

**ISTC 1866-2000**

**Final  
Project Technical Report  
of ISTC 1866p-2000**

**Investigation of Discharges Influence  
on Boundary Layer in Supersonic Airflow**

**(From 1 October 2000 to 30 September 2001 for 12 months)**

**Valery Mikhailovich Shibkov  
(Project Manager)  
Department of Physics of Moscow State University**

**October 2001**

---

This work was supported financially by the European Office of Aerospace Research and Development (EOARD)  
and performed under the contract to the International Science and Technology Center (ISTC), Moscow.

REPORT DOCUMENTATION PAGE				Form Approved OMB No. 0704-0188	
Public reporting burden for this collection of information is estimated to average 1 hour per response, including the time for reviewing instructions, searching existing data sources, gathering and maintaining the data needed, and completing and reviewing this collection of information. Send comments regarding this burden estimate or any other aspect of this collection of information, including suggestions for reducing this burden to Department of Defense, Washington Headquarters Services, Directorate for Information Operations and Reports (0704-0188), 1215 Jefferson Davis Highway, Suite 1204, Arlington, VA 22202-4302. Respondents should be aware that notwithstanding any other provision of law, no person shall be subject to any penalty for failing to comply with a collection of information if it does not display a currently valid OMB control number. PLEASE DO NOT RETURN YOUR FORM TO THE ABOVE ADDRESS.					
1. REPORT DATE (DD-MM-YYYY) 04-10-2001		2. REPORT TYPE Final		3. DATES COVERED (FROM - TO) 01-10-2000 to 01-10-2001	
4. TITLE AND SUBTITLE Investigation of Discharges Influence on Boundary Layers in Plasma Unclassified				5a. CONTRACT NUMBER	
				5b. GRANT NUMBER	
				5c. PROGRAM ELEMENT NUMBER	
6. AUTHOR(S) Shibkov, Valery ;				5d. PROJECT NUMBER	
				5e. TASK NUMBER	
				5f. WORK UNIT NUMBER	
7. PERFORMING ORGANIZATION NAME AND ADDRESS Moscow State University (MSU) Faculty of Physics Moscow Moscow 11989, Russiaxxxx				8. PERFORMING ORGANIZATION REPORT NUMBER	
9. SPONSORING/MONITORING AGENCY NAME AND ADDRESS EOARD PSC 802 BOX 14 FPO, 09499-0014				10. SPONSOR/MONITOR'S ACRONYM(S)	
				11. SPONSOR/MONITOR'S REPORT NUMBER(S)	
12. DISTRIBUTION/AVAILABILITY STATEMENT APUBLIC RELEASE					
13. SUPPLEMENTARY NOTES					
14. ABSTRACT This report results from a contract tasking Moscow State University (MSU) as follows: The contractor will develop methods of creation of plasmas of different types of gas discharges near the surface of airplanes and in the boundary layers. He will also develop methods of analysis of plasma properties in plasma regions near the surface. The following experimental work will be done in supersonic air flow (M<2) at pressures between 1 and 200 Torr: a) measurement of friction drag on a flat plate without plasma flow; b) same as (a) with plasma jet flow, and with corona discharge; and c) measurement of friction drag of the plate treated with plasma. A theoretical analysis of the obtained results will also be delivered.					
15. SUBJECT TERMS EOARD; Aviation Technology; Aerodynamics					
16. SECURITY CLASSIFICATION OF:		17. LIMITATION OF ABSTRACT Public Release	18. NUMBER OF PAGES 116	19. NAME OF RESPONSIBLE PERSON Fenster, Lynn lfenster@dtic.mil	
a. REPORT Unclassified	b. ABSTRACT Unclassified	c. THIS PAGE Unclassified		19b. TELEPHONE NUMBER International Area Code Area Code Telephone Number 703767-9007 DSN 427-9007	
				Standard Form 298 (Rev. 8-98) Prescribed by ANSI Std Z39.18	

REPORT DOCUMENTATION PAGE				Form Approved OMB No. 0704-0188	
Public reporting burden for this collection of information is estimated to average 1 hour per response, including the time for reviewing instructions, searching existing data sources, gathering and maintaining the data needed, and completing and reviewing the collection of information. Send comments regarding this burden estimate or any other aspect of this collection of information, including suggestions for reducing the burden, to Department of Defense, Washington Headquarters Services, Directorate for Information Operations and Reports (0704-0188), 1215 Jefferson Davis Highway, Suite 1204, Arlington, VA 22202-4302. Respondents should be aware that notwithstanding any other provision of law, no person shall be subject to any penalty for failing to comply with a collection of information if it does not display a currently valid OMB control number. <b>PLEASE DO NOT RETURN YOUR FORM TO THE ABOVE ADDRESS.</b>					
<b>1. REPORT DATE (DD-MM-YYYY)</b> 04-10-2001		<b>2. REPORT TYPE</b> Final Report		<b>3. DATES COVERED (From – To)</b> 01-Oct-00 - 01-Oct-01	
<b>4. TITLE AND SUBTITLE</b> Investigation of Discharges Influence on Boundary Layers in Plasma			<b>5a. CONTRACT NUMBER</b> ISTC Registration No: 1866		
			<b>5b. GRANT NUMBER</b>		
			<b>5c. PROGRAM ELEMENT NUMBER</b>		
<b>6. AUTHOR(S)</b> Professor Valery Shibkov			<b>5d. PROJECT NUMBER</b>		
			<b>5d. TASK NUMBER</b>		
			<b>5e. WORK UNIT NUMBER</b>		
<b>7. PERFORMING ORGANIZATION NAME(S) AND ADDRESS(ES)</b> Moscow State University (MSU) Faculty of Physics Moscow Moscow 11989 Russia				<b>8. PERFORMING ORGANIZATION REPORT NUMBER</b>  N/A	
<b>9. SPONSORING/MONITORING AGENCY NAME(S) AND ADDRESS(ES)</b>  EOARD PSC 802 BOX 14 FPO 09499-0014				<b>10. SPONSOR/MONITOR'S ACRONYM(S)</b>	
				<b>11. SPONSOR/MONITOR'S REPORT NUMBER(S)</b> ISTC 00-7005	
<b>12. DISTRIBUTION/AVAILABILITY STATEMENT</b> Approved for public release; distribution is unlimited.					
<b>13. SUPPLEMENTARY NOTES</b>					
<b>14. ABSTRACT</b>  This report results from a contract tasking Moscow State University (MSU) as follows: The contractor will develop methods of creation of plasmas of different types of gas discharges near the surface of airplanes and in the boundary layers. He will also develop methods of analysis of plasma properties in plasma regions near the surface. The following experimental work will be done in supersonic air flow (M<2) at pressures between 1 and 200 Torr: a) measurement of friction drag on a flat plate without plasma flow; b) same as (a) with plasma jet flow, and with corona discharge; and c) measurement of friction drag of the plate treated with plasma. A theoretical analysis of the obtained results will also be delivered.					
<b>15. SUBJECT TERMS</b> EOARD, Aviation Technology, Aerodynamics					
<b>16. SECURITY CLASSIFICATION OF:</b>			<b>17. LIMITATION OF ABSTRACT</b> UL	<b>18. NUMBER OF PAGES</b>  118	<b>19a. NAME OF RESPONSIBLE PERSON</b> Charbel N. Raffoul
<b>a. REPORT</b> UNCLAS	<b>b. ABSTRACT</b> UNCLAS	<b>c. THIS PAGE</b> UNCLAS			<b>19b. TELEPHONE NUMBER</b> (Include area code) +44 (0)20 7514 4299

## CONTENTS

INTRODUCTION	3
CHAPTER I REVIEW OF THE LITERATURE	5
1.1. Frontal drag reduction	5
1.2. Reduction of boundary friction	8
1.3. Surface microwave discharges	20
CHAPTER II PHYSICAL MODEL OF THE MICROWAVE DISCHARGE ON A DIELECTRIC ANTENNA SURFACE	37
2.1. Introduction	37
2.2. Complete set of equation for discharge description	39
2.2.1. Maxwell equations	39
2.2.2. Kinetics of charged particles without negative ions	40
2.2.3. Kinetics of charged particles with negative ions	41
2.2.4. Electron energy balance and calculation of electron temperature	47
2.3. Surface and dielectric waveguide waves in homogeneous bounded plasma	50
2.4. Surface wave discharge classification	53
2.5. Simplified set of equations	59
2.5.1. Electron heat transfer equation	59
2.5.2. Electron density distribution near antenna surface	61
2.6. Discharge characteristics	64
CHAPTER III EXPERIMENTAL INSTALLATIONS	70
3.1. Experimental set-up	70
3.2. Set-up for creation of surface microwave discharge	73
3.3. Set-up for creation of surface transversal pulsed-periodical discharge	75
3.4. Automated circuit of probe measuring	75
CHAPTER IV DIAGNOSTICS METHODS	78
4.1. Probe application for diagnostics of the surface microwave discharge in supersonic flow	78
4.2. Spectral methods of measurement of gas temperature	80
4.3. Spectral methods of measurement of vibration temperature	82
CHAPTER V EXPERIMENTAL RESULTS	84
5.1. Surface microwave discharge	84
5.2. Threshold characteristics of the surface microwave discharge	87
5.3. Dynamics of the surface microwave discharge	90
5.4. Gas heating under condition of the surface microwave discharge	96
5.5. Surface transversal pulsed-periodical discharge	102
CONCLUSIONS	107
REFERENCES	110

## INTRODUCTION

During many years the intensive theoretical and experimental investigations of a boundary layers existing near the bodies streamlined by the flow of gas or fluid were studied. The development of a modern aviation and especially the supersonic one requires effective means for the control of characteristics of flow near the aeroplane's surface, boundary layer heat and mass transfer in these regions, flow separation and boundary layer friction drag reduction. With the purpose of improvement of the aerodynamic characteristics of flight vehicles the set of the methods of an external influence on a boundary layer was offered. However existing methods of an application of energy to a boundary layer are ineffective or economically unprofitable. Therefore the development of new ways of influence on the characteristics of gas flow near a flight vehicle exists.

Recently the interest to use for various applied tasks of low-temperature plasma has revived again. So, for example, a new direction of aerodynamics - so-called plasma supersonic aerodynamics was arisen [1-4]. In this case the various type of the gas discharges are used with the purpose of influence on the characteristics of gas flow near a surface of the flying bodies. However a physics of the discharge in supersonic flow of gas until the present time is in a phase of development. There are many unsolved questions, among which a problem of a gas breakdown in supersonic flow, a creation and maintenance of the stable discharge in supersonic flow of air, an influence of flow on parameters of plasma of the gas discharge and an influence of the discharge on the characteristics of supersonic flow are dominant problems.

The first laboratory experiments [1-3] have shown an opportunity of a drag reduction at creation of the discharges of direct and alternative currents before a body streamlined supersonic airflow. However, the electrode discharges in flow are unstable and spatially non-uniform. Such discharges result in strong erosion of electrodes and model surface and reliably are not reproduced in various realizations [1].

A task of search of optimum ways of creation of non-equilibrium plasma in supersonic flows was appeared. One of such ways, offered in our laboratory, is the new version of a surface microwave discharge, namely, the microwave discharge on an external surface of the dielectric bodies, streamlined supersonic flow of air. In this case the economically efficient influence on the delay of laminar-turbulent transition and on the reduction of a turbulent friction coefficient at the external action on a turbulent boundary layer can take place.

The Project "Investigation of discharges influence on boundary layer in supersonic airflow" is devoted to the development of methods of creation of plasma of different types of the gas discharges near the surface of bodies and in the boundary layers. The main objective is to investigate the physics of non-equilibrium plasma of the surface microwave discharge in supersonic airflow.

## CHAPTER I

### REVIEW OF THE LITERATURE

In the recent years the task of improvement of the aerodynamic characteristics of flight vehicles by the new methods is an actual problem. For this purpose it is necessary to lower a drag reduction and to reduce a friction coefficient in a boundary layer.

The reduction of a drag can be achieved by creating an area of heated gas before a flight vehicle. Such area can be formed as a result of absorption of electromagnetic energy of the different frequency ranges or by plasma creating in this area. For this purpose in some laboratories it is offered to use the discharges of different types.

With the purpose of influence on the characteristics of boundary-layer flow near a body, streamline supersonic gas flow, such methods as heating of a body surface, action on a boundary layer of acoustic oscillations, application of vibrators, suction of a boundary layer etc. are considered.

#### 1.1. Frontal drag reduction

The system of shock waves existing near a body moving in the Earth's atmosphere with supersonic velocity causes a continuous acceleration of air masses in direction of the flight. It leads to the frontal drag of the supersonic aeroplane. In paper [4] it is offered to minimize the acceleration of air in a direction of a motion of a flight vehicle. For it the airflow should be subsonic everywhere. For elimination of frontal shock waves it is enough to create before a nose of a flight vehicle the area with the heightened values of the local velocity of a sound  $v_s$ , for example, to heat air with the help of absorption of beam energy. It is important, that the gas heating should not be bound up to an injection of a preheated continuous medium - plasma or gas: otherwise in a direction of "x" on boundary with cold gas the local velocity of a sound in cold gas will be exceeded, the shock wave will be formed and the radical drag reduction will fail.

It is necessary to generate such area in air even before approach of a flight vehicle. If the shape of this area is elongated enough on "x" direction, the gas expanding at a heating has (in a laboratory frame) practically only radial component of velocity  $v_r$ . This velocity depends on the radial co-ordinate and the time-space allocation of an energy release on cross section at co-

ordinate "?", but does not depend on velocity of a flight vehicle  $v$ . Apparently, the velocity  $v_r$  can be enough small in comparison not only with  $v$ , but also with  $v_s$ , i.e. it is possible ensure its subsonic expansion without formation of strong shock waves. If the area of an energy release insufficiently elongates (for example, quasi-spherical zone) it is streamlined by cold gas almost as a solid body and the shock wave is formed.

In order that the motion of a flight vehicle in an atmosphere happened without formation of frontal shock waves two requirements should be executed.

First,

$$v_s = \sqrt{\frac{\gamma k T}{m}} > v, \quad (1.1)$$

where  $k$  is Boltzmann constant,  $T$  is temperature,  $m$  is mean molecular mass,  $\gamma$  is adiabatic index.

Second, the final radial dimension of the gas-plasma channel  $r_p$  should be more then the radial size  $r_a$  of a nose of a flight vehicle.

Let's consider the problem on creation of the heated area. It can be generated as a result of absorption of electromagnetic energy of the different frequency bands or at creation of plasma of a gas discharge. One or two electrodes are required for formation of the direct current, pulsed-periodic or high-frequency discharges. In this case before a body it is necessary to dispose electrodes so that to ensure the greatest frontal drag reduction at a relative supersonic motion of a body.

In paper [5] the model was placed along a wind tunnel axis, the cathode was placed at the front of model, and anode was behind it. In experiment two types of models (with spherical and conical frontal parts) were used. The anode consisted of 8 electrodes, each of which was included to the power source through the ballast resistance. The plasma was created on the frontal surface of model. Thus the frontal drag reduction up to 15 % for model to a spherical surface and up to 10 % with conical one took place.

The diminution of a frontal drag reduction can be explained by two mechanisms. At the considerable gas heating the translational temperature of molecules has increased up to 1000-2000 K. Therefore for some modes the drifted plasma has a subsonic speed, that gives in an uniform distribution of pressure in plasma, and to absence of shock waves in plasma area. The Reynolds's numbers are much lower than for the same stream without the discharge. The creation of the discharge probably hinders with laminar-turbulent transition and, thus, reduces to a viscous component.

Attempt to investigate a degree of influence of one of these mechanisms on a frontal drag reduction was conducted and enunciated in paper [6]. During experiment the efforts were guided



on separation of plasma and thermal effects. But the obtained data have not yielded results due to the large errors.

In paper [7] the chemical reactions were taken into account at examination of plasma effects in non-equilibrium plasma. The detailed experimental and theoretical examination of plasmachemical reactions which are taken place at a microwave discharge in air enunciated in the monograph [8]. In these papers the conditions of realization of experiment are close to requirements of the plasma aerodynamic experiments.

At usage of the microwave or the laser radiations they spoke about an electrodeless discharge. The adaptability to manufacture of energy transportation and its input into the discharge chamber, the efficiency of absorption of electromagnetic energy in the discharge plasma, the absence of plasma instability initiated by electrodes, the long-lived maintenance of cleanness of plasma because of absence of contact with electrodes and walls of the discharge chamber, the opportunity of creation of the extended homogeneous discharge, the achievement of the high specific supplied powers, the selectivity at redistribution of energy from electrons in the internal degrees of freedom of molecules are the features of a microwave.

The application of a microwave energy to plasma can be executed as follows [9]. The dielectric tube from a material transparent for a microwave (for example, quartz) is interposed into a waveguide of the rectangular section perpendicularly to its broad wall. The vector of an electric field in a wave such as  $H_{01}$  is parallel to the narrow wall of a waveguide, the electric field  $E$  in this direction is constant, and in perpendicular direction it changes under the sine law. The discharge is formed in the zone of cross of a tube with a waveguide. The plasma is supported at the expense of a dissipation of energy of a running electromagnetic wave.

However the peculiar properties of a microwave allows to conduct experiments in free space in absence of a contact of the discharge with walls of the chamber and electrodes. In [10] the discharge formed in the resonator in which the standing electromagnetic waves such as  $H_{01}$  were excited. The discharge was formed on an axis in the zone of a maximum electric field. The plasma was drawn out along vector of an electric field and looked like a cord at large powers.

The successes in development of an electronics of ultrahigh frequencies have resulted in an opportunity of creation of the new form of the discharge – the electrodeless microwave discharge in the focused beam of electromagnetic energy in a free space. In [11] the microwave discharge was observed at argon pressure  $p=100$  torr. The focused beam was formed with the help of a mirror. The radiation of the microwave generator working in a continuous mode power  $W=2$  kW on a wavelength  $\lambda=3$  cm was used. The pulsed microwave discharge in the focused beam of radiation was explored in [12] too.

The microwave discharge arising in the focal zone of electromagnetic energy beam represents a complex nonlinear phenomenon including a non-stationary breakdown of gas, spreading of ionization fronts interacting with electromagnetic radiation, maintenance of nonequilibrium plasma, heating and excitation of neutral gas. Under action of the powerful focused beam of electromagnetic waves of a very high frequency, provided that the electric field intensity exceeds threshold value, a gas breakdown takes place in the focal zone of the discharge chamber. A microwave discharge in the focused beam was investigated in detail in a cycle of paper [8, 13-23].

## **1.2. Reduction of boundary friction**

The laminarization of airflow is one of the few possibilities of reducing of a friction resistance and, consequently, improving the aerodynamic quality and efficiency of flight vehicles. For subsonic aircraft the friction resistance makes up till 80-90 %, and for supersonic till 50-60 % from total resistance. It is known, that the friction coefficient at laminar flow almost on the order is less than at turbulent one. From here, the importance of a problem of a laminarization of airflow is obvious for flight vehicles. In recent years, much attention has been given to the study of new possibilities for laminarization of flow, i.e. delay of transition to the turbulent flow mode in the boundary layer up to the highest possible Reynolds's numbers. One of the unconventional methods of controlling the laminar-turbulent transition [24] is the heating of a small area of the surface of a body being flown around.

It has been established in [24] that the heating of a part of a body surface in the vicinity of the leading edge helps to considerably increase the extent of the laminar portion of boundary layer. In paper [24] was shown, that the heating of a small surface area in the vicinity of the leading edge to temperatures two to four times higher than the forward flow temperatures leads to delay of transition even if the body surface is heat-insulated downstream of a heating area. An example is provided of the surface temperature distribution, when the energy savings due to reduction of friction exceed the energy spent to heat the surface by a factor of three.

In [25] the results of experimental examination of an opportunity of a laminarization of a boundary layer by the method of suppression of Tollmien-Schlichting waves, existing in a boundary layer and responsible for transition, were represented. Thus, the artificial created waves of perturbation were inlet into a boundary layer in an antiphase to Tollmien-Schlichting waves. The opportunity of such laminarization was shown. The experiments were conducted on a direct wing in a low turbulent subsonic wind tunnel. The boundary layer, perceiving external

fluctuations, quenches them in a broad band of frequencies except for the some narrow strip. Thus, it is possible to receive diminution of amplitude of the most dangerous vibration by introduction in a boundary layer the artificial created waves of perturbation. In such a way, a retardation of development of a dominant wave of instability takes place and, as result, the line of transition displaces downstream.

The problem of transition of a laminar boundary layer in a turbulent condition during several decades causes a big interest of the researchers. It is stipulated, at first, by necessity of the solution of practical problems, for example, the problem of control of a boundary layer with the purpose of a reduction of resistance of aircraft and calculation of its aerodynamic characteristics. Secondly, the study of process of appearance of a turbulence is a part of more general fundamental problem of the description of a turbulence.

In the literature the conception of "the transition" is understood, as a rule, concept alone process of decay of a laminar mode and formation of a turbulent flow. A beginning of transition usually connects to occurrence of rough processes in the form of turbulent spots and low-frequency pulsations of large amplitude. However it became now absolutely understandable, that the long sequence of physical processes, resulting in a laminar flows destroying, takes the beginning much earlier, namely, in transformation of external perturbations of a different nature in an external flow in waves of a boundary layer or in their generation into the boundary layer happening on unevenness' of a streamline surface (ledges, roughness etc.).

At the end of XIX century Reynolds expressed the assumption that the instability of laminar flow is the reason of transition of laminar flow in a turbulent condition. In other words, the waves in a boundary layer amplify and it is the reason of destruction of a laminar mode of stream. Much later Taylor was expressed other hypothesis, according to which the transition is caused by pulsation's of an external flow resulting in to local boundary layer separation and its turbulization.

The theory of magnetohydrodynamic stability started by Relay's transactions on a boundary of ?? century. The first calculations of boundary layer stability were carried out by Tollmien and Schlichting much later at the end of 20 - at the beginning of 30 years. However right up to 40 years Taylor's hypothesis was preferred in a stability theory. Only Schubauer's and Skramstad's experiments carried out at the beginning of 40 years have confirmed validity of the concept of instability. Schubauer and Skramstad have found out both oscillation of a boundary layer and their determining role during destruction of a laminar mode. Now it is absolutely clear that in case of small intensity of all external perturbations and smooth surface of a plate the

transition to a turbulence in a boundary layer happens owing to development of instability of an initial laminar flow.

The process of transition of a laminar boundary layer in a turbulent condition at small intensity of external perturbations consists of three conditionally parted stages: the generation of waves of a boundary layer, their amplification under the laws of the linear theory and non-linear destruction of a laminar mode of flow. Each stage of this sequence corresponds the typical area in space in accordance with increase of distance from a leading edge of model. The described sequence of stages of transition is diagrammatically shown in a Fig.1.1 [26].

In [27] the opportunities of improvement of the aerodynamic characteristics of a plate are investigated at the expense of a combined laminarization including the optimization of pressure distribution and temperature of a surface. The class of the temperature distribution of a surface corresponding to a heating of a leading edge and cooling of a remaining part of a surface up to the recovery temperature of an incident flow was surveyed. It was shown, that thus it was possible: i) to increase a lift coefficient of a plate at invariable resistance and ii) to lower resistance and to increase a critical Mach number at invariable lift. In [27] was shown, that the energy expedient reduction of resistance can achieve by a heating of a part of a wing surface in a combination to other methods of flow laminarization.

The behaviour of a separated flow at a motion of flight vehicles is considered in [28]. The aerodynamic characteristics of flight vehicles are determined by features of their streamlining, that is relative motion of a surrounding medium. The flow separation is one of the fundamental phenomena of a mechanics of a fluid and gas. It consists that under certain conditions (for example, unfavourable gradient of pressure) the medium in vicinity of a streamlined body ceases to move along its surface and starts to moves away from it. In result the area of the separation flow will be formed. The flow separation renders influence on a manoeuvrability, controllability and aerodynamic efficiency of a vehicle. The behaviour of the separation flow differs for different aeroplane speeds, wing shapes and attack angles. At a separation of a stationary laminar stream the separated flow can again join a wing surface. Thus, the local separation zone arises. It has the small sizes as contrasted to the wing sizes (Fig.1.2, a). In this case separated area on a wing exists as a narrow strip elongate along its total wing-span. The position of a separated zone on a wing depends on an angle of attack. At its increasing the separation zone is shifted closer to a leading edge of a wing. One more separation of a non-stationary turbulent flow is appeared on back edge of a wing (Fig.1.2, b). At a turbulent separation there is no repeated connection of a separated flow to a wing surface and zone of a separation includes all area of flow from a line of a separation up to a back edge of a wing. A flow separation from a leading edge arises at further

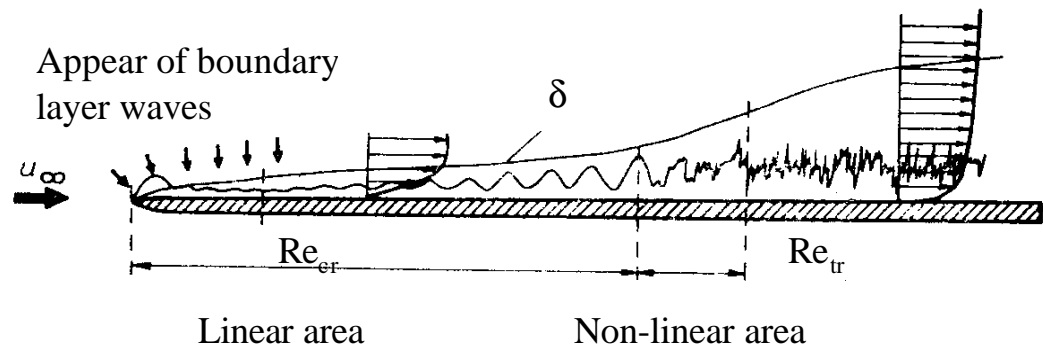


Fig.1.1.1. The diagram of main stages of transition process in a boundary layer [26].

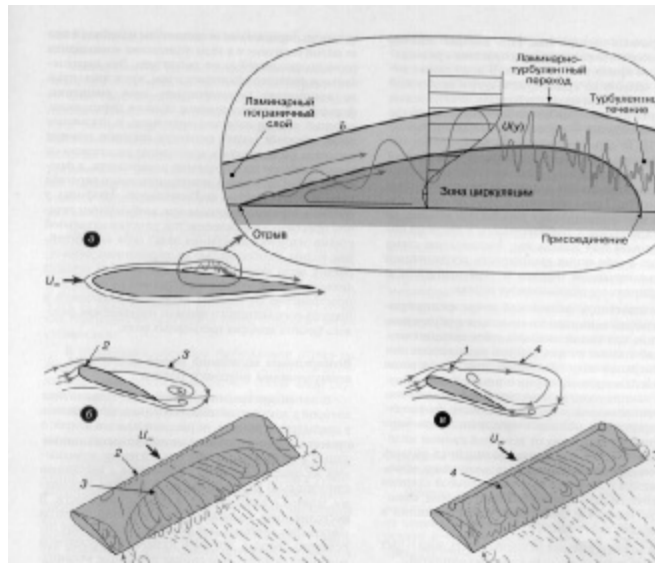


Fig.1.2. The diagrams of the flow separation at different values of an attack angle of a wing [28].

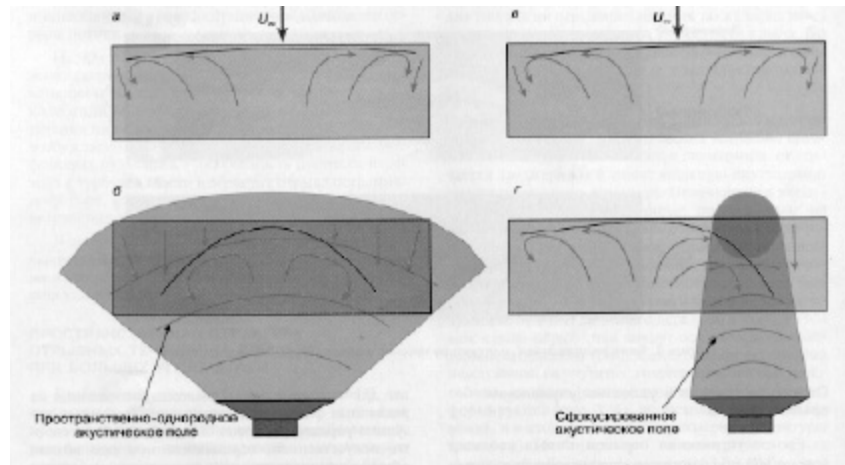


Fig.1.3. The scheme of flow in vicinity of a wing surface at the excitation of the spatially homogeneous acoustic field and at the focused acoustic field [28].

magnification of an angle of attack and reaching it of critical value. It is called global or complete separation (Fig.1.2, c). The complete separation is accompanied by sharp decrease of lift of a wing, by magnification of its drag and gives in unfavourable consequences.

For the first time the preventing of a complete separation from a leading edge of a wing at excitation of acoustic oscillations was fulfilled in [29] in representation about two-dimension flow. The scheme of flow in vicinity of a wing surface are represented in Fig.1.3. The excitation of the spatially homogeneous acoustic field from a remote source of oscillations causes the connection of the separated flow. In result the complete separation from a leading edge is replaced by a separation of a turbulent flow downstream (Fig.1.3, a,b). Thus, the streamlining of the wing remains to symmetric concerning its central section. If the wing is in the focused acoustic field the behaviour of the vortexes in a zone of a separation depends on what area of flow is put to the test. If the oscillations focused on the edge of model they have an effect in a zone of one of vortexes and the influences do not render in the area of other vortex (Fig.1.3, c,d). From here it is possible to make a conclusion that the spatial structure of flow at acoustical action and the result of control of a complete separation depend on transport of gas in a transverse direction, in spite of the fact that the acoustical excitation of oscillations of the separated layer realizes near to a leading edge of a wing and the large-scale turbulent motion is formed downstream.

In paper [30] the experimental study of a susceptibility of a boundary layer is investigated at modelling of process of excitation of own oscillation of a boundary layer by external, artificial caused, acoustical perturbations. The discharge-boundary layer system was used as a source of the determined perturbations. The surface electric discharge in a laminar boundary layer of first plate causes the perturbations which amplifies in some times at a motion downstream. This process is accompanied by acoustical radiation in an external stream. The distribution of the perturbation amplitude, radiated in a free stream, depends on longitudinal coordinate  $x$  and has two maximums. The first, rather narrow maximum, is caused by electric discharge and is spread on Mach line from it. The second maximum corresponds to radiation from a transitional zone and is spread on a line by close to Mach line. The frequency of radiation coincides frequency of an electrical arc ignition. When the second plate moves in a field of perturbations, the maximums of radiation fall on different parts of a plate and cause different response of a boundary layer on external perturbations. From experiment one can see that the most intensive transformation of external acoustical perturbations to own oscillations of a boundary layer of a flat plate happens in neighbourhoods of a leading edge of a plate, sound branch of a neutral curve, and lower branch of a curve of neutral stability.

The method of a reduction of friction based on a heating of a part of a surface of a flat plate near to its leading edge was offered in [31]. In this case the diminution of a total resistance of friction on a plate was reached due to increase of stability of gas flow heated near to a leading edge and further travelling above more cold surface, that result in to essential magnification of length of a laminar part of boundary layer flow. However at large enough values of a typical Reynolds's number the extent of a turbulent part of a boundary layer considerably exceeds the length of a laminar part, owing to what in this case further diminution of a friction drag is possible only by a reduction of the turbulent friction. It is known that on an isothermal surface, which temperature is higher than the flow recovery temperature, the friction is less than that on an adiabatic surface. However uniform heating of all streamline surface is bound up to considerable technical difficulties and in this case the energy cost of a boundary layer heating considerably exceeds the profit received owing to a friction reduction.

In paper [32] the results of numerical investigations of influence of a heating of a local part of a surface of a flat plate on a flow in a developed turbulent boundary layer are submitted. The surface was assumed to be heat-insulated downstream of the heated portion. It is shown that at the beginning of the heating portion the friction is increased and then the friction coefficient decreases, and its minimum values are reached on the heat-insulated part of a surface following behind the heated portion. The reduction of coefficient of turbulent friction as contrasted to its value on an isothermal adiabatic surface is spread to considerable distance downstream from a heated portion. Due to "long memory effect" of a turbulent boundary layer the considerable friction reduction is reached at local heat input in comparison with the uniform heating of all streamline surface. At presence of several following one after another the heating portion this "long memory effect" intensifies and more essential diminution of value of the turbulent friction can be obtained. At identical total energy consumption the reduction of an integrated friction coefficient almost twice is more than in case of an uniformly distributed on all surface energy supplied to gas in a boundary layer.

The article [33] is development of the paper [32]. In [33] the calculations are performed of a supersonic boundary layer on a flat plate with one and five zones of local heating of its surface. Within the concept of "displacement body", allowance is made for the interaction between the boundary layer and external nonviscous flow. It is shown that the inclusion of viscous-nonviscous interaction leads to significant variation in the distribution of the local friction coefficient.



It is known that the friction resistance decreases under conditions of heating of the surface being flown about [34, 35]. Based on the results of calculation of a compressible turbulent boundary layer using the algebraic model of turbulence, it was shown in [36] that the efficiency of the thermal method of reducing turbulent friction may be raised considerably owing to localization of the region of heat input to the boundary layer. In [37] the theoretical studies were made into the effect of the thermal properties of the material of the surface being flown about on the reduction of turbulent friction under conditions of local heating of a flat plate.

The localization of regions of heat input to gas under conditions of fairly intense heating leads to the emergence of appreciable gradients of the displacement thickness of boundary layer. In this case, the interaction between external nonviscous flow and the boundary layer results, even under conditions of flow past a flat surface, in the emergence of a longitudinal pressure gradient. The presence of a pressure gradient obviously leads to a variation of the characteristics of the turbulent boundary layer. In view of this, it becomes necessary to include the viscous-nonviscous interaction and assess its effect on the parameters of the boundary layer in the presence of localized regions of heat input.

The authors of the article [33] treat the flow past a plate with the Mach number in the incident flow  $M_\infty = 2$  and the velocity, density, temperature, and dynamic viscosity  $u_\infty^*, \rho_\infty^*, T_\infty^*$  and  $\mu_\infty^*$ , respectively. The initial section is identified in the region of the developed boundary layer, which is characterized by the value of Reynolds number  $Re_\theta = \rho_\infty^* u_\infty^* \theta_0^* / \mu_\infty^* = 4000$ , calculated by the parameters of incident flow and momentum thickness in this section  $\theta_0^*$ .

Located at the distance  $L^*$  downstream of the above-identified section is the beginning of the heated portion of the plate surface, which has the length  $h^*$ . Two options will be treated below, namely, (a) a single heated portion, and (b) five series-arranged heated surface portions of the same length  $h^*$  with the constant distance  $H^*$  between the beginnings of two neighboring portions. Outside of the heated portions, in which the heat flux distribution is preassigned, the plate surface is assumed to be adiabatic.

The simulation of the compressible turbulent boundary layer is performed using the two-parameter k- $\epsilon$  model of turbulence [38]. For numerical solution of the system of equations of the turbulent boundary layer in view of viscous-nonviscous interaction, in [33] dimensionless variables (without the superscript \*) are introduced, defined by the following relations:

$$\begin{aligned}
x^* &= l^* x, & y^* &= l^* \delta y, & \delta^* &= l^* \delta, \\
u^* &= u_\infty^* u_e u, & v^* &= u_\infty^* u_e \delta \left( V + \frac{yu}{\delta} \frac{d\delta}{dx} \right), \\
k^* &= \frac{u_\infty^{*2}}{Re^{1/2}} k, & \varepsilon^* &= \frac{u^{*3}}{l^*} \varepsilon, & T^* &= T_\infty^* T, \\
\rho^* &= \rho_\infty^* \rho, & \mu^* &= \mu_\infty^* \mu, & Re &= \frac{\rho_\infty^* u_\infty^* l^*}{\mu_\infty^*}.
\end{aligned} \tag{1.2}$$

Here,  $\delta(x)$  is the dimensionless displacement thickness of the boundary layer,  $u_e(x)$  is the velocity on its external boundary, and  $k^*$  and  $\varepsilon^*$ , respectively, denote the kinetic energy of turbulence and its dissipation rate. Relations (1.2) further include the characteristic linear size  $l^*$  and characteristic Reynolds number  $Re$ , which may be preassigned arbitrarily, because the parameters of the developed boundary layer in the initial section are defined by the value of the Reynolds number.

The values of  $l^*$  and  $Re$ , preassigned in the calculations, define the value of the momentum thickness in the initial section according to the expression  $\theta_0^* = l^* Re_\theta / Re$ . In the calculations, the values of  $l^* = 1\text{m}$ ,  $Re = 2 \cdot 10^6$  and, consequently,  $\theta_0^* = 0.002\text{m}$  were preassigned.

In order to include the interaction between the turbulent boundary layer and external supersonic flow, in [33] the concept of "displacement body" is employed, according to which the effect of the boundary layer on external flow is equivalent to nonviscous flow past the effective surface formed by adding the displacement thickness of boundary layer to the real surface of the body.

In the calculations, constant values were preassigned for the distance from the initial section  $x_0$  to the beginning of the first heated portion  $L^* = 250\theta_0^* = 0.5\text{ m}$  and for the length of each portion  $h^* = 20\theta_0^* = 0.04\text{ m}$ . The distribution of heat flux  $q_w$  in the heated portions was preassigned in the sine form. In the presence of one heated portion, the total amount of heat, equal to the integral of  $q_w$  over the portion length, was  $Q_w = 10^{-4}$  (option 1) and  $2 \times 10^{-4}$  (option 2). When five heated portions were treated, the distance between the beginnings of two adjacent portions was  $H^* = 100\theta_0^* = 0.2\text{ m}$ , and the amount of heat supplied to every one of them was  $Q_w = 10^{-4}$ .

Fig.1.4 gives the distribution of the displacement thickness of boundary layer and of the velocity gradient on its external boundary for a single heated portion for two above-identified values of total thermal power supplied to the boundary layer [33]. The dashed curves indicate,

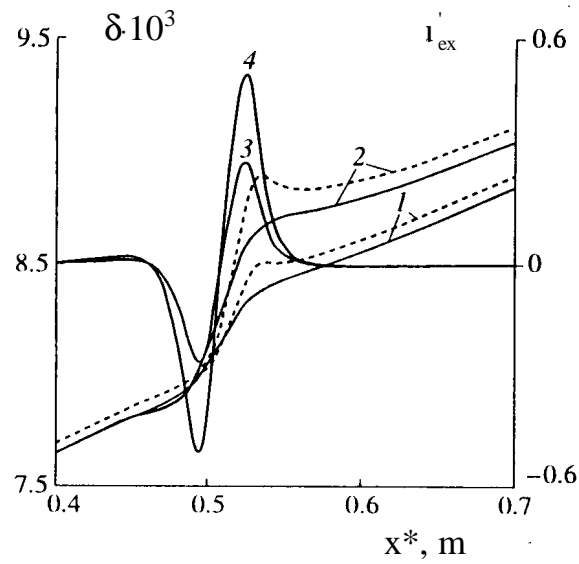


Fig.1.4. The distribution of (1, 2) the displacement thickness of boundary layer and (3, 4) of the velocity gradient on its external boundary: (1, 3)  $Q_w=10^{-4}$ , (2, 4)  $2 \cdot 10^{-4}$ . Dashed curves indicate  $\delta$  in the case of ignoring the viscous-nonviscous interaction, and continuous curves indicate  $\delta$  in the case of including the interaction [33].

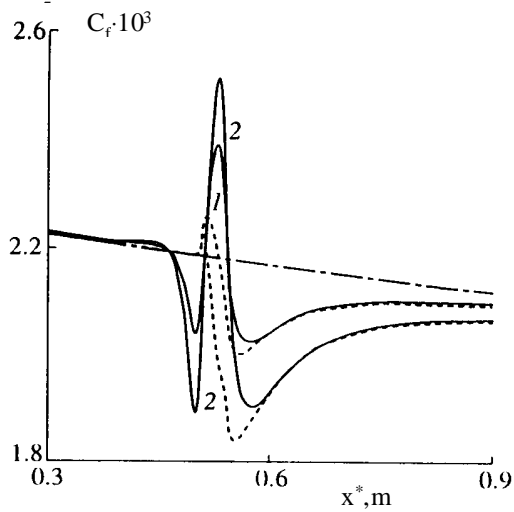


Fig.1.5. The distribution of the local friction coefficient for a single heated portion: (1)  $Q_w=10^{-4}$ , (2)  $Q_w=2 \cdot 10^{-4}$  [33].

for comparison, the distribution of the displacement thickness ignoring the viscous-nonviscous interaction. Naturally, the displacement thickness in the heated portion and behind it increases with  $Q_w$ . The interaction between the boundary layer and external flow results, first, in a smaller increase of the displacement thickness than in the case of ignoring the interaction and, second, in the upstream propagation of the effect of surface heating on the boundary layer thickness.

As a result of viscous-nonviscous interaction before the boundary layer, a fairly considerable gradient of velocity occurs on the external boundary of the boundary layer, whose absolute magnitude is the greater, the higher the power of heat input. A fairly intensive acceleration of external flow is observed in the greater part of the heated portion.

The longitudinal gradient of pressure, emerging upon inclusion of viscous-nonviscous interaction, affects considerably the local friction, as is shown in Fig.1.5 [33] which gives the distribution of the local friction coefficient for two values of  $Q_w$  defined by the expression

$$C_f = \frac{2}{\rho_e u_e \text{Re } \delta} \left( \mu \frac{\partial u}{\partial y} \right)_w. \quad (1.3)$$

The dot-and-dash curve in Fig.1.5 indicates the distribution of the friction coefficient on a fully adiabatic surface, calculated for  $u_e = 1$ , and the dashed curves indicate the distribution of  $C_f$  on a heated surface ignoring the interaction.

The deceleration of external flow before the heated portion is accompanied by a considerable decrease of the friction coefficient. Due to acceleration of flow, the friction coefficient throughout almost the entire heated portion is higher than that on the adiabatic surface. This increase of  $C_f$  is the higher, the greater the heat input. The inverse dependence is observed when the interaction is ignored. As in the case of  $u_e = 1$ , the maximum reduction of local friction is attained behind the heated portion.

The interaction between the boundary layer and external flow has a marked effect both on the distribution of the local friction coefficient and on integral friction. The total reduction of friction due to local surface heating, attained at  $x_m^* = 1.5 \text{ m}$ , is less than in the case of ignoring the interaction by approximately 3% with  $Q_w = 10^{-4}$  and by 10% with  $Q_w = 2 \times 10^{-4}$ .

In the presence of several heated portions with one and the same value of  $Q_w$  the distribution of the velocity gradient on the external boundary of the boundary layer in the region of heat input is almost periodic, as is seen in Fig.1.6 [33]. A gradual downstream decrease is observed of the maximum (in absolute magnitude) values of  $u'_{ex}$ . The dashed curve in Fig.1.6 indicates the distribution of displacement thickness, calculated ignoring the interaction.

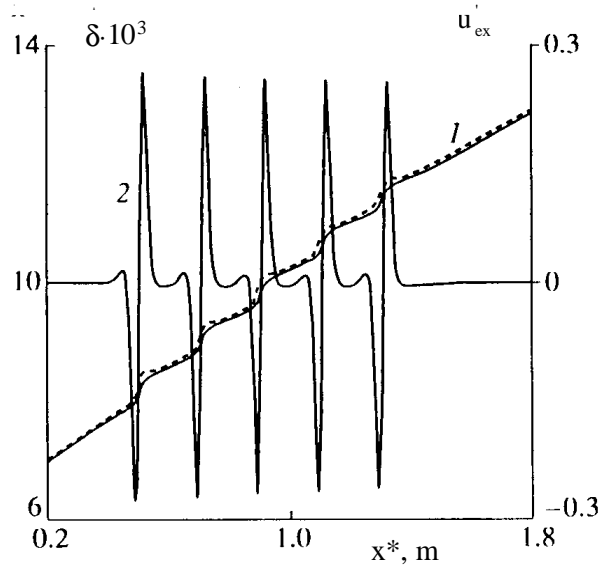


Fig.1.6. The distribution of (1) the displacement thickness of boundary layer and (2) velocity gradient on its external boundary for five heated portion [33].

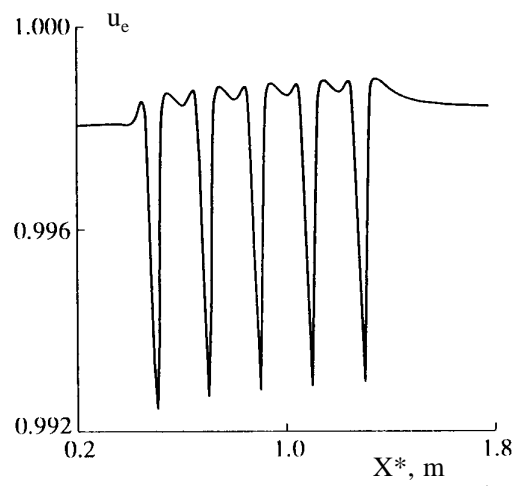


Fig.1.7. The distribution of the velocity of external nonviscous flow [33].

Fig.1.7 reflects the effect of the boundary layer on external supersonic flow [33]. As a result of periodic deceleration-acceleration, the maximum value of velocity of nonviscous flow increases slowly downstream.

Fig.1.8 gives the distribution of the local friction coefficient both ignoring (dashed curve) and including (continuous curve) the interaction for five heated portions [33]. The dot-and-dash curve indicates the distribution of the friction coefficient on the adiabatic surface. No qualitative changes are observed in the behaviour of  $C_f$  as compared with the case of a single heated portion.

From the obtained in [33] results one can make conclusions that the interaction between turbulent boundary layer and supersonic flow has a considerable effect on both local and integral friction. This effect increases with the power of heat input to the gas. In optimizing the thermal method of reducing turbulent friction, based on local heat input to the boundary layer, the viscous-nonviscous interaction must be included.

### **1.3. Surface microwave discharge**

One of the ways for obtaining of a stable plasma column of considerable length in a large range of gas pressures and in a big diapason of frequencies is use of the surface electromagnetic wave of the microwave region. In cycle of papers [40-46] the problems bound up with creation of surface high-frequency and microwave discharges and study of their properties are considered. The plasma was formed in a discharge tube, the energy was supplied with the help of a wave guide through the special device - surfatron.

In a microwave surfatron the discharge represents a plasma waveguide on which the surface wave supporting ionization of gas is distributed. Thus for a wide range of frequencies it is possible to receive a plasma column of significant extent and forms determined by a dielectric wall limiting the discharge. A high electron concentration (exceeding critical density) and its appreciable unhomogeneity in a direction of a surface wave distribution are main feature of such discharge. It is known [41,42] that at creation of the high-frequency and microwave discharges inside dielectric tube filled by gas at low pressure, the electromagnetic energy delivered to system is transformed to a surface wave. Thus, there is a self-sustaining system when a plasma medium created by the surface wave is necessary for a surface wave existence, i.e. the presence of plasma is a necessary condition for spreading of a surface wave. The surface wave is travelled in space so long as its energy is sufficient for creation of plasma with an electron density no less than a critical value. Sufficient microwave absorption for plasma generation can only be

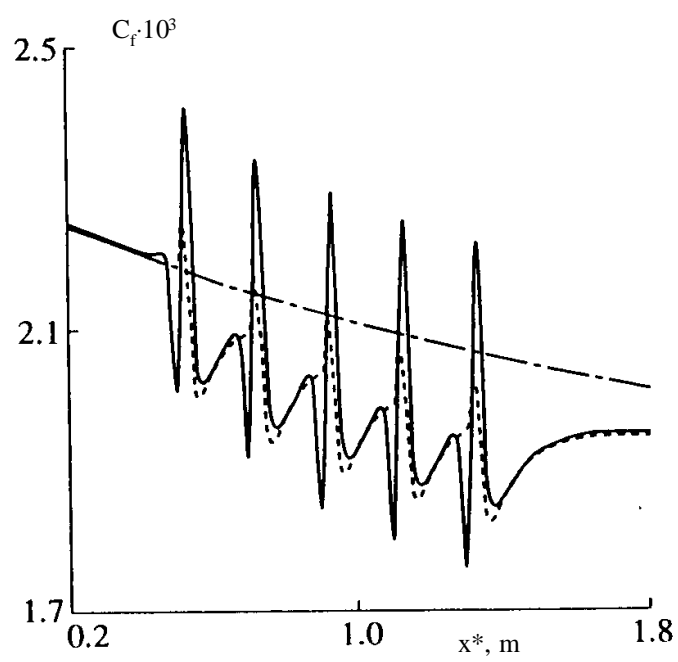


Fig.1.8. The distribution of the local friction coefficient for five heated portion [33].

achieved for overcritical electron densities  $n_e > n_c$ . The critical density is determined by the angular frequency of the electromagnetic field  $\omega$  and the permittivity of the free space  $\epsilon_0$  :

$$n_c = m_e \epsilon_0 \omega^2 / e^2 \quad (1.4)$$

( $e$  and  $m_e$  are the electron charge and mass, respectively). This way of plasma production and device for its creation refer to as a surfatron.

The feature of such kind of the surface discharge is the longitudinal density gradient  $dn_e/dz$  of electrons. It is explained by a consecutive supply of a microwave energy to different segments on its length. At not too small gas pressure a high electron concentration and its longitudinal gradient should give in considerable non-uniform heating of gas. This heating leads to change of the reduced gas density and, therefore, of kinetic coefficients in plasma. The energy balance in the discharge changes also.

The paper [47] is specially focused on large area microwave plasma. It briefly reviews recent results in the field. Only their basic principle are analyzed. The discharges are classified according to operating principle: large diameter plasma, radiating structures and based on evanescent waves structures. Basic properties and operating conditions are described. Most of these structures have been designed as plasma reactors dedicated to plasma material processing.

Interest for plasma processes strongly increased in the 90's particularly considering the microwave plasma. A very large variety of applications is investigated as materials processing, plasma processing, plasma chemistry, depollution... New plasma sources have been designed for use in such applications. At low (or medium) pressure, microwave plasma produce high densities of charged particles and further they exhibit exciting qualities for the manufacturer as versatility (without contamination), improved throughput and reduced processing cost. Surfaguides have been extensively reported [48-57] but only a few recent papers dealt with the production of large plasma [58-60].

The paper [61] discusses basic concepts of slotted waveguide microwave plasma excitation which is technically very reasonable for the generation of long extended and large area plasmas. Results of different experiments aimed at the details of the spatial plasma structure are reported for an improved version of slotted waveguide plasma excitation which allows maximum suppression of plasma homogeneity limiting effects.

Microwave plasma generation is determined by the specific propagation properties of microwaves and by their strong absorption in the plasma. This is of special importance for plasmas with dimensions comparing to or exceeding the microwave free space wavelength. In a comprehensive comparison of radio frequency and microwave plasma reactors Moisan et al.



pointed out that regarding a constant power density operation it is always better to operate at high frequencies for processes with a threshold energy below about half that for ionization [62].

To generate a plane wavefront, a field antenna with characteristic dimensions comparing to the microwave window dimension has to be operated under far field conditions. Far field conditions are characterized by the relation

$$r_o > 8(r_s^2 / \lambda_o) \quad (1.5)$$

with  $r_o$  is distance between source and microwave window,  $r_s$  is characteristic source dimension, and  $\lambda_o$  is the wavelength in free space [63]. Following this, a setup is necessary which is extremely space consuming. Further, shielding against leaky waves which is needed for security reasons will be a problem. It needs additional space and can cause unwanted waveguiding effects disturbing plane wave propagation. A much more appropriate solution to spread microwave power over a large plasma area is to use waveguiding structures which are directly coupled to the plasma.

A very convenient method often used method for power spreading are slotted waveguides. Slotted waveguides are in widespread use for waveguide couplers and antennas. The basic problem of spreading microwave power over large plasma areas is the compensation of power losses due to absorption. For the linear slow wave structures a small tilt between structure and vessel was used to improve plasma homogeneity. For slotted waveguides the use of resonance effects [64, 65] and tuning of the power coupling efficiency of the slots [66, 67] is reported.

However, in any case slotted waveguides are inhomogeneous waveguides by principle. Characteristic dimensions of the slotted waveguides compare to characteristic dimensions of power transfer to the plasma. The question is to which extend this discreteness of the coupling slots will limit the generation of homogeneous plasmas.

The interesting effect of a slot in a waveguide wall is that it may interrupt surface currents on the inner side of the waveguide wall. This way an electric field can be formed in the slot which can leak out or radiate to the surrounding. The level of the radiated power, its radiation pattern and its feedback on the waveguide depend on size and location of the slot and on the type of transmission mode in the waveguide. Here only a brief summary necessary for basic understanding is given. It refers to the case of slots in the broad plane of a rectangular waveguide with  $H_{11}$  - transmission mode [68]. The situation for a general inclined-displaced slot is illustrated in Fig.1.9 [61].

A single narrow rectangular slot acts like a dipole radiator. When the slot has been tuned

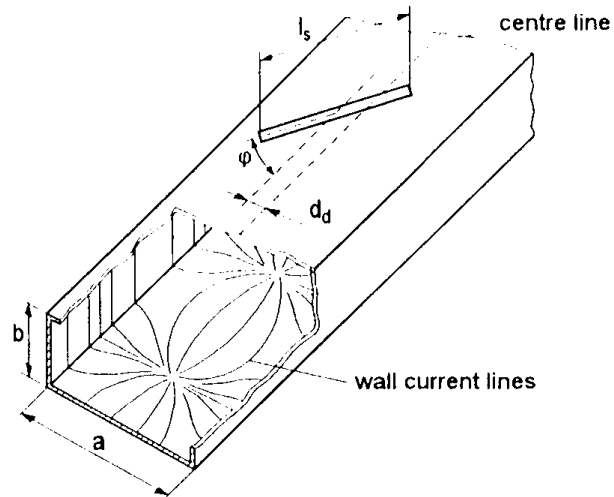


Fig.1.9. Scheme of a section of a slotted rectangular waveguide showing a general inclined-displaced slot.  
On the inner walls the wall current distribution for  $H_{10}$  - mode traveling waves is indicated [61].

by cutting to a length  $l_s$ , close to one half of the free space wavelength  $\lambda_o$  it is resonant and presents a pure resistance to the wave. Therefore, it has no influence on the phase velocity of wave propagation. A longitudinal slot ( $\phi=0$ ) presents a shunt load. It is excited by the transverse component of the surface current in the inner side of the waveguide wall. This means that it remains unexcited if the displacement  $d_d$  to the center line of the broad face is zero. The transverse component  $j_{st}$  of the surface current increases with the distance  $d_d$  to this line ( $j_{st} \approx \cos \pi x / a$ ) and, therefore, the power coupling increases ( $\approx \cos^2 \pi x / a$ ). A transverse slot symmetrically cut in the broad face ( $\phi=90^\circ, d_d=0$ ) is excited by the longitudinal component of the surface current. It presents a series load to the wave in the waveguide. It may be rotated about its center and still remains a series load while the coupled power varies from zero (at  $\phi=0$ ) to maximum (at  $\phi=90^\circ$ ).

Since resonant slots present pure resistances they have no influence on the phase velocity of wave propagation in the waveguide. This is the reason why they are often used to construct antenna arrays. If the single slots are in phase, the radiation pattern formed by the superposition of the single slot dipole pattern has a maximum in the direction normal to the broad plane of the waveguide can be obtained. This is the case for slots which are arranged at a distance of about one half of the wavelength in the waveguide  $\lambda_h/2$ . If an even number of slots are arranged at distances of a quarter wavelength  $\lambda_h/4$  the array radiates in the forward direction of the wave, basically. Similarly, directional waveguide couplers can be constructed on the basis of resonant slots which transmit power in the forward direction only.

In the simplest case the dimensions of slotted waveguides used for microwave discharge excitation are similar to linear-array slotted waveguide antennas for radiating waves [69]. The only difference is that a discharge vessel with a microwave transparent wall is placed parallel to the waveguide at a certain distance  $d_g$  which is short compared to the far field condition. This way, the antenna becomes a nearly perfect transmission line applicator.

Slotted waveguide microwave applicators are intended to generate large area long extended plasmas. Therefore, large microwave windows with considerable thicknesses are necessary. Especially, if these windows are inserted in a conducting vessel wall they can act as an additional waveguide which is now inserted between the waveguide face and the plasma and which can be resonant.

Another design problem for long linear microwave field applicators and, therefore, also for slotted waveguide microwave applicators is to get a long extended plasma with maximum

homogeneity. Special care has to be taken to ensure homogeneous power distribution since power absorption along the waveguide is not negligible. In this context, it is necessary to subdivide between two configurations of the waveguiding, power distributing field applicators, the one which carries standing waves and the other which carries travelling waves. The travelling-wave structure is terminated by a matched load. The standing-wave structure is terminated by fully reflecting, usually tunable, loads. Both configurations possess advantages and disadvantages.

There are different methods to improve slotted waveguide applicator performance. It is well known, that external static magnetic field can be used to control the homogeneity of microwave plasma. The use of magnetic fields, however, is limited to lower pressures  $<0.1$  mbar. At higher pressures the electron cyclotron resonance effect is suppressed by collisional damping. Therefore, other means to influence plasma homogeneity are necessary.

Yasui et al. [65] describe a standing-wave applicator where an adjustable T-shaped ridge is inserted in the slotted waveguide. It is used to control the electromagnetic field pattern in the waveguide.

Another method to improve the performance of standing-wave applicators is the use of closed loop waveguides. This has the advantage that standing wave modes with very regular power distribution to the single slots can be obtained. In [64,70] a setup using circular waveguides with circumferential lengths of the middle line of the cavity of about integer multiples of the waveguide wavelength is described.

The examples reported in [64, 67, 69, 70] indicate that an appropriate arrangement of the gap between slotted waveguide face and discharge vessel surface is of great importance for the obtained plasma distribution. It is, therefore, strongly recommended to use microwave applicators which exhibit well defined microwave propagation properties in this gap. A traveling-wave applicator where this is realized was first described in [66].

The basic problem of large area homogenous microwave plasma generation is to avoid inhomogeneous power coupling. This concerns the scheme of power distribution over the whole plasma area and the localization of power absorption in the plasma. An ideal microwave applicator should generate a microwave field distribution which is homogeneous over the entire microwave window. It was the aim of the development of the so called "planar microwave plasma applicator" to adapt the technical advantages of slotted waveguide power distribution to this requirement. The design of this applicator is based on a principle of distributed and tunable coupling of microwave power in conjunction with the use of an additional smoothing waveguide which supports homogeneous plasma excitation. In Fig.1.10 and Fir.1.11 the technical

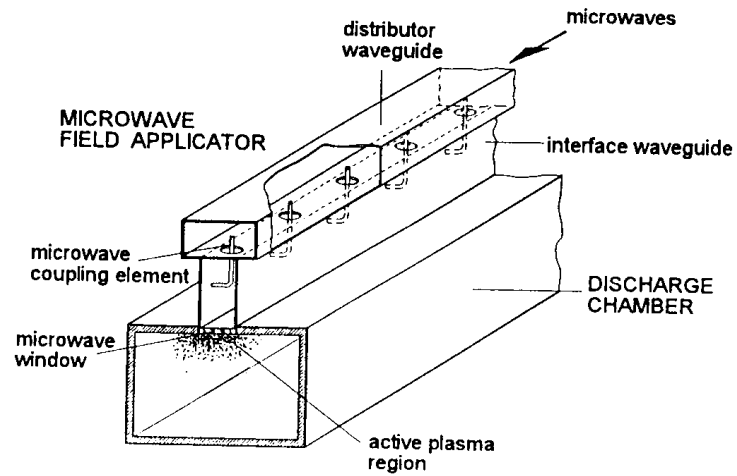


Fig.1.10. Schematic description of a planar microwave plasma source with a modified slotted waveguide microwave field applicator consisting of two rectangular waveguide in T-shape configuration [61].

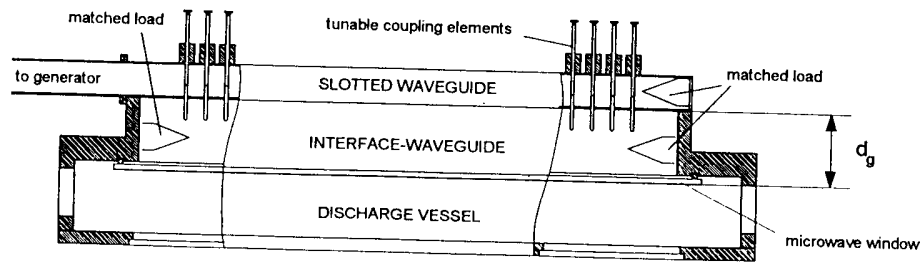


Fig.1.11. Scheme of the side view of a long planar plasma source with the modified slotted waveguide applicator described in Fig.1.10 [61].

realization of this principle using two rectangular waveguides in T-shape configuration is described schematically. A modified traveling-wave slotted waveguide is used to distribute microwave power over the desired length. Instead of rectangular slots coupling holes at distances of  $\lambda_h / 4$  are used. These holes contain movable metallic hooks which improve the efficiency and the tuning range of power coupling considerably. Since the hooks are polarized elements, they can be used to determine the orientation of the coupled microwave field.

Microwaves coupled to this additional, so called "interface waveguide" can propagate in both directions to the ends of the applicator. These ends are terminated by matched loads which are located above the ends of the microwave window to avoid resonance effects of the window slot. Following this, only travelling waves exist in the interface waveguide. This way, a smoothing effect is obtained. At each position of the waveguide, field components originating from different coupling points superpose to a complex wave package without any interferences. Therefore, for positions between the coupling points the effect of power losses due to the strong absorption in the plasma can be reduced. Further, power losses of the wave in the distributing waveguide can be compensated by tuning of the coupling hooks. This way, a good plasma homogeneity over the whole length of the plasma can be obtained.

Finite-area plane microwave plasma source has been designed by H.Sugai and coworkers [71]. A pair of slots formed on a waveguide base plane couples the microwave power (2.45 GHz – 1 kW) to the plasma as shown in Fig.1.12. These two slots (width = 10 mm and length = 61 mm = half a wavelength) are separated by 79.6 mm, a half of guide wavelength. Angle of slots with respect to the waveguide axis is  $27^\circ$  (matching of the radiation resistance with the characteristic resistance of the guide). Slots plane is separated from the cylindrical plasma chamber (diameter = 22 cm) by a 17 mm thick quartz window. Plasma is created in argon in the range 20 to 350 Pa (gas flow is 715 sccm). Axial field distribution is found quasiconstant from the quartz window surface ( $z=0$ ) at low density over 8 mm and sharply decreasing as the electron density becomes higher than the critical one ( $7.4 \cdot 10^{10} \text{ cm}^{-3}$ ). The measured electron temperature is  $T_e \sim 2 \text{ eV}$  for these high density plasma. As these surface waves are evanescent in the axial direction and propagate in the  $r-\theta$  directions on a large plasma surface, the surface wave excitation from small slots antennas would provide a new method for production of large "flat panel" plasma.

The SLAN structure proposed by J.Engemann [72] is based on the principle of a slotted radiating guide whose the slots are perpendicular to the waveguide axis. But SLAN system consists of an annular waveguide, called a ring resonator, whose slots antennas are parallel to the

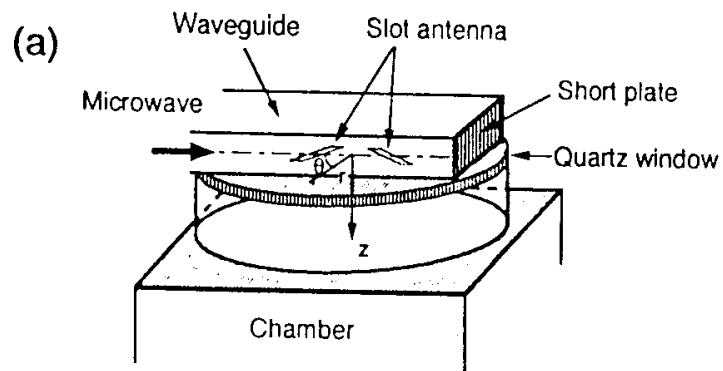


Fig.1.12. Finite area planar microwave plasma [71].

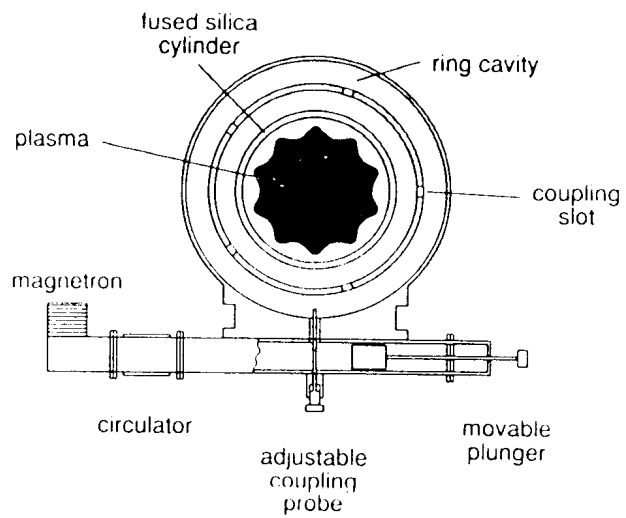


Fig.1.13. SLAN structure. Chamber diameter = 16 cm [72].

ring axis and positioned at regular intervals. Basic structure (Fig.1.13) is such the middle line of the annular waveguide has a circumferential length of five waveguide wavelengths. Five coupling slots are on the inner side of the ring resonator and are half of a free-space wavelength long. Diameter of the ring is chosen to develop a standing  $TE_{10}$  wave inside. Plasma tube is positioned inside and coaxially to the ring. A coupling probe transfers the magnetron power to the ring and its distance from the nearest slot is a quarter of waveguide wavelength. Hence, the standing wave nodes of the electric field are at the slots positions and, in vacuum, each slot antenna constructively interfere forming in the plasma chamber a  $TE_{51}$  mode as in a cylindrical cavity.

The all structures producing large diameter plasma exhibit several common features. They are multimodes structures, nevertheless the plasma is produced along a dominant mode which is determined by the applicator geometrical configuration, the microwave power and the pressure. The spatial distribution of the microwave power is never homogeneous, hence the homogenization of the plasma strongly depends on the diffusion efficiency. As a consequence, increasing the plasma diameter requires lower operating pressures. In all structures, an appropriate magnetic field can be added either for obtaining the ECR conditions or only a plasma confinement.

General principle of the radiating structures is based on gas ionization by a radiated wave. This wave is produced either by slots or by antennas, the excitator being designed in such a way as every slot antenna is radiating the same power. Further, the dimensions of the plasma chamber are much larger than the wavelength of the radiated wave. Hence, on the opposite of the large diameter plasma, no eigenmodes can occur and the microwave field distribution does not depend on the chamber geometry. We briefly present four of these structures.

Fig.1.14 shows the principle of the planar microwave plasma source. It consists of two waveguides arranged parallel to each other in a T-shape cross-section configuration. Waveguide 1 is a guide on one end and is connected with the microwave generator on the other end with a matched load. Waveguide 2 is connected at both ends to matched loads. Coupling of microwave power from guide 1 to guide 2 is obtained by means of radiating antennas shaped into hooks. These hooks act as discrete adjustable coupling elements distributed along the guides and enable the ignition of an homogeneous plasma provided the elements yield the same power (radiated waves from every element overlap to an integral field distribution of nearly constant amplitude over the whole plasma length). Obviously, the lower side of guide 2 is replaced by a quartz window separating it from the plasma vessel, the plasma itself acting as a conducting wall. The structure operates at 2.45 GHz, in the pressure range 1 Pa to 10 kPa with argon, hydrogen plasma



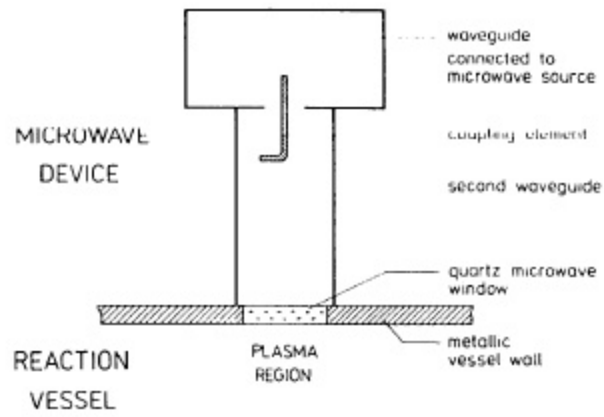


Fig.1.14. Planar microwave plasma source [47].

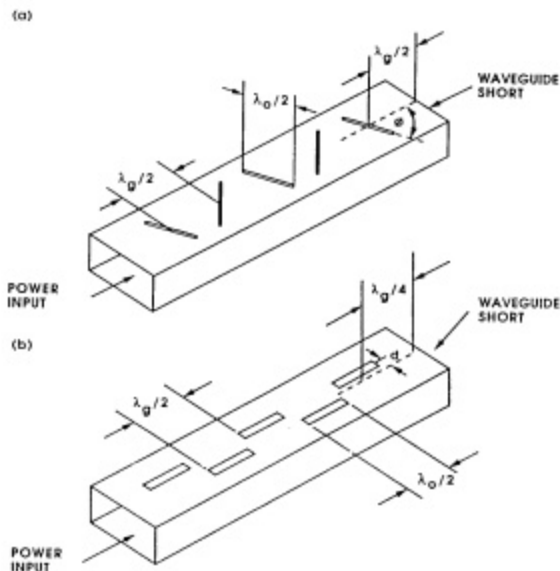


Fig.1.15. Resonant field applicators [47]

- (a) array of centred, inclined series-slots in the broad wall of a waveguide
- (b) array of longitudinal shunt-slots placed off the centre line of the broad wall of a waveguide.

with power ranging from 0.1 to 1 kW. Gases are injected near the quartz window with maximum flows of  $10^3$  sccm. Homogeneity better than 5% has been obtained over 30x100 cm plasma. It is expected that scaling-up to 200 cm could be obtained.

Fig.1.15 shows the principle of the resonant field applicators. A waveguide terminated by a short-circuit plane establishes a standing wave within it. It delivers power to the plasma by means of slots at positions closely correlated to the standing wave pattern. The configuration of the slots ensures that the phase of the field radiated by each slot is the same yielding a broadside radiation pattern. The slots are located at minima or maxima of the electric field and their dimensions ensure that slots susceptance or reactance vanishes at the operating frequency (so-called resonant slots). Two such configurations are shown in Fig.1.15. The length of each slot is one half of the free-space wavelength  $\lambda$  (hence the resonance) and the slots are spaced one half of the waveguide wavelength  $\lambda_g$ . In Fig.1.15 a, the applicator aperture consists of an array of centred, inclined series-slots in the broad wall of the waveguide, the short-circuit being located  $\lambda_g/2$  past the last slot in the array. In Fig.1.15 b, the aperture consists of longitudinal shunt-slots placed off the centre line of the broad wall of the guide, the short-circuit being located  $\lambda_g/4$  past the last slot in the array. More details could be found in [73, 74].

Gigatron and Duoplasmaline structures are described in more details in [75]. Gigatron is an example of structure based both on radiating structures principle and propagation of evanescent surface waves. As shown in Fig.1.16, it consists of an inner copper rod surrounded by a quartz tube filled with atmospheric pressure air. The rod radiates the microwave power coming from a coaxial line (supplied by a 2.45 GHz magnetron) the centre conductor of which is the rod. Either one or two magnetron sources can be used giving the name of "Gigatron" or "Duoplasmaline". The radiated wave yields an evanescent surface wave which propagates along the dielectric interface. The strong absorption of the wave yields the gas ionization in the surrounding chamber. As for surface waves produced plasma, the plasma length depends on the microwave power. Therefore, with the Gigatron, the plasma density decreases along the tube whereas this axial decrease is compensated by the use of two magnetron sources with the Duoplasmaline.

Two types of structures based on evanescent waves are described [76-78]. Surface wave along a dielectric line applicator is schematically shown in Fig.1.17. A rectangular microwave waveguide is ended by a fluorocarbon polymer sheet covering an aluminum plate and they consist the dielectric line. The wave coming from the guide generates a surface wave which

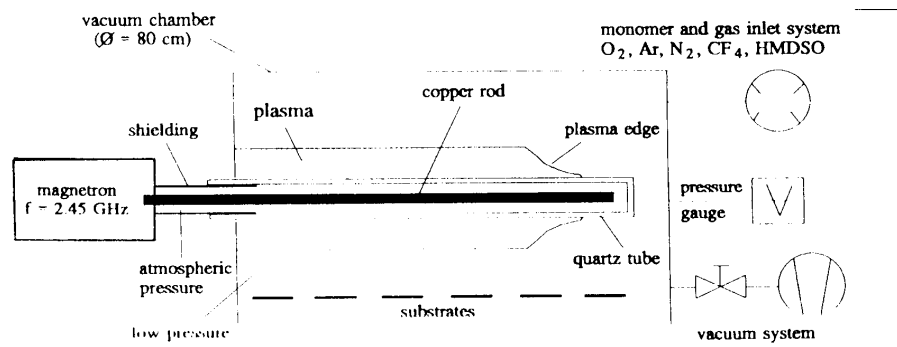


Fig.1.16. Duoplasma line structure [75].

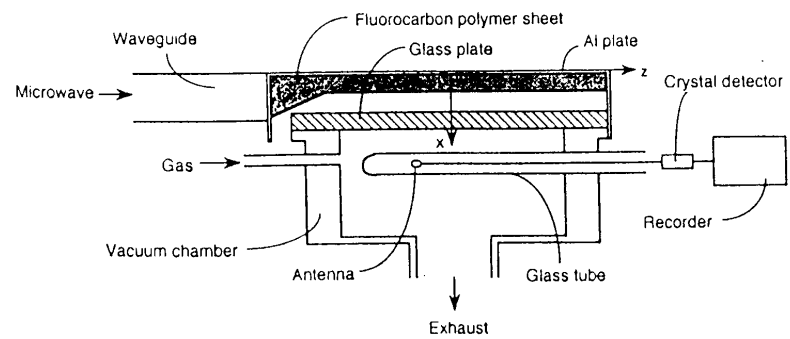


Fig.1.17. Structure of the surface wave dielectric line [76].

propagates along the dielectric line. This wave couples the microwave power to the gas chamber via the evanescent field along the glass window separating the line from the plasma chamber. Profiles of the electric field in the chamber exhibit a standing wave pattern imposed by the chamber walls. Although this pattern is complex, it has been found a good agreement with computations assuming, in a first approximation that the chamber is a rectangular guide where the microwave mode is a complex mode consisting of  $TM_{4m}$  and  $TM_{6m}$  without plasma. Almost the all microwave power is absorbed near the microwave window producing a  $180 \times 300 \text{ mm}^2$  plasma, the pressure ranging in the 10 to 100 Pa.

The coaxial-type open-ended dielectric cavity structure, shown in Fig.1.18 is described in more details in [79]. The microwave power of a  $TE_{10}$  mode within a rectangular guide is coupled to a TEM coaxial waveguide mode in the same way as in rectangular coaxial transitions. Coaxial guide is then widened and funnel-shaped upside-down. The bottom of this part is opened on a coaxial-type cavity whose typical dimensions of inner and outer diameters 199 and 254 mm respectively. At the open end of the coaxial-type cavity is placed a Pyrex window of 20 mm thickness and 175 mm diameter in contact with the inner conductor. Finally, the cavity gap runs into the circumferential side of the Pyrex window. Accounting for the cylindrical TEM mode propagating in the coaxial guide, the Pyrex window is the dielectric line in which microwave propagate from the edge towards the centre. Therefore, the surface wave radiates into the chamber. The microwave power decreases from the edge towards the centre but the waves interfere with another as they are circularly propagated nearly yielding uniform electric field on the window surface, hence generating uniform plasma. This structure produces argon plasma in the pressure range of 10-300 mTorr with densities of the order of  $10^{11}$ - $10^{12} \text{ cm}^{-3}$ , typical microwave power being 500 W.

The examples of structures we have briefly reviewed show that most of them are based on surface wave excitation principle, radiated or evanescent waves coupling or a combination of them. In many cases, the structure is a multimodes one and it finally operates on a specific mode depending on the matching conditions or the resonant conditions which are used. In any way, we have seen that the design of the structure is really depending on the wanted plasma configuration accounting for the aimed application.

Nevertheless, regarding the main characteristics of these structures, we have observed, in all cases, that a threshold power is required in order, at least, to generate a plasma filling the chamber. This threshold particularly depends on the power balance, say, the  $\theta/N$  parameter where  $\theta$  is the mean power for electron-ion pair maintaining and  $N$  is the neutral density. Concerning the plasma homogeneity, the overcoming difficulty is the general inhomogeneity of

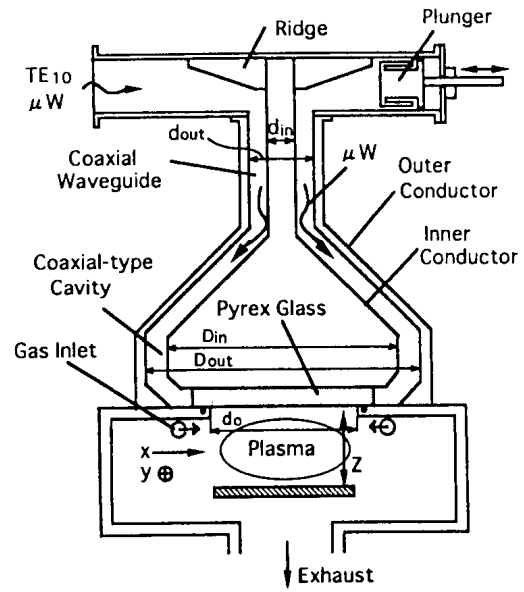


Fig.1.18. Coaxial-type open-ended dielectric cavity [79].

the electric field. Therefore, many innovative devices have been conceived to yield nearly homogeneous distribution of the electric field. The plasma homogeneity is then obtained decreasing the pressure toward the low pressure range provided the plasma diffusion length is larger than the inhomogeneity length of the field.

## CHAPTER II

### PHYSICAL MODEL OF THE MICROWAVE DISCHARGE ON A DIELECTRIC ANTENNA SURFACE

#### 2.1. Introduction

The microwave discharge on a dielectric antenna surface being flown about can be used for boundary gas layer modification, changing gas flow in the antenna vicinity. For understanding of the physical processes taking place in such kind of the discharge the mathematical model of the surface microwave discharge should be worked out and the theoretical analysis should ensure the following results:

(•) the calculation of the dispersion curves of a surface wave taking into account inhomogeneity of a plasma layer (self-consistent solution with the ionized non-linearity);

(••) the calculation of a field penetration depth in plasma and thickness of a plasma layer created by both direct and reflected surface waves, in dependence on wave amplitude and frequency, and also gas pressure and airflow velocity;

(•••) the dependence of longitudinal length of the discharge supported by a surface wave from power, transferred by a microwave;

(••••) the analysis of requirements of electromagnetic waves reflection from antenna butt-end at the different shape of the latter;

(•••••) the analysis of two dimensional field structure in a plane of the antenna.

The geometry of installation, in which the microwave discharge is created, is given in Fig.2.1. A microwave energy forming plasma is supplied to one edge of a dielectric antenna. The direction of the supersonic gas flow reverses the direction of the microwave spreading. At the initial moment the plasma forms by strong microwave fields at the boundary between waveguide and antenna. Then the plasma starts to propagate along the antenna covering only its part surface at small power (Fig.2.2), or its entire surface at high microwave power (Fig.2.3). Electron plasma density (marked by 4 in Fig.2.2 and Fig.2.3) in a steady-state mode exceeds critical density that enables an electromagnetic field to propagate along plasma as a surface wave. The electromagnetic field penetrates into plasma on distance of the order  $c/\omega_{pe}$  ( $c$  is the light velocity,  $\omega_{pe}$  is the electron plasma frequency), therefore plasma exists as a flat sheet near antenna. The sheet thickness depends on microwave wave power, energy transfer and diffusion

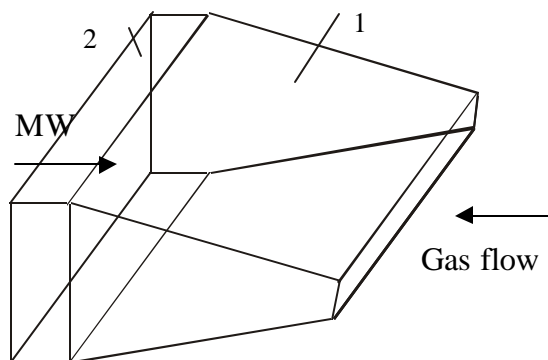


Fig.2.1. Installation for creation of microwave discharge on antenna surface.

- 1 – Dielectric wave-guide antenna
- 2 – Waveguide carrying microwave

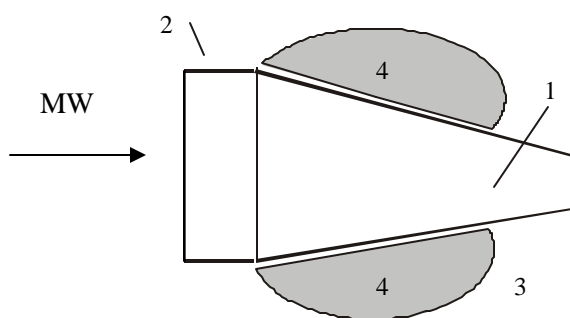


Fig.2.2. Structure of surface discharge at small power of microwave.

- 1 – Dielectric wave-guide antenna
- 2 – Waveguide carrying microwave
- 3 – Non-ionized gas
- 4 – Space, occupied by plasma.

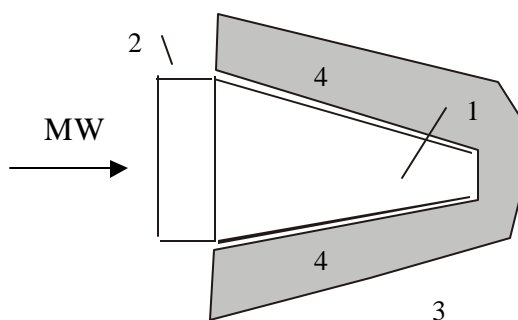


Fig.2.3. Structure of surface discharge at high-power of microwave.

- 1 – Dielectric wave-guide antenna
- 2 – Waveguide delivering microwave
- 3 – Weakly ionized gas region
- 4 – Plasma region



coefficients in plasma. At a large distance from the antenna the electric field absents, therefore electrons intensively disappear due to attachment. In this area (marked by 3 in a Fig.2.2 and Fig.2.3) the electrons density is small (usually plasma in this area forms by photoionization).

In surveyed model the gas flow in the antenna vicinity is considered to be given. The discharge influence to gas flow (for example, owing to a neutral heating by discharge) is not taken into account.

## 2.2 Complete set of equation for discharge description

### 2.2.1. Maxwell equations

The mathematical model grounded on set of Maxwell equations

$$\text{rot} \vec{E} = -\frac{1}{c} \frac{\partial \vec{B}}{\partial t}, \quad (2.1)$$

$$\text{rot} \vec{B} = \frac{1}{c} \frac{\partial \vec{E}}{\partial t} + \frac{4\pi}{c} \vec{j}, \quad (2.2)$$

$$\text{div} \vec{E} = 4\pi e \rho, \quad (2.3)$$

$$\text{div} \vec{B} = 0, \quad (2.4)$$

and equations of charged and neutral particles kinetics. Here  $\vec{E}$  and  $\vec{B}$  are electric and magnetic field intensity,  $\vec{j}$  is electric current density and  $\rho$  is density of a space charge. We shall consider that the frequency of microwave, supporting plasma, is much greater then the frequency of inelastic collisions and reverse time of energy exchange between electrons and neutrals and character size of a microwave field inhomogeneity is much greater then thermal conductivity length  $\lambda_{Te} = \lambda_e (M/2m)^{1/2}$ , where  $m$  and  $M$  are electronic and ion masses,  $\lambda_e$  is the mean electron free path. In this case we can consider that electrons temperature will be local function of coordinate and it is quasistationary function of time. The plasma can be considered as quasistationary medium with time, but without a spatial dispersion, with slow time-dependent dielectric permittivity, that means  $\partial \ln(n_e)/\partial t \approx \nu_i \ll \omega$ . ( $\nu_i$  is ionization frequency). Thus, the microwave field in plasma will be harmonic:

$$\vec{E}(\vec{r}, t) = \tilde{\vec{E}}(\vec{r}, t) \exp(-i\omega t), \quad (2.5)$$

$$\vec{B}(\vec{r}, t) = \tilde{\vec{B}}(\vec{r}, t) \exp(-i\omega t). \quad (2.6)$$

Therefore the equations (2.1-2.4) can be rewritten as following equation:

$$\text{rot} \tilde{\vec{E}} = \frac{i\omega}{c} \tilde{\vec{B}}, \quad (2.1')$$

$$\text{rot} \tilde{\vec{B}} = -\frac{i\omega}{c} \epsilon(\omega, \vec{r}) \tilde{\vec{E}}, \quad (2.2')$$

$$\text{div} \epsilon(\omega, \vec{r}) \tilde{\vec{E}} = 0, \quad (2.3')$$

$$\text{div} \tilde{\vec{B}} = 0, \quad (2.4')$$

where  $\epsilon(\omega, \vec{r}) = 1 - \frac{4\pi n_e(\vec{r}) e^2}{m\omega(\omega + i\nu_{en})}$ ,  $\nu_{en}$  – collision frequency between electrons and charged

particles,  $e > 0$  – elementary electric charge,  $n_e(\vec{r})$  – density of electrons.

The similar approach is usual for microwave discharge calculation [1-6], the large list of paper is given in [2], [24].

The alternate approach, grounded on a numerical integration of Maxwell equations during a field period [5], essentially increases volume of calculation and is justified in a case when it is necessary to take into account non-linear electromagnetic field interactions (for example, microwave field rectification in space charge layer on plasma boundary). This method can be used for discharge modelling in specific regimes.

### 2.2.2. Kinetics of charged particles without negative ions

To determine of the spatial distribution of plasma density it is necessary to solve the kinetics equations for electrons, ions and neutral excited particles. As it was shown these equations are essentially various in plasma (where characteristic length of inhomogeneity more than Debye radius) and in weakly ionized gas (where the reverse condition takes place).

In first case we have to take into account:

1. Direct and step ionization of atoms (molecules) by electron impact,
2. Atoms and molecules exciting by electron impact,
3. Ionization at heavy particles collisions,
4. Dissociative recombination.

The time-space evolution of charged particles density is determined by the balance equation ( $n_e = n_i = n$ )

$$\frac{\partial n}{\partial t} + \text{div} (n \vec{C}_S) - \vec{\nabla} D_a \vec{\nabla} n = F(n, T_e). \quad (2.7)$$

The equation (2.7) describes plasma density distribution in all space except for a space charge layer and Knudsen's layer near to antenna surface. In the formula (2.7) the denotation for an ambipolar diffusion coefficient

$$D_a = \frac{\mu_e D_+ + \mu_+ D_e}{\mu_e + \mu_+} \quad (2.8)$$

is used. The electron  $\vec{G}_e = n_e \vec{V}_e$  and ion  $\vec{G}_+ = n_+ \vec{V}_+$  current satisfy the equations.

$$\vec{G} = \vec{G}_e - \vec{G}_+ = 0. \quad (2.9)$$

$$\vec{G}_e = \vec{G}_+ = n_e \vec{C}_S - D_a \vec{\nabla} n_e.$$

The relation (2.9) assumed, that plasma has no electric current, that can be created only by external electrodes. In (2.7)–(2.9) and below the denotations  $V_e$ ,  $V_+$ ,  $C_S$  are velocities of electrons, ions and neutrals,  $\mu_e$  and  $\mu_+$  are mobilities of electrons and ions,  $D_e$  and  $D_i$  are coefficients of a free electron and ion diffusion,  $e$  is elementary electric charge,  $E$  is electric field strength in plasma,  $F$  is expression for sources of electron and ions which are taking into account that they are born only by pairs. The items, containing  $C_S$ , take into account motion of a gas stream concerning antenna resulting in to ions and electrons drift downstream. The standard expression for  $F$  is

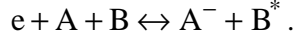
$$F = \nu_i n_e - \alpha n_e n_+ - \beta n_e^2 n_+. \quad (2.10)$$

The expression (2.10) takes into consideration a direct ionization by electronic impact ( $\nu_i$  is frequency of ionization), and two- and three-particles recombination ( $\alpha$  and  $\beta$  are recombination coefficients). Frequency of ionization and the recombination rates are functions of temperature of electrons. At recording of equation (2.9) we have limited by slow processes with typical frequencies less then ion-neutral collision frequency. It is possible because the character time of electrons density change is determined by ionization frequency and it is usually on some order below.

### 2.2.3. Kinetics of charged particles with negative ions

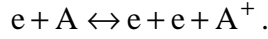
The set of equations, used in 2.2.1, satisfactorily describes processes in steady discharge at high electron density. For the description of formation of a transversal profile of electron density and discharge propagation along the antenna the kinetics of electrons at small density, which should take into account attachment-detachment reaction, will play essential role.

The majority of reaction including negative ions can be described by the scheme <sup>1</sup>



Constants of a forward reaction (attachment) and reverse reactions (detachment) we designate  $k_a$  (dimension -  $\text{cm}^3/\text{s}$ ) and  $k_d$  ( $\text{cm}^6/\text{s}$ ). Except for attachment and detachment we take into account also recombination positive and negatively ionized atoms (reaction constant  $\beta_+$  ( $\text{cm}^6/\text{s}$ )) Density of negatively charged ions we designate  $n_-$  and their current density -  $\vec{G}_-$

In the given paragraph we use also  $v_i$  ( $\text{cm}^3/\text{s}$ ) and  $\beta$  ( $\text{cm}^6/\text{s}$ ) as notations for ionization constants by electronic impact and three-body recombination



Thus initial set of equations will accept a view:

$$\frac{\partial n_e}{\partial t} + \text{div} \vec{G}_e = (v_i N - \beta n_e n_+) n_e - (k_a N n_e - k_d n_-) N, \quad (2.11)$$

$$\frac{\partial n_+}{\partial t} + \text{div} \vec{G}_+ = (v_i N - \beta n_e n_+) n_e - \beta_+ n_e n_+, \quad (2.12)$$

$$\frac{\partial n_-}{\partial t} + \text{div} \vec{G}_- = (k_a N n_e - k_d n_-) N - \beta_- n_e n_-. \quad (2.13)$$

Electron  $\vec{G}_e = n_e \vec{V}_e$  and positive and negative  $\vec{G}_+ = n_+ \vec{V}_+$  and  $\vec{G}_- = n_- \vec{V}_-$  ion flows fit to equations

$$\vec{G}_e = n_e \vec{C}_S - \mu_e n_e \vec{E} - D_e \vec{\nabla} n_e, \quad (2.14)$$

$$\vec{G}_+ = n_+ \vec{C}_S + \mu_+ n_+ \vec{E} - D_+ \vec{\nabla} n_+, \quad (2.15)$$

$$\vec{G}_- = n_- \vec{C}_S - \mu_- n_- \vec{E} - D_- \vec{\nabla} n_-, \quad (2.16)$$

$$\vec{j} = e \vec{G} = e (\vec{G}_i - \vec{G}_e - \vec{G}_-), \quad (2.17)$$

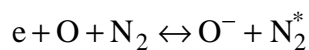
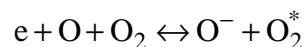
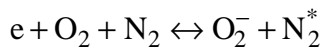
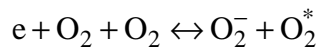
$$\text{div} \vec{E} = -4\pi e (n_e + n_- - n_+), \quad (2.18)$$

$$\text{rot} \vec{E} = 0. \quad (2.19)$$

In this system we take into account attachment and detachment of electrons (constant of reaction  $k_a$  and  $k_d$ ) and also recombination of positive and negatively ionized atoms.

---

<sup>1</sup> As an example it is possible to record reaction [42]



In the region of small electron densities ( $r_{De} \gg L$ ), the equations (2.11)–(2.18) yield:

$$\Delta\phi = 0, \quad (2.20)$$

$$\vec{E} = -\vec{\nabla}\phi, \quad (2.21)$$

$$\frac{\partial n_e}{\partial t} + \text{div} \left( n_e \vec{C}_S + \mu_e n_e \vec{\nabla}\phi \right) - D_e \Delta n_e = (v_i N - \beta n_e n_+) n_e - (k_a N n_e - k_d n_-) N, \quad (2.22)$$

$$\frac{\partial n_+}{\partial t} + \text{div} \left( n_+ \vec{C}_S - \mu_+ n_+ \vec{\nabla}\phi \right) - D_+ \Delta n_+ = (v_i N - \beta n_e n_+) n_e - \beta_- n_+ n_-, \quad (2.23)$$

$$\frac{\partial n_-}{\partial t} + \text{div} \left( n_- \vec{C}_S + \mu_- n_- \vec{\nabla}\phi \right) - D_- \Delta n_- = (k_a N n_e - k_d n_-) N - \beta_- n_+ n_-. \quad (2.24)$$

In a reverse limiting case ( $r_{De} \ll L$ ,  $n_e + n_- = n_+$ ,  $\text{div} \vec{G} = 0$ ) we have

$$\text{div} \left\{ ((\mu_e + \mu_+) n_e + (\mu_- + \mu_+) n_-) \vec{\nabla}\phi \right\} - (D_e - D_+) \Delta n_e - (D_- - D_+) \Delta n_- = 0, \quad (2.25)$$

$$\vec{E} = -\vec{\nabla}\phi, \quad (2.26)$$

$$\vec{j} = e \vec{G} = e \left( -((\mu_e + \mu_+) n_e + (\mu_- + \mu_+) n_-) \vec{\nabla}\phi + (D_e - D_+) \vec{\nabla} n_e + (D_- - D_+) \vec{\nabla} n_- \right), \quad (2.27)$$

$$\frac{\partial n_e}{\partial t} + \text{div} \left( n_e \vec{C}_S + \mu_e n_e \vec{\nabla}\phi \right) - D_e \Delta n_e = (v_i N - \beta n_e n_+) n_e - (k_a N n_e - k_d n_-) N, \quad (2.28)$$

$$\frac{\partial n_-}{\partial t} + \text{div} \left( n_- \vec{C}_S + \mu_- n_- \vec{\nabla}\phi \right) - D_- \Delta n_- = (k_a N n_e - k_d n_-) N - \beta_- (n_e + n_-) n_-. \quad (2.29)$$

On the contrary in this case both ambipolar field and field supporting a direct current appear not potential (contain a vortex component), though a general electrical field is potential. Therefore equation (2.25) includes expressions, keeping the second derivative of density of charged particles.<sup>2</sup>

<sup>2</sup> The alternate approach, founded on the introduction of a current vector-potential does not result in simplification of equations because the vortex electric current can exist in plasma without external electrodes, that follows from equation (2.30). In this case set of equations becomes

$$\text{rot} \left\{ \frac{\text{rot} \vec{A} + (D_e - D_+) \vec{\nabla} n_e + (D_- - D_+) \vec{\nabla} n_-}{(\mu_e + \mu_+) n_e + (\mu_- + \mu_+) n_-} \right\} = 0, \quad (2.30)$$

$$\frac{\partial n_e}{\partial t} + \text{div} \left( \vec{G}_e \right) = (v_i N - \beta n_e (n_e + n_-)) n_e - (k_a N n_e - k_d n_-) N, \quad (2.31)$$

$$\frac{\partial n_-}{\partial t} + \text{div} \left( \vec{G}_- \right) = (k_a N n_e - k_d n_-) N - \beta_- (n_e + n_-) n_-, \quad (2.32)$$

$$\vec{E} = \frac{\text{rot} \vec{A} - (D_e - D_+) \vec{\nabla} n_e - (D_- - D_+) \vec{\nabla} n_-}{(\mu_e + \mu_+) n_e + (\mu_- + \mu_+) n_-}, \quad (2.33)$$

The simplification of a set of equations is possible, if in plasma the electron conduction predominates  $(\mu_e + \mu_+)n_e \gg (\mu_- + \mu_+)n_-$ , or, that practically is equivalent,  $n_e \gg (m/M)^{1/2} n_-$ . In this case at the description of an ionic flow, neglecting an ionic diffusion and conductivity, we receive

$$\text{div} \{(\mu_e n_e) \vec{\nabla} \psi\} = 0, \quad (2.37)$$

$$\vec{E} = -\vec{\nabla} \psi - \frac{D_e}{\mu_e} \vec{\nabla} \ln n_e, \quad (2.38)$$

$$\begin{aligned} \frac{\partial n_e}{\partial t} + \text{div} \left( n_e \vec{C}_S + \mu_e n_e \vec{\nabla} \psi - \frac{(\mu_+ n_+ - \mu_- n_-) D_e}{\mu_e n_e} \vec{\nabla} n_e \right) = \\ = (v_i N - \beta n_e (n_e + n_-)) n_e - (k_a N n_e - k_d n_-) N \end{aligned} \quad (2.39)$$

$$\frac{\partial n_+}{\partial t} + \text{div} \left( n_+ \vec{C}_S - \mu_+ n_+ \vec{\nabla} \psi - \frac{\mu_+ n_+ D_e}{\mu_e n_e} \vec{\nabla} n_e \right) = (v_i N - \beta n_e n_+) n_e - \beta_- n_+ n_-, \quad (2.40)$$

$$\frac{\partial n_-}{\partial t} + \text{div} \left( n_- \vec{C}_S + \mu_- n_- \vec{\nabla} \psi + \frac{\mu_- n_- D_e}{\mu_e n_e} \vec{\nabla} n_e \right) = (k_a N n_e - k_d n_-) N - \beta_- (n_e + n_-) n_-. \quad (2.41)$$

In a reverse limiting case  $(\mu_e + \mu_+)n_e \ll (\mu_- + \mu_+)n_-$  ambipolar condition bind motion of positive and negative ions, at the same time electrons moves as free particles, as the reference value of an ambipolar potential will be equal to  $k(T_+ + T_-)/e$ . The set of equations will accept a view:

$$\text{div} (n(\mu_- + \mu_+) \text{grad} \psi) = 0, \quad (2.42)$$

$$\begin{aligned} \vec{G}_e = n_e \vec{C}_S - \frac{\mu_e n_e \text{rot} \vec{A}}{(\mu_e + \mu_+)n_e + (\mu_- + \mu_+)n_-} - \\ - \frac{(\mu_e D_+ + \mu_+ D_e) n_e + (\mu_- + \mu_+) D_e n_-}{(\mu_e + \mu_+)n_e + (\mu_- + \mu_+)n_-} \vec{\nabla} n_e + \frac{\mu_e n_e (D_- - D_+)}{(\mu_e + \mu_+)n_e + (\mu_- + \mu_+)n_-} \vec{\nabla} n_-, \end{aligned} \quad (2.34)$$

$$\begin{aligned} \vec{G}_- = n_- \vec{C}_S - \frac{\mu_- n_- \text{rot} \vec{A}}{(\mu_e + \mu_+)n_e + (\mu_- + \mu_+)n_-} - \\ - \frac{(\mu_- D_+ + \mu_+ D_-) n_- + (\mu_e + \mu_+) D_- n_e}{(\mu_e + \mu_+)n_e + (\mu_- + \mu_+)n_-} \vec{\nabla} n_- + \frac{\mu_- n_- (D_e - D_+)}{(\mu_e + \mu_+)n_e + (\mu_- + \mu_+)n_-} \vec{\nabla} n_e \end{aligned}, \quad (2.35)$$

$$\begin{aligned} \vec{G}_+ = (n_e + n_-) \vec{C}_S + \frac{\mu_+ (n_e + n_-) \text{rot} \vec{A}}{(\mu_e + \mu_+)n_e + (\mu_- + \mu_+)n_-} - \\ - \frac{(\mu_e D_+ + \mu_+ D_e) n_e + (\mu_+ D_e + \mu_- D_+) n_-}{(\mu_e + \mu_+)n_e + (\mu_- + \mu_+)n_-} \vec{\nabla} n_e - \\ - \frac{(\mu_e D_+ + \mu_+ D_-) n_e + (\mu_- D_+ + \mu_+ D_-) n_-}{(\mu_e + \mu_+)n_e + (\mu_- + \mu_+)n_-} \vec{\nabla} n_- \end{aligned} \quad (2.36)$$

$$\bar{E} = -\bar{\nabla}\psi - \frac{D_- - D_+}{\mu_- + \mu_+} \bar{\nabla} \ln n_+, \quad (2.43)$$

$$\begin{aligned} \frac{\partial n_+}{\partial t} + \text{div} \left( n_+ \bar{C}_S - \mu_+ n_+ \bar{\nabla} \psi - \frac{\mu_+ D_- + \mu_- D_+}{\mu_- + \mu_+} \bar{\nabla} n_+ \right) = \\ = (v_i N - \beta n_e (n_e + n_-)) n_e - \beta_- n_+ n_- \end{aligned} \quad (2.44)$$

$$\begin{aligned} \frac{\partial n_-}{\partial t} + \text{div} \left( n_- \bar{C}_S + \mu_- n_- \bar{\nabla} \psi - \frac{\mu_+ D_- + \mu_- D_+}{\mu_- + \mu_+} \bar{\nabla} n_- \right) = \\ = (k_a N n_e - k_d n_-) N - \beta_- (n_e + n_-) n_- \end{aligned} \quad (2.45)$$

$$\frac{\partial n_e}{\partial t} + \text{div} (n_e \bar{C}_S - D_e \bar{\nabla} n_e) = (v_i N - \beta n_e (n_e + n_-)) n_e - (k_a N n_e - k_d n_-) N. \quad (2.46)$$

The description of electron detachment kinetics is principle for the description of discharge processes. Detachment is connected to interaction with excited atoms and molecules, and also with heating of negatively ionized atoms in an electrical field (in a corona discharge). The fullest models of a kinetics used for the description of streamers propagation include up to 150 [7–10] of chemical reactions. Features of our system is the availability of two areas of discharge. The first area is the area of weak ionization. In this area the excited atom density is small, and thus detachment is unessential  $k_d^{(1)} = 0$ . The second area is area of high density of electrons. In this area the electron and excited atoms concentrations are great. Approximately it is possible to consider, that the electrons, excited atoms and negatively ionized atoms are in equilibrium in this area.

$$\frac{n_e N}{n_-} = \frac{g_N}{g_-} \left( \frac{2\pi k T_e}{m} \right)^{3/2} \exp \left( -\frac{\varepsilon_-}{k T_e} \right). \quad (2.47)$$

where  $\varepsilon_-$  is the bond energy of electron in negative ion.

At application of a principle of detail equilibrium the ratio (2.47) allows to calculate a detachment constant

$$k_d^{(2)} = k_a \frac{n_e N}{n_-} = k_a \frac{g_N}{g_-} \left( \frac{2\pi k T_e}{m} \right)^{3/2} \exp \left( -\frac{\varepsilon_-}{k T_e} \right). \quad (2.48)$$

At small electron concentrations the excited atoms are formed by electronic impact, therefore  $N^* \sim k n_e$ , and detachment probability  $k_d^{(1)} = \tilde{k} n_e / N$ . With growth of an electron density the number of electrons borne due to detachment should increase from  $dN^{(1)}/dt \sim k n_e n_- N$  up to  $dN^{(2)}/dt \sim k_d^{(2)} n_- N$ . In the given report we model this transition by

the introducing of a phenomenological function  $\Phi(n_e)$  such, that  $\lim_{n_e \rightarrow 0} \Phi(n_e) = 0$ ,  $\lim_{n_e \rightarrow \infty} \Phi(n_e) = 1$ . Detachment rate we shall model by expression

$$dN/dt = dN^{(1)}/dt (1 - \Phi(n_e)) + dN^{(2)}/dt \Phi(n_e).$$

The complete set of chemical reactions in air can be found in papers [7-14]. In the initial equations set we can neglect a space charge in area of weak ionization, therefore these equations can be reduced to the form

$$\Delta\phi = 0, \quad (2.49)$$

$$\frac{\partial n_e}{\partial t} + \text{div} \vec{G}_e = F_e(n_e, n_+, n_-, T_e), \quad (2.50)$$

$$\frac{\partial n_+}{\partial t} + \text{div} \vec{G}_+ = F_+(n_e, n_+, n_-, T_e), \quad (2.51)$$

$$\frac{\partial n_-}{\partial t} + \text{div} \vec{G}_- = F_-(n_e, n_+, n_-, T_e), \quad (2.52)$$

$$\vec{G}_e = n_e \vec{C}_S + \mu_e n_e \vec{\nabla} \phi - D_e \vec{\nabla} n_e, \quad (2.53)$$

$$\vec{G}_+ = n_+ \vec{C}_S - \mu_+ n_+ \vec{\nabla} \phi - D_+ \vec{\nabla} n_+, \quad (2.54)$$

$$\vec{G}_- = n_- \vec{C}_S + \mu_- n_- \vec{\nabla} \phi - D_- \vec{\nabla} n_-, \quad (2.55)$$

$$\vec{E} = -\vec{\nabla} \phi. \quad (2.56)$$

The subsequent perturbation on small parameter  $\eta^{-1} = (r_{De}/L)^{-1}$  can be received with the equation

$$\Delta\phi^{(1)} = 4\pi e(n_e - n_+ + n_-). \quad (2.57)$$

The requirements of particle fluxes through boundary and ambipolar field potential continuity are executed on boundary between weakly ionized gas and plasma. On plasma and antenna boundary the space charge layer takes place. The boundary conditions can be noted in the form of the equality of electrons and ions currents on wall

$$\vec{j}_{en} + \vec{j}_{-n} = \vec{j}_{in}, \quad (2.58)$$

and Bohm criterion [15, 16]

$$\vec{j}_{in} = n_i V_S. \quad (2.59)$$

The frequencies of chemical processes are determined by electron and neutral temperatures defined by energy balance equations.



#### 2.2.4. Electron energy balance and calculation of electron temperature

As follows from equation (2.9), in a limiting case of strongly ionised gas ( $L \gg r_{De}$ ,  $n_e = n_+ = n$ ) the electrical field exists in two forms: ambipolar (longitudinal) field

$$\vec{E} = -\frac{D_e - D_+}{\mu_e + \mu_+} \vec{\nabla} \ln(n) = \frac{\mu_e kT_e/e - \mu_+ kT_+/e}{\mu_e + \mu_+} \vec{\nabla} \ln(n),$$

and field that supported electric current, flowing past on plasma, (transversal field)

$$\vec{E} = \frac{\vec{G}}{(\mu_e + \mu_+)n} = -\vec{\nabla} \psi.$$

In double-fluid hydrodynamics approximation the electron energy balance equation reduced to [39, 40]

$$\frac{3}{2} \frac{\partial nkT}{\partial t} + \text{div} \left( \frac{3}{2} nkT \vec{V} \right) + nkT \text{div} \vec{V} + \text{div} \vec{q} = Q_+ - Q_- . \quad (2.60)$$

The terms in the left-hand part of the equation (2.60) take into account the action of electron pressure. In a right-hand one  $Q_+$  is heat energy transmitted to electrons by an electrical field (action of the conforming friction force),  $Q_-$  is thermal energy transmitted from electrons to the neutrals by collision.

Power of an electrical field transmitted to electrons, can be counted as work of an electrical field in coordinate system, bound with driving neutral gas

$$Q_{+e} = -e \left( (\vec{G}_e - n\vec{C}_S) \vec{E} \right). \quad (2.61)$$

Substituting the expressions for electric field and current (2.9) in (2.60) we shall receive:

$$Q_{+e} = \frac{\mu_e \vec{G}^2}{n(\mu_e + \mu_+)^2} - \frac{D_a(D_e - D_+)}{(\mu_e + \mu_+)} \frac{(\vec{\nabla} n)^2}{n} - \frac{(\vec{G} \vec{\nabla} n)}{n} \frac{\mu_e D_e - 2\mu_e D_+ - \mu_+ D_e}{(\mu_e + \mu_+)^2}. \quad (2.62)$$

It is more convenient to use expression which is taking into account a smallness of ion temperature in comparison to electron one.

$$Q_{+e} = \frac{\mu_e \vec{G}^2}{n(\mu_e + \mu_+)^2} - \frac{\mu_+ D_e^2}{(\mu_e + \mu_+)^2} \frac{(\vec{\nabla} n)^2}{n} - \frac{(\vec{G} \vec{\nabla} n)}{n} \frac{\mu_e D_e}{(\mu_e + \mu_+)^2}. \quad (2.62a)$$

The first term in equation (2.62) responds for electrons heating by electric current, flowing past on plasma, the second one accounts energy expended for ambipolar field creation by electrons, the last term is cross addends which are taking into account electron current through an ambipolar barrier. In microwave field it is necessary to add into equation (2.62) the

power of high frequency field transferred to electrons (including both collisional  $\frac{n_e e^2 v_{en} \bar{E}^2}{2m(\omega^2 + v_{en}^2)}$ , and collisionless absorption of energy) (see for example [1] - [5]).

The similar expression can be recorded for energy transferred from electric field to ions

$$Q_{++} = \frac{\mu_+ \bar{G}^2}{n(\mu_e + \mu_+)^2} + \frac{D_a(D_e - D_+)}{(\mu_e + \mu_+)} \frac{(\bar{V}_n)^2}{n} - \frac{(\bar{G}\bar{V}_n)}{n} \frac{\mu_e D_+ + 2\mu_+ D_e - \mu_+ D_+}{(\mu_e + \mu_+)^2}. \quad (2.63)$$

The conforming simplified expression which is taking into account the smallness of electron temperature looks like

$$Q_{++} = \frac{\mu_+ \bar{G}^2}{n(\mu_e + \mu_+)^2} + \frac{\mu_+ D_e^2}{(\mu_e + \mu_+)^2} \frac{(\bar{V}_n)^2}{n} - \frac{(\bar{G}\bar{V}_n)}{n} \frac{2\mu_+ D_e}{(\mu_e + \mu_+)^2}. \quad (2.63?)$$

As well as it was necessary to expect, the energy spent by electrons for creation of an ambipolar barrier, is transmitted to heating of ions, so that as a whole ambipolar field does not work, it only reallocate energy between components of plasma.<sup>3</sup> The effect of ions acceleration

---

<sup>3</sup> The indicated result can be illustrated by following calculation. Let the electron is in an electrical field  $\bar{E}$  and let it experiences only isotropizing collisions  $t_1, t_2, \dots, t_n$  in points with coordinates  $\bar{r}_1, \bar{r}_2, \dots, \bar{r}_n$ . Then

$$\bar{V}_j = \bar{V}_{j-1} + \frac{e\bar{E}}{m}(t_j - t_{j-1}), \quad \bar{r}_j = \bar{r}_{j-1} + \bar{V}_{j-1}(t_j - t_{j-1}) + \frac{e\bar{E}}{2m}(t_j - t_{j-1})^2, \\ \frac{m(V_j^2 - V_{j-1}^2)}{2} = e(\bar{V}_{j-1}\bar{E})(t_j - t_{j-1}) + \frac{e^2\bar{E}^2}{2m}(t_j - t_{j-1})^2.$$

Substituting in last expression  $\bar{V}_{j-1}$  from first and summarizing on all interferences we receive

$$\frac{m(V_j^2 - V_{j-1}^2)}{2} = e((\bar{r}_j - \bar{r}_{j-1})\bar{E}), \\ \frac{m(V_n^2 - V_0^2)}{2} = e((\bar{r}_n - \bar{r}_0)\bar{E}).$$

Thus, as well as it was necessary to expect, the change of a thermal energy of an electron is equal to change of its potential energy

$$\frac{3}{2}n \frac{\partial kT}{\partial t} = (j\bar{E}),$$

where the current  $j$  includes all possible causes of electron movement both the current caused by an electrical field (conduction current) and current conditioned by inhomogeneous distribution of electrons in space and their Brownian motion (diffusive current). Allowing follow up elastic energy losses of electrons in interferences, the equation of electron energy balance can be reduced to the form (thermodiffusion and heat conduction can be taken easily into account)

$$\frac{3}{2}n \frac{\partial kT}{\partial t} = \left( \left( \frac{ne^2}{mv} \bar{E} + eD_e \bar{V}_n \right) \bar{E} \right) - \frac{3}{2} \kappa v k (T_e - T_g).$$

by an ambipolar field is well-known in low pressure discharge, restricted by walls, where this ions energy is transferred to a wall. In freely localized discharges this energy transmitted to heavy neutral particles due to ion neutral collisions. The estimations demonstrate, that this energy can play a noticeable role in heating heavy plasma components<sup>4</sup>.

Similar calculation for not quasi-neutral area, where  $\eta = r_{De}/L \gg 1$  for electrons and similar ratio for ions results in

$$Q_{+e} = \mu_e n_e e (\vec{\nabla} \phi)^2 - D_e (\vec{\nabla} n_e \vec{\nabla} \phi), \quad (2.64)$$

$$Q_{++} = \mu_+ n_+ e (\vec{\nabla} \phi)^2 - D_+ (\vec{\nabla} n_+ \vec{\nabla} \phi). \quad (2.65)$$

The electrical fields in this area can be great, and density of charged particles is small, therefore we can neglected the second term in equations (2.64), (2.65).

The calculation of power transmission from electrons in a other component should take into account the ionization losses, excitation of electronic, vibratory and rotary levels and elastic losses. All losses we can take into consideration by introducing an effective energy transfer coefficient  $\kappa$  [30]. In this case expression for  $Q_{e-}$  has the form

$$Q_{e-} = \kappa v_{en} n_e \frac{3}{2} (kT_e - kT_g). \quad (2.66)$$

Thus, the electron temperature in a quasi-stationary mode can be calculated under expression:

$$T_e = T_g + \frac{2(Q_{e+} - Q_{e-} - W_p)}{3\kappa v_{en} n_e}, \quad (2.67)$$

where  $W_p$  is energy lost due to ambipolar field creation, spotted by the left-hand part of an equation (2.60).<sup>5</sup>

---

This yields the expressions (2.62) and (2.62?). The physical sense of diffusive cooling of electrons is, that the majority of electrons located in a point  $\vec{r}$  were born and acquire energy in the field of large integrated electron densities, therefore having come exactly to  $\vec{r}$ , they have expended a part of the thermal energy on overcoming of a potential hill.

<sup>4</sup> It follows from mass equality of ions and neutrals. The heating of the neutrals at transition of ionization front can be estimated approximately under the expression

$$\Delta T = A \rho T_e,$$

where  $A$  - factor about units dependent on a spacing distribution of chemical reactions at the front of ionization,  $\rho$  - degree of ionization.

<sup>5</sup> At record of equation (2.67) we have determined the temperature  $T_e$  as 3/2 squares of mean energy in coordinate system, bound with driving electrons, thus temperature is determined by an isotropic part of a cumulative distribution function in this coordinate system. The ionization frequency is determined through a cumulative distribution function in coordinate system bound with neutral gas, therefore we should characterize mean electron energy in this coordinate

### 2.3. Surface and dielectric waveguide waves in homogeneous bounded plasma

The dispersion characteristics of surface waves were esteemed in number of papers. Among the 24 works of Russian scientists it is necessary to mark the monographies [17-23]. The fullest review of the articles, concerning surface wave discharge structure investigation keeping more of 160 links, was published by Zhelyazkov, and Atanasov [24]. The fullest subsequent reviews of recent works are contained in stuffs of conferences [25, 26].

For surface wave dispersion curve calculation in a considered case it is convenient to use the approach offered in [27]. Let's consider, that the surface wave is propagated in z-direction, and the plasma is inhomogeneous only in a direction, perpendicular to its boundary (this direction we shall designate X). As it is known, the field of a surface wave has three components  $E_x$ ,  $E_z$  and  $B_y$ . Let's search for the solution by the way:

$$\begin{Bmatrix} E_x \\ E_z \\ B_y \end{Bmatrix} = \begin{Bmatrix} \tilde{E}_x(x) \\ \tilde{E}_z(x) \\ \tilde{B}_y(x) \end{Bmatrix} \exp(-i(\omega t - i h z)). \quad (2.68)$$

In this case Maxwell equations are resulted in

$$\frac{dE_z}{dx} = \frac{i\omega}{c} \left( \frac{h^2 c^2}{\omega^2 \epsilon(x)} - 1 \right) B_y, \quad (2.69)$$

$$\frac{dB_y}{dx} = \frac{i\omega \epsilon(x)}{c} E_z, \quad (2.70)$$

$$E_x = \frac{c}{i\omega \epsilon(x)} i h B_y. \quad (2.71)$$

In range of parameters, interesting us, we can leave out a spatial dispersion. Therefore

$$\epsilon(x) = 1 - \frac{4\pi n e^2}{m\omega(\omega + i\nu_{en})}. \quad (2.72)$$

The boundary conditions for an equation (2.69)–(2.72) include conditions of radiation non reflection from infinity and conditions of electrical and magnetic field continuity on plasma

---

system (conforming quasi-temperature we shall designate as  $\tilde{T}_e = T_e + mV_e^2/3$ ) And this mean energy will determine frequencies of chemical processes, bound with interferences of electrons and neutrals. It is determined by an equation

$$\tilde{T}_e = T_g + \frac{2Q_{e+}}{3k\nu_{en}n_e}. \quad (3.10)$$

Also is in the full consent with an equation of an energy balance recorded for one electron.

and dielectric antenna boundary. The field inside the antenna can be shown by the way

$$\begin{Bmatrix} E_x \\ E_z \\ B_y \end{Bmatrix} = B_0 \begin{Bmatrix} (hc/\mathbf{w}\mathbf{e}_D)ch\left(\sqrt{(h^2 - \mathbf{w}^2\mathbf{e}_D/c^2)}(x - x_0)\right) \\ \sqrt{(h^2c^2/\mathbf{w}^2\mathbf{e}_D - 1)}sh\left(\sqrt{(h^2 - \mathbf{w}^2\mathbf{e}_D/c^2)}(x - x_0)\right) \\ ch\left(\sqrt{(h^2 - \mathbf{w}^2\mathbf{e}_D/c^2)}(x - x_0)\right) \end{Bmatrix} \exp(-i(\mathbf{w}t - ihz)), \quad (2.73)$$

where  $x_0$  is x-coordinate of a central plane of the antenna.

If the electron oscillation frequency in an electric field in a direction perpendicular to the border exceeds the typical size of a non-uniformity of a space charge layer (electronic radius of Debye) the process of UHF field rectification in a space charge layer and the process of the harmonic generations, which are capable to update process of absorption of energy in plasma, are essential.

The electromagnetic fields in such system can be separated into three groups (Fig. 2.4).

1. The waves of an continuum spectrum, radiated by system at  $h^2 < \omega^2 \epsilon_p / c^2$  (if  $\epsilon_p < 0$  this waves damp along the antenna and exist only near to sharp structural inhomogeneities - at transferring point from a waveguide to the antenna and near to a point of plasma slab abruption).

2. The waves of a dielectric wave guide (their field is periodic on X direction inside waveguide and damps exponentially outside). The expression for the dispersion characteristics of these waves has no analytical form for arbitrary plasma density, however at defined values of  $\epsilon_p$  the wave propagation coefficient easily evaluate ( $m=0,1,2\dots$ ).

$$\epsilon_p = 0, \quad h_m^2 = k_0^2 \epsilon_D - \frac{(2m+1)^2 \pi^2}{L^2}$$

$$\epsilon_p \rightarrow \infty, \quad h_m^2 \rightarrow k_0^2 \epsilon_D - \frac{4(m+1)^2 \pi^2}{L^2}$$

(The wave for which  $h_m^2 < k_0^2 \epsilon_p$  does not exist).

3. The surface wave existing at  $\epsilon_p < -\epsilon_D$ . The surface wave concentrates near to plasma and antenna boundary and exponentially damps in both sides from it.

$$\epsilon_p \rightarrow -\epsilon_D, \quad h^2 \rightarrow k_0^2 \frac{\epsilon_D \epsilon_p}{\epsilon_D + \epsilon_p} \quad (2.74)$$

$$\epsilon_p \rightarrow \infty, \quad h_m^2 \rightarrow k_0^2 \epsilon_D$$

The penetration depth of a surface wave and waves of a dielectric waveguide in plasma determines by relations

$$L = \text{Im } k_x^{-1}, \quad k_x^2 = k_0^2 \epsilon_p - h^2.$$

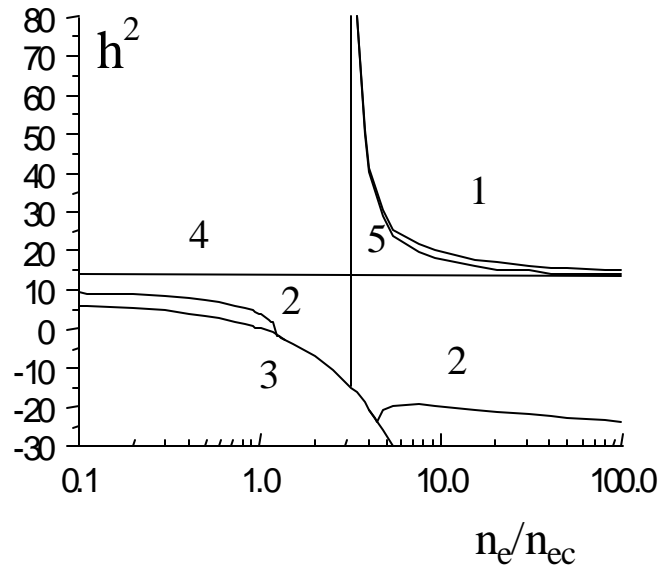


Fig. 2.4. The waves in system a plasma - dielectric waveguide in absence of collisions.

- 1 - The surface wave existing in an area  $\epsilon_p < -\epsilon_D$ ;
- 2 - dielectric waveguide wave existing in an area  $\epsilon_p > \epsilon_D$ ;
- 3 - boundary infinite spectrum, 4 -  $k_o^2 \epsilon_D$ ;
- 5 - calculation under the equation (2.7) ( $\epsilon_D = 5$ , antenna thickness  $L=8$  mm, microwave length  $\lambda=2.4$  cm,  $n_C = m\omega^2/4\pi e^2$ ).

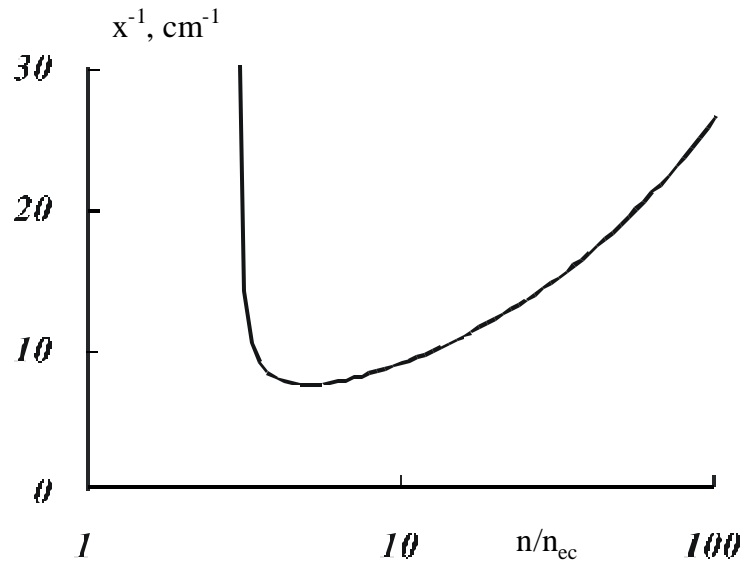


Fig. 2.5. Inverse penetration depth  $x^{-1}$  of a surface wave as a function of electron density at  $\nu/\omega=0$ .

The calculations results for surface wave and dielectric waveguide waves for geometry used in experiment ( $L=1$  cm) are given in Fig. 2.4.

The dependence of return depth of penetration of a surface wave in plasma corresponding to a dispersion curve in Fig. 2.4 is submitted on Fig. 2.5. In area  $\epsilon_p \rightarrow -\epsilon_D$  it can be described by equation

$$x^{-1} = \frac{\omega}{c} \frac{|\epsilon_p|}{\sqrt{\epsilon_D + \epsilon_p}}.$$

An utilized earlier estimation

$$x^{-1} = \frac{\omega_{pe}}{c}$$

is take place at  $n_e \rightarrow \infty$ .

Maximum UHF field penetration depth in plasma

$$x^{-1} = \frac{\omega_{pe}}{c} \frac{2\epsilon_D}{\epsilon_D - 1}$$

is watched at  $\epsilon_p = -2\epsilon_D$  or, that is the same,  $n_e = n_{ec}(1 + 2\epsilon_D)$ .

At  $n_e \rightarrow n_{ec}(\epsilon_D + 1)$  the depth of penetration of a field in plasma decreases up to zero point (at absence of collisions) and at definite density of plasma becomes equal or more than thickness of a diffusive layer. Therefore at  $n_e = n_{ec}(1 + 2\epsilon_D)$  the considered model requires in refinement. It is possible to expect, that in this area the electromagnetic wave will be absorbed much more strongly, than follows from our model.

The electrons collisions result in attenuation both surface and waveguide modes, at that the surface wave exists in area  $\text{Re } h^2 > k_0^2 \text{Re } \epsilon_D$ , and it turns in strongly attenuated wave with a reverse dispersion at  $k_0^2 \text{Re } \epsilon_p < \text{Re } h^2 < k_0^2 \text{Re } \epsilon_D$ . The results of calculation of the surface wave dispersion characteristics at the account of collisions are given in Fig. 2.6.

## 2.4. Surface wave discharge classification

A microwave discharge on a surface of a dielectric wave-guide antenna can be supported in pressure range  $10^{-3}$ - $10^3$  torr. In general case such wide pressure range results in necessity of the account of all possible kinetic processes:

1. Direct and step ionization by electron impact and ionization at collision of excited molecules.

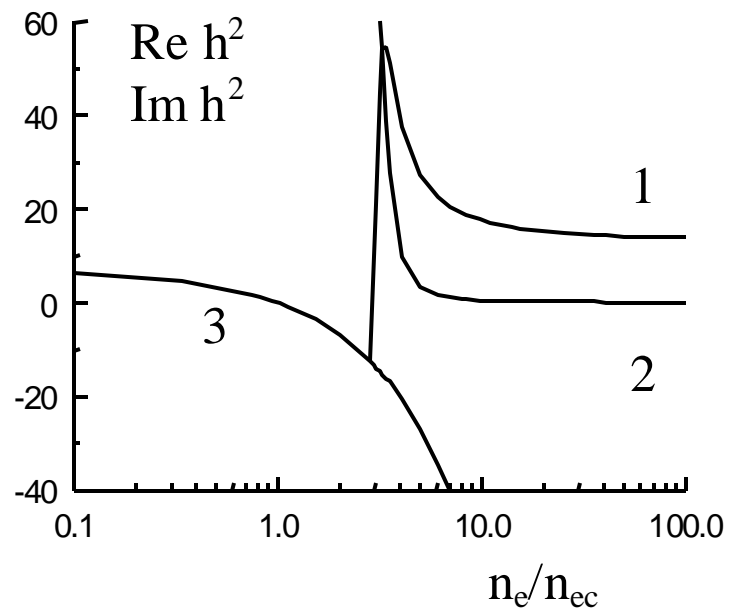


Fig. 2.6. The surface wave dispersion characteristics in system of a plasma - dielectric waveguide at the account of collisions  $\nu/\omega=0,01$ . Surface wave: 1 –  $\text{Re } h^2$ , 2 -  $\text{Im } h^2$ . Continuum spectrum boundary - 3.



2. Attachment and detachment.
3. Electron - ion and ion – ion recombination.
4. Excitation of the oscillatory and rotary freedom degree of molecules.
5. Ambipolar diffusion.
6. Particles and energies balance can be both local and non-local depending on external conditions.
7. At low pressures it is necessary to include a spatial dispersion in electrodynamics' model.
8. The discharge can be transparent and opaque (at high pressures) for self-radiation.
9. The plasma non-uniformity along an electrical field direction results in additional energy absorption in a resonance region, where the real part of complex permittivity of plasma is close to zero point. There is a considerable change of an electron distribution function due to additional energy absorption in a resonant layer.
10. Sharp changing of the electric field near plasma boundary can change the spatial distribution of the plasma density, and caused the generation of the electric field harmonic due to striction plasma nonlinearity.
11. The role of the gas heating can be different depending on a part of energy transmitted to the heating of neutrals and on a microwave pulse duration's.

The complete set of the constant rates of chemical reactions for air plasma is given in [7-10].

We shall use notifications below:  $e$  and  $m$  – electron charge and mass;  $c$  – light velocity;  $n_e$  – charged particles density;  $\nu_{en}$  – electron collision frequency;  $\omega$  – microwave field frequency;  $\lambda_{en}$  – mean free path of electron-neutral collision;  $\omega_{pe} = (4\pi n_e e^2 / m_e)^{1/2}$  – plasma frequency;  $n_{ec} = m_e \omega^2 / 4\pi e^2$  – critical density;  $k_0 = \omega / c$ ;  $E$  and  $B$  – electric and magnetic fields;  $\epsilon(\omega)$  – dielectric permittivity; in antenna region  $\epsilon(\omega) = \epsilon_D$ ; in plasma  $\epsilon(\omega) = \epsilon_P = 1 - \omega_{pe}^2 / (\omega(\omega + i\nu_{en}))$ ;  $D_a$  – ambipolar diffusion coefficient;  $\nu_i$  – ionization frequency;  $\alpha$  – recombination coefficient;  $c_V$  – thermal capacity;  $\chi$  – electron thermal conductivity (heat transfer) coefficient;  $T_e$  and  $T_g$  – electron and gas temperatures. For estimation of field penetration length into plasma we will be used the value  $c / \omega_{pe}$  as for surface microwave discharges  $\omega_{pe} > \omega$ .

As the position of one of the discharge boundaries does not fixed by a wall, the usual analysis based on the solution of the ambipolar diffusion equations and direct - current analogy can not be used. In the report we shall give approximate model for stationary microwave

discharge valid at middle gas pressure ( $p=1-100$  torr) and on its base the classification of the main processes taking place in plasma of surface microwave discharge will be given.

If the condition  $c/\omega_{pe} < \lambda_{en}$  is satisfied the skin layer on plasma boundary is collisionless, therefore processes of energy transfer from microwave field to electrons should be considered in kinetic approach. Otherwise the hydrodynamic equations are possible to use. The border of the kinetic and hydrodynamic description on the diagram  $(n_e-p)$  – (charged particles density - pressure of the neutrals) is described by a curve

$$n_e = \frac{c^2 m}{4\pi e^2 \lambda_{e1}^2} p^2, \quad (2.75)$$

where  $\lambda_{e1}$  is the mean free path of electrons at pressure  $p=1$  torr.

The energies balance is local if the characteristic size of absorption of microwave energy  $c/\omega_{pe}$  for typical case exceeds the length of thermal conductivity  $\lambda_{Te} = \lambda_{en}/(\delta)^{1/2}$ , where  $\delta$  is a mean part of energy, which electrons loss in collisions with molecules (at elastic collisions  $\delta=2m/M$ , that yields a lower limit of possible values). The equation of border of local and non-local modes looks like

$$n_e = \frac{c^2 m \delta}{4\pi e^2 \lambda_{e1}^2} p^2. \quad (2.76)$$

Particles balance is local at condition  $\alpha n_e > D(\omega_{pe}/c)^2$  for the local energies balance case and  $\alpha n_e > D\delta/(\lambda_{en})^2$  in the opposite case. The boundary position between these areas on the diagram  $(n_e - p)$  results in equations ( $D_1$  is an ambipolar diffusion coefficient at pressure 1 torr)

$$p = \frac{D_1}{\alpha} \frac{4\pi e^2}{mc^2}, \quad (2.77)$$

$$n_e = \frac{D_1}{\alpha} \frac{\delta}{\lambda_{e1}^2} p. \quad (2.78)$$

In the case of a three-particle recombination predominance (third particle is an electron,  $\beta$  is a recombination coefficient) the equations (3.3) and (3.4) become

$$n_e > \frac{4\pi e^2}{mc^2} \frac{D_1}{\beta p}, \quad (2.77?)$$

$$n_e > \left( \frac{D_1 \delta}{\beta \lambda_{e1}^2} p \right)^{1/2}. \quad (2.78?)$$

Thus the electrons density and temperature will be connected by Sakha equation.

The conducted above reasoning are fair for plasma by transparent for own radiation, otherwise the energy absorbed by electrons leaves the discharge volume only by heat conduction (including radiant heat conduction), and the cooling of discharge descends only from a surface. The Rosseland's path of a photon can be estimated under the expression

$$L = \frac{AT_e^{7/2}}{n_e^2},$$

where the value of a constant A depends on a kind of gas and on a photons scattering mechanism [28], [29]. As the value  $\lambda_{en}/\sqrt{\delta}$  is the typical size of discharge at local energies balance and  $c/\omega_{pe}$  is the typical one at non-local energies balance the conditions of the discharge opacity look like

$$n_e > \left( \frac{AT_e^{7/2}}{\lambda_{e1}} \right)^{1/2} \delta^{1/4} p^{1/2}, \quad (2.79)$$

$$n_e > 4^{1/3} \pi^{1/3} A^{2/3} T_e^{7/3} \left( \frac{e^2}{mc^2} \right)^{1/3}. \quad (2.80)$$

If the conditions (2.79) or (2.80) are fulfilled the discharge will be equilibrium. The discharge transition from the non-equilibrium form to equilibrium usually occurs in time as development of the overheated instabilities [30].

The neutral gas heating in discharge area results in two effects.

1. There is a hydrodynamic gas movement leading to equalising of a gas pressure in the discharge with the pressure of the environmental medium. The typical time  $\tau$  of this process is

$$\tau \approx \frac{c}{\omega_{pe} C_S} = \left( \frac{m}{4\pi n_e e^2} \right)^{1/2} \frac{c}{C_S} \quad (2.81)$$

for the systems with local energy balance and

$$\tau \approx \frac{c\sqrt{\delta}}{\lambda_{e1} C_S} p \quad (2.82)$$

for the system with non-local one.

2. At large times the gas heating leads to slow gas convection due to Archimedes force. This class of phenomena we do not consider in this work.

The areas with different character of discharge kinetic processes depending on electron density and the gas pressure are given on Fig. 2.7.

At all conditional character of similar division due to a proximity of the estimations of a

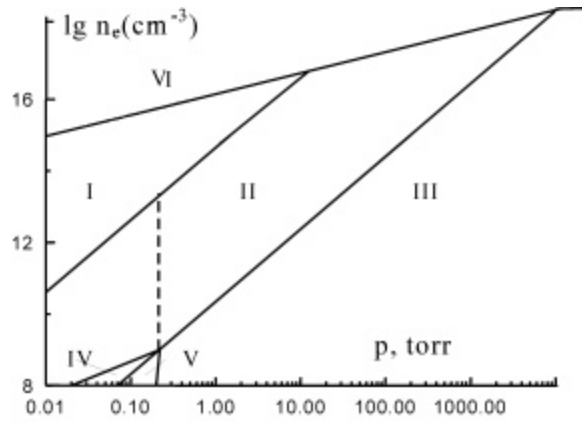


Fig. 2.7. Different discharge kinetics areas:

I is area of kinetic viewing,  
 II is local particles balance and non-local energy balance,  
 III is local particles and energy balance,  
 IV is non-local particles balance and non-local energy balance,  
 V is non-local particles balance and local energies balance,  
 VI is the area of the discharge opaque for optical radiation.

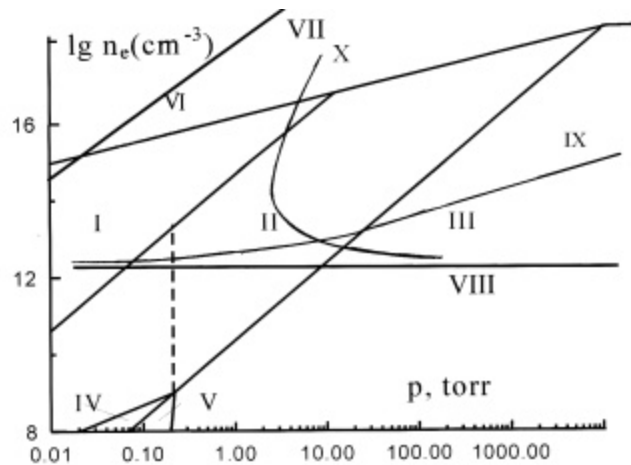


Fig. 2.8. Different discharge kinetics areas:

I is area of kinetic viewing,  
 II is local particles balance and non-local energy balance,  
 III is local particles and energy balance,  
 IV is non-local particles balance and non-local energy balance,  
 V is non-local particles balance and local energies balance.  
 VI is region of discharge opaque for optical radiation.  
 VII is the boundary of 100% ionisation.  
 VIII is the critical density (for 2.45 cm microwave).  
 IX is the boundary of field absorption in resonance point and collisionless field absorption on plasma boundary,  
 X is the boundary of elementary homogeneous plasma model.

field penetration depth and dependence of the chemical reactions constants rates and part of energy, loss electrons, on temperature, this analysis allows to make a deduction about possible methods of the plasma description. According to the carried out analysis in large range of requirements it is possible to consider that the particles balance is local, but at the same time, it is necessary to take into account the electronic thermal conductivity.

The analysis of the discharge processes we shall begin from most simple (and at the same time most often meeting) particular case of discharge with local balance of the particles and non-local balance of energies. On the first stage we also shall not take into account the hydrodynamic movement of gas due to its heating.

Let's consider that the longitudinal plasma inhomogeneity is small and the distribution of electromagnetic wave along the plasma – antenna surface it is possible to describe in a geometric optics approximation [7,8]. It is usual condition for discharges supported by a surface wave, generated near to one of the plasma borders. As the area of the microwave field localization in plasma is much less than thermal conductivity length it is possible to account that the energy absorption distribution in a direction, perpendicular to a boundary, is described as

$$W_{\perp} = W_{\perp 0} \exp\left(-x\sqrt{\delta}/\lambda_{en}\right). \quad (2.83)$$

Considering that the part of energy expended on ionization does not depend on energy (it means, that electron density is proportional to absorbed energy, that executed only approximately), it is possible to receive following expression for dependence of electrons density on cross coordinate

$$n_e(x) = n_{eo} \exp\left(-x\sqrt{\delta}/\lambda_{en}\right), \quad (2.84)$$

where  $n_{eo} = v_i(W_{\perp 0})/\alpha$ . Thus the characteristic size of plasma exceeds the depth of electric field penetration in plasma therefore from an electrodynamic point of view it is possible to consider plasma to be uniform with electron density equals to its boundary value. Strictly speaking, on plasma and dielectric antenna boundary the electron density is close to zero, therefore the diffusive layer is formed in this area.

## 2.5. Simplified set of equations

### 2.5.1. Electron heat transfer equation

The homogeneous plasma model can be use for calculation of surface wave dispersion characteristics, if the reference size of a diffusive layer is much shorter then the surface wave

penetration depth in plasma. The matching demonstrates that the plasma non-uniformity should essentially change surface wave spectra, at first, in the area of small electron densities  $|\epsilon_D| \leq |\epsilon_p| \leq 2|\epsilon_D|$ , and secondly, in the area of high densities  $\frac{n}{n_C} \geq \frac{c^2}{\omega^2} \frac{v_i}{D_a}$ . In intermediate area

$2\epsilon_D < \frac{n}{n_C} < \frac{c^2}{\omega^2} \frac{v_i}{D_a}$  the elementary model must work, except, maybe, the account of absorption in a resonant point [30], [31]. The boundary of this area is showed in a Fig. 2.8 by curves X. Thus, the model of homogeneous plasma works presumptively only in the field of high-pressure discharge, at pressure below than 30 torr, one has to use the numerical models.

At a discharge numerical modelling one can outline some possible problems:

1. Simulation of longitudinal discharge structure (along a direction of a wave propagation).
2. Simulation of discharge parameters distribution on the whole antenna surface.
3. Simulation of stationary discharge structure in a direction, perpendicular to antenna boundary.
4. Simulation temporary evolution of transversal discharge structure.

The independent consideration of "longitudinal" and "transversal" processes can be done because the longitudinal discharge size, as a rule, is much greater then its transversal size and thus stationary longitudinal structure is reached much earlier than the longitudinal one. At the same time the discharge time evolution modelling should include the hydrodynamic motion of neutral gas, which one can include its convective motion. This motion depends on a plenty of the factors, including arrangement of the antenna in a horizontal or vertical plane. Therefore simulation of process of installation of fixed frame of discharge in many respects has conditional nature.

As follows from the previous analysis for discharge mathematical modelling under our condition (pressure of the neutrals 10-1000 torr, microwave wavelength 2.4 cm) it is necessary to take into account following processes:

1. Electron energy transfer described by an equation of electrons energy balance

$$\frac{3}{2}nk \frac{\partial T_e}{\partial t} = \bar{\nabla} \chi \bar{\nabla} T_e + Q(x) - w_l(x)n, \quad (2.85)$$

where  $\chi$  is electronic heat conduction coefficient;  $Q(x)$  is power transmitted from a surface wave to electrons, which include both collisional (ohmic) and collisionless mechanisms;  $w_l$  is energy lost by an electron in interferences, including elastic losses, loss on excitation and ionisation [30]. Let's mark, that we consider discharge to be transparent for radiation, behind exception, may be, resonance emission.

2. Excited atoms and molecules density transfer, including resonant condition, described by an integral Biberman-Holstein equation, and the metastable atoms, described by a usual diffusion equation. It is necessary to account excitation transfer separately from electrons energy transfer (though the some energy levels can be in equilibrium with electrons) because region, where the electronic heat conduction is possible, is limited to a potential barrier built by an ambipolar field, while area, where excitation transfer in neutral gas is possible, is not limited.

3. The electrons transfer in space is described by an ambipolar diffusion equation (2.7) taking into account the ionization from excited states

Distribution of an electromagnetic field in space we shall describe by equations (2.2) – (2.4). Energy absorption in a resonant point or collisionless absorption of an electromagnetic wave on plasma boundary we shall allow by the introducing of the conforming surface resistance.

### 2.5.2. Electron density distribution near antenna surface

In §2.6 the different types of UHF discharge in neighbourhood of a dielectric antenna (see Fig. 2.3) are analyzed and the approximated qualitative model of the discharge supported by a surface wave is constructed. This model used the assumption of local charged particles balance and a non-local energy balance in plasma. This model corresponds to the most widespread discharge maintenance conditions (Fig. 2.7).

The surface waves characteristics used in model, leave out of the corrections, bound with a plasma non-uniformity near to a dielectric antenna and electromagnetic field absorption in a resonance region, where  $\text{Re } \epsilon \approx 0$ , and also possible non-linear processes in a space charge layer between plasma and antenna.

At calculation of electron density distribution near plasma boundary we will use the approach of ambipolar diffusion. Thus the electron density distribution is subject to an equation

$$\frac{\partial n}{\partial t} - \bar{\nabla} D_a \bar{\nabla} n = v_i n - \alpha n^2 - \beta n^3. \quad (2.85)$$

The notations are entered in (2.85):  $n$  is density of charged particles,  $D_a$  is coefficient of an ambipolar diffusion. The expression (2.85) takes into consideration a direct ionization by electron impact ( $v_i$ , is frequency of ionization;  $\alpha$  and  $\beta$  are two and three body recombination coefficients). Frequency of ionization and the frequencies of a recombination are functions of temperature of electrons. As we consider processes in a diffusive layer, which has size of the

order  $\sqrt{D_a/v_i}$ . Its size is much less than heat conduction length  $\lambda_{Te} = \lambda_{en}/\sqrt{\delta}$ . we shall consider electron temperature and, therefore, constant of chemical reactions not dependent from co-ordinates.

This equation should be resolved with boundary conditions on infinity and on plasma boundary with a dielectric antenna. The former is  $n \rightarrow n_o$  at  $x \rightarrow \infty$ , where  $n_o$  is the root of equation

$$v_i - \alpha n_o^2 - \beta n_o^3 = 0. \quad (2.86)$$

The elementary version of boundary conditions on a wall  $n=0$  at  $x=0$  was suggested by Shottky. However we must determine the plasma density on the boundary with space charge layer (CPL). We shall use a condition following from Bohm's criterion

$$nV_S = D_a \frac{\partial n}{\partial x}. \quad (2.87).$$

At a solving the equation (2.87) it is most convenient to consider that the maximum value of an electron density is  $n_o$ , entering a new variable  $\eta = n/n_o$ . Thus in a stationary approach the equation (2.85) is reduced to

$$\frac{d^2 \eta}{dx^2} = \eta [\tilde{\alpha}(1 - \eta) + \tilde{\beta}(1 - \eta^2)], \quad (2.88)$$

where the notations

$$\tilde{\alpha} = \alpha n_o / D_a, \quad \tilde{\beta} = \alpha n_o^2 / D_a \quad (2.89)$$

are entered. The equation (2.88) can be integrated

$$\frac{d\eta}{dx} = \sqrt{\frac{\tilde{\alpha}}{3} + \frac{\tilde{\beta}}{2} + \frac{\tilde{\beta}}{2}\eta^4 + \frac{2\tilde{\alpha}}{3}\eta^3 - (\tilde{\alpha} + \tilde{\beta})\eta^2}. \quad (2.90)$$

The reference depth of a diffusive layer can be evaluated as

$$\bar{x} = \sqrt{D_a/v_i} = (\tilde{\alpha} + \tilde{\beta})^{-1/2}. \quad (2.91)$$

In Schottky-type boundary condition the second integrating leads to simple relation between electron density and coordinate

$$x = \int_0^\eta \frac{d\eta}{\sqrt{\frac{\tilde{\alpha}}{3} + \frac{\tilde{\beta}}{2} + \frac{\tilde{\beta}}{2}\eta^4 + \frac{2\tilde{\alpha}}{3}\eta^3 - (\tilde{\alpha} + \tilde{\beta})\eta^2}}. \quad (2.92)$$

Bom's criterion-type boundary condition (2.87) yields



$$x = \int_{\eta_s}^{\eta} \frac{d\eta}{\sqrt{\frac{\tilde{\alpha}}{3} + \frac{\tilde{\beta}}{2} + \frac{\tilde{\beta}}{2}\eta^4 + \frac{2\tilde{\alpha}}{3}\eta^3 - (\tilde{\alpha} + \tilde{\beta})\eta^2}}. \quad (2.93)$$

The value  $h_s$  is determined from a condition (2.87) together with an equation (2.90).

Thus, we have

$$V_s \eta_s = D_a \sqrt{\frac{\tilde{\alpha}}{3} + \frac{\tilde{\beta}}{2} + \frac{\tilde{\beta}}{2}\eta_s^4 + \frac{2\tilde{\alpha}}{3}\eta_s^3 - (\tilde{\alpha} + \tilde{\beta})\eta_s^2}. \quad (2.94)$$

Thus, the electron density on boundary is determined as the root of equation

$$\frac{\tilde{\alpha}}{3} + \frac{\tilde{\beta}}{2} + \frac{\tilde{\beta}}{2}\eta_s^4 + \frac{2\tilde{\alpha}}{3}\eta_s^3 - \left( \tilde{\alpha} + \tilde{\beta} + \frac{V_s^2}{D_a^2} \right) \eta_s^2 = 0. \quad (2.95)$$

Considering  $\eta_s \ll 1$ , we shall receive approximately

$$\eta_s = \sqrt{\left( \frac{\tilde{\alpha}}{3} + \frac{\tilde{\beta}}{2} \right) / \left( \tilde{\alpha} + \tilde{\beta} + \frac{V_s^2}{D_a^2} \right)}. \quad (2.96)$$

After substitution of values  $\tilde{\alpha}$  and  $\tilde{\beta}$  from a ratio (2.89) we shall receive:

$$\eta_s = \sqrt{\left( \frac{\alpha n_o}{3} + \frac{\beta n_o^2}{2} \right) / \left( \alpha n_o + \beta n_o^2 + \frac{V_s^2}{D_a^2} \right)} = \sqrt{\left( \frac{\alpha n_o}{3} + \frac{\beta n_o^2}{2} \right) / (\alpha n_o + \beta n_o^2 + v_{in})}, \quad (2.97)$$

where  $v_{in}$  - ion neutral collision frequency.

Last ratio demonstrates, that the plasma resonance area [31, 32] exists in plasma if conditions

$$n_o > n_C = \frac{m\omega^2}{4\pi e^2}, \quad (2.98)$$

$$\eta_s n_o < n_C = \frac{m\omega^2}{4\pi e^2} \quad (2.99)$$

is fulfilled, where  $\omega$  – frequency of microwave field supporting plasma. The ratio (2.99) results in following connection of electron density and pressure  $p$

$$n_C > \sqrt{\left( \frac{\alpha n_o}{3} + \frac{\beta n_o^2}{2} \right) / (\alpha n_o + \beta n_o^2 + v_{ioP})} n_o. \quad (2.100)$$

If condition (2.100) is fulfilled, additional surface wave energy absorbs in the plasma resonance, which results in surface wave dispersion curve change (increase of absorption), and, therefore, change the relations between electron density and wavelength, that leads to more strong dependence of electron density from longitudinal coordinate. It gives the possibility to

support discharge at smaller microwave powers. The boundary, which separates area where the resonance area is present at plasma, showed by curves VIII and IX in Fig. 2.8. Thus the microwave length was considered equal to 2.4 cm. Above the curve IX the plasma resonance is inside of a spatial charge layer, therefore the collisionless absorption of a surface wave can be taken into account in this case as absorption on plasma boundary, similar to absorption of a HF field in a capacitive HF discharge [15]. The discharge with density is less then critical one  $n_c = m\omega^2/4\pi e^2$  (below by curve VIII) as a rule, will not be realized<sup>1</sup>.

Except for curves VIII and IX Fig. 2.8 contains the straight line VII representing limit of 100 % ionization. Strictly speaking, all reduced estimations are fair much below by curve VII. Besides Fig. 2.8 contains a position of boundaries of discharge with different types of kinetics (curves I-VI), which position and physical sense were discussed in §2.2.

At low electronic density, when the double recombination dominates, it follows from (4.18) that the influence of a diffusive layer on the dispersion characteristics of an electromagnetic field is essential at

$$\frac{D_1}{\omega n_{ep}} < \frac{c^2}{\omega_{pe}^2}, \quad (2.101)$$

that results in a condition coincidence with a condition (2.76), however having sense not only on border of III and V areas but also inside II area. In this case the qualitative analysis of discharge characteristics reduced in the given section is inapplicable and the numerical solution of a problem is necessary.

## 2.6. Discharge characteristics

The equations set (2.1')-(2.4') and (2.7)-(2.9) were solved in several cases.

(•) The dispersion curves of a surface wave taking into account inhomogeneity of a plasma layer (self-consistent solution with the ionized non-linearity) were calculated. In this case set of equations were solved on segment ( $0 < y < L$ ) as eigenvalues problem for a nonlinear wave propagated along the antenna. Solution of a problem is searched as

$$\begin{pmatrix} \tilde{\vec{E}} \\ \tilde{\vec{H}} \end{pmatrix} = \begin{pmatrix} \hat{\vec{E}}(y) \\ \hat{\vec{H}}(y) \end{pmatrix} \exp(ihz), \quad n = n(y). \quad (2.102)$$

---

<sup>1</sup> Usually, to create discharge with density below critical it is necessary to use discharge in a resonator, when even the little density change results in sharp decreasing of a microwave field due to resonance frequency shift.

Boundary conditions for a field are requirement of symmetry at  $y=0$  and the requirement not reflections of a wave in a point  $y=L$  (which with adequate accuracy by virtue of a field shielding can be exchanged zero). The eigenvalue of the task is propagation constant  $h$ .

The similar problem for a wave, supporting the discharge in the waveguide, was solved in article [33], where the discharge tube was introduced in a rectangular waveguide. The analogous calculation for a surface wave discharge was fulfilled by Moisan and Zakrzhevsky. In distinction from the indicated works, in our case, one of plasma boundaries is free, i.e. its position should be found from calculation. The similar problems were considered in a Boev's cycle of papers [34-37] and paper [38], where the plasma dielectric permittivity was considered as local nonlinear function of a high frequency field. In these papers the field solutions, looking as wave channels propagating along plasma waveguides (created by power microwave itself), were found. Unfortunately, direct comparison of results of the articles [34-37] with experiment is impossible as the authors have not taken into account the electrons temperature and density space relaxation processes (i.e. diffusion and thermal conductivity).

In a nonlinear task on eigenvalues (opposite linear one) the value of propagation constant  $h$  appears to be the function of field amplitude. Calculation of dependence  $h = h(E_0)$ , as well as the calculation of the profile of the transversal distributions of plasma density  $n = n(E_0, y)$  and fields  $\vec{E} = \vec{E}(E_0, y)$ , is a main problem.

(••) The surface wave attenuation constant usually has a peak near to resonance point  $n = \frac{m\omega^2}{4\pi e^2}(1 + \epsilon_{ant})$ , therefore at low powers the surface wave is well absorbed and the reflection from back plasma boundary is insignificant (Fig. 2.8). In this case it is possible approximately to consider that the plasma is supported by a surface wave, running along antenna from microwave source.

At large powers the plasma covers whole antenna. The antenna butt-end became the short-circuited plunger and it is possible to expect the essential reflection of a surface wave. Such reflection can change a cross profile of created plasma, and it is essential to affect on efficiency of energy transfer from magnetron to plasma and magnetron operation regime. The energy deposition to a neutral gas also becomes periodic function of longitudinal coordinate. Under these conditions the problems (•••) and (••••) is planned to consider analytically and then to include them in numerical discharge model. One of the problems is the analysis of a surface wave reflection from butt-end of the different shape antenna with the purpose to achieve minimum wave reflection coefficient.

The propagated surface wave energy, absorbed per unit plasma length, can be expressed through an energy flux density along the antenna

$$W_{\text{abs}} = 2W \operatorname{Im} h(n_e) \quad (2.103)$$

that allows by virtue of a requirement (2.102) to calculate power necessary for maintaining of the surface discharge plasma with density  $n_e$ :

$$W = \frac{n_e w_1}{2 \operatorname{Im} h(n_e)}, \quad (2.104)$$

where  $w_1$  is the power expended for creation of one free electron. The calculated dependencies (2.104) in relative units for the different values of ratio  $\nu/\omega$  of collision frequency  $\nu$  to microwave field frequency  $\omega$  is represented in Fig. 2.9.

The joint solution of the equation (2.104) and Maxwell equations allows to receive approximate dependence of plasma parameters on the propagated surface microwave power flow.

Distribution of surface wave power along a plasma slab one can find from the equation:

$$\frac{dW(z)}{dz} = -2 \operatorname{Im}(h(n_e(W(z))))W(z) \quad (2.105)$$

The equation (2.105) is equivalent to the equation for electron density:

$$\frac{dn_e(z)}{dz} = -\frac{2 \operatorname{Im}(h(n_e(z)))}{\frac{d}{dn_e} \ln(W(n_e(z)))}, \quad (2.106)$$

where the dependence  $W(n_e(z))$  is shown in Fig. 2.9. We neglect wave reflection from back butt-end of plasma. It is obviously possible if the wave does not reach the butt-end of the antenna.

The calculated dependencies of plasma density on coordinate  $Z$  along the antenna are given in Fig. 2.10. In summary on Fig. 2.11-2.14 the results of calculation of distribution of a very high frequency field in neighbourhood vicinity of the antenna at different integrated electron densities in plasma  $n_e/n_{ec}$  are submitted. The existence of a diffusive layer on border of plasma is not taken into account. As well as it was necessary to expect, at  $n_e \rightarrow \infty$  field allocation comes nearer to allocation in a metal wave guide.

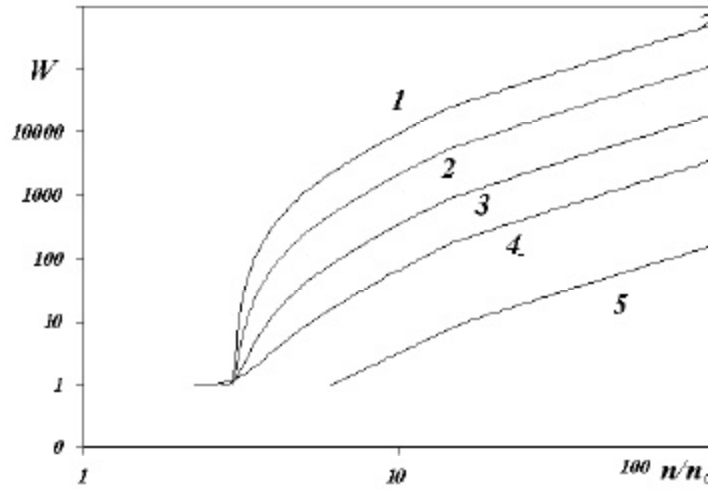


Fig. 2.9. Electrons density to electrons critical density ratio  $n_e/n_{ec}$  as a function of power  $W$  (in relative units) of a surface wave propagated along the antenna at different collision frequencies  $\nu/\omega$ : 1–0.01; 2–0.03; 3–0.1; 4–0.3; 5–1.

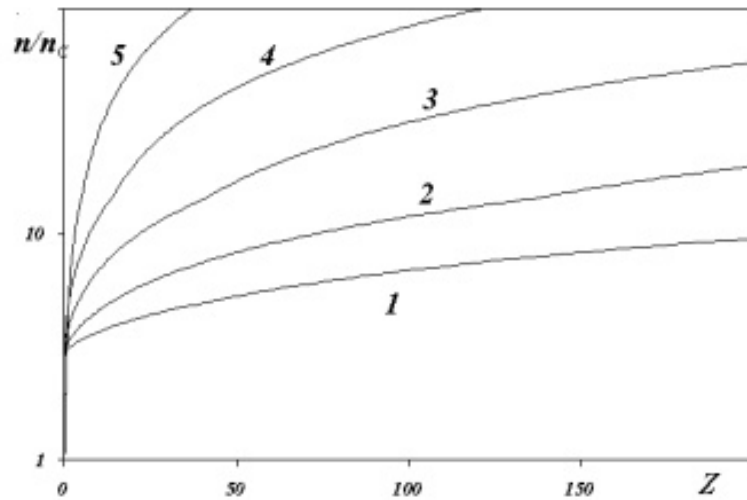


Fig. 2.10. Electrons density to electrons critical density ratio  $n_e/n_{ec}$  as a function of coordinate  $Z$  at different frequencies of collisions  $\nu/\omega$ : 1 – 0.01; 2 - 0.03; 3 – 0.1; 4 – 0.3; 5 – 1.0.

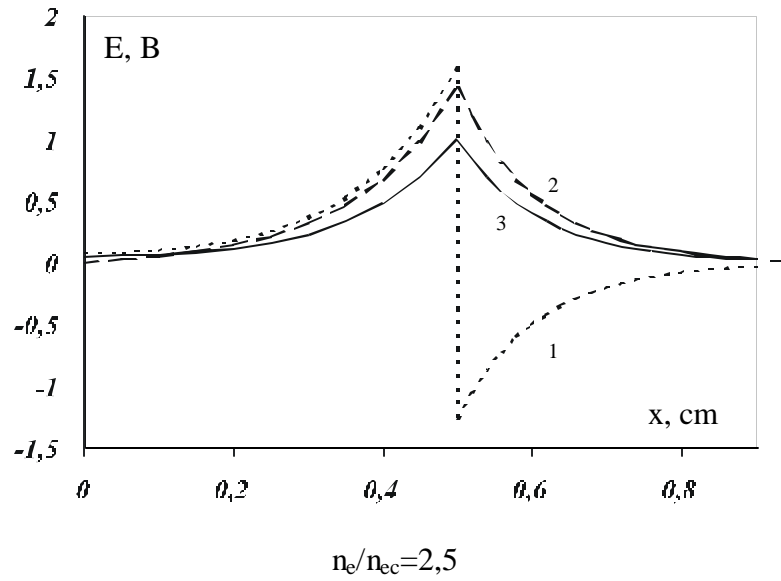


Fig. 2.11. A space distribution of electrical ( $E_y$ , - curve (1) and  $E_z$  - curve (2)) and magnetic ( $B_y$  - curve (3)) fields in a surface wave.

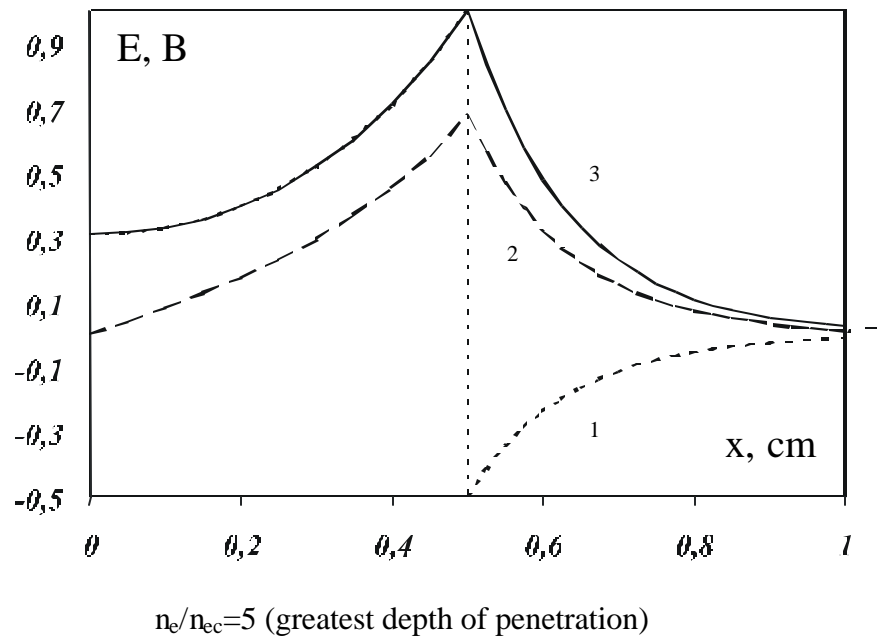


Fig. 2.12. A space distribution of electrical ( $E_y$ , - curve (1) and  $E_z$  - curve (2)) and magnetic ( $B_y$  - curve (3)) fields in a surface wave.

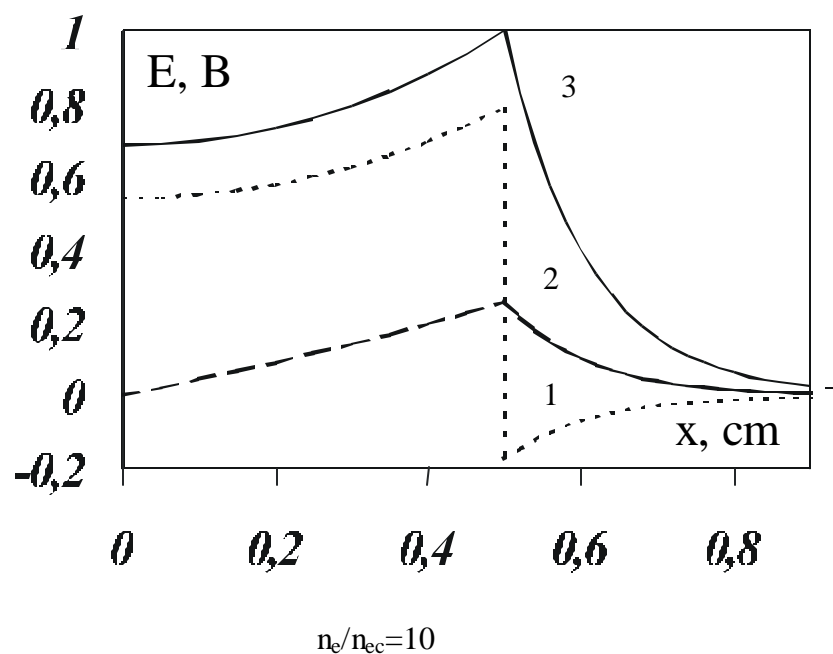


Fig. 2.13. A space distribution of electrical ( $E_y$ , - curve (1) and  $E_z$  - curve (2)) and magnetic ( $B_y$  - curve (3)) fields in a surface wave.

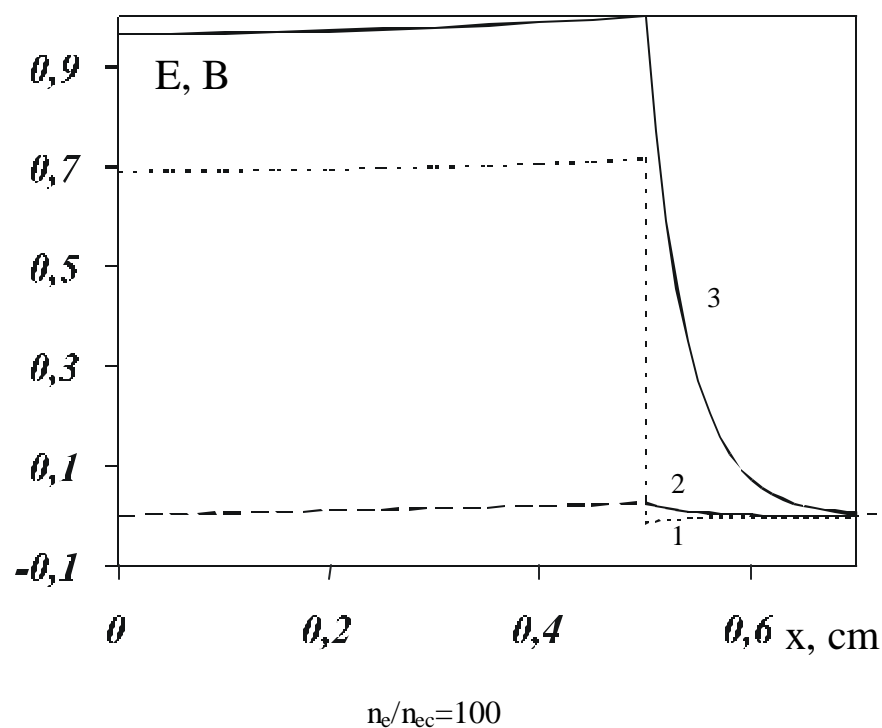


Fig. 2.14. A space distribution of electrical ( $E_y$ , - curve (1) and  $E_z$  - curve (2)) and magnetic ( $B_y$  - curve (3)) fields in a surface wave.

## CHAPTER III

### EXPERIMENTAL INSTALLATIONS

#### 3.1. Experimental set-up

The experimental set up is based on a stainless steel cylindrical gas/vacuum chamber three meters long with about a meter in diameter (Fig.3.1). Supersonic airflow can be organized in it. Twenty six windows with different diameters (10-50 cm) are situated on its lateral surface, that has allowed to visualize the discharge processes and to provide a vacuum-tight transport of electric current and electric signals. The gas/vacuum chamber consists of two sections that can form a vacuum-tight junction with help of a lever-operated gate. At installation and adjustment of diagnostic and experimental equipment inside the chamber its sections can be easily separated. A vacuum pump has allowed to achieve a pressure level of 1 torr for 10-15 minutes of pumping.

The supersonic airflow was formed at filling the chamber with the atmospheric air through specially profiled converging-diverging nozzles with Mach number  $M=2$ . A detailed calculation of the nozzle shape has been carried out. The nozzle convergent part was made close to the ideal form providing a plane  $M=1$  interface. The walls near the critical cross section had a sharp edge. The angle of the wall of the divergent part near the critical cross section was calculated from the theoretical formulae with use of the gas dynamic functions. The whole profile of the divergent part was calculated to obtain the output parallel supersonic airflow. This uniform  $M=M_0$  airflow region in case of negligible pressure in the vacuum chamber is restricted by a surface with a shape of two Mach angle cones based on the nozzle exit circle; upstream  $M<M_0$ , downstream  $M>M_0$ . The nozzles were made of a dielectric (caprolactone). A cylindrical nozzle had an outlet diameter 3 cm and a diameter 15.4 mm of critical cross section. The characteristic period of time of regular nozzle operation was about 2 second.

The nozzles were screwed on a dielectric tube 5 cm in diameter. On its opposite end a electric hydraulic valve with  $\varnothing 5$  cm channel was fixed. All this construction was installed on a flange of a window of the chamber so that to position the supersonic airflow along the chamber's diameter. The nozzle end was situated on the level of big transparent windows on the lateral surface of the chamber. The electric hydraulic valve operated with a power supply unit which was synchronized with the discharge power supply units.



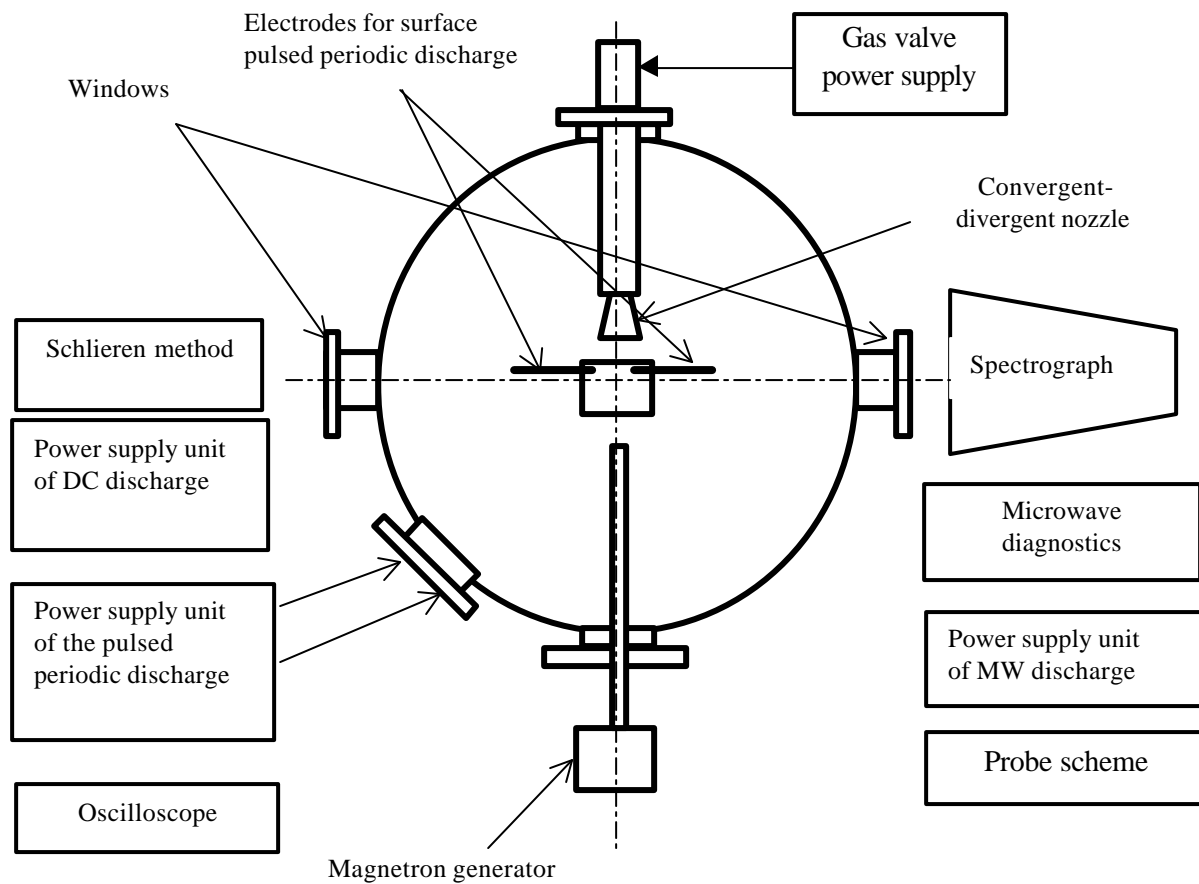


Fig.3.1. General scheme of the experimental set up

The experimental set up was equipped with different types of diagnostics.

A Schlieren device with  $\varnothing 15$  cm outlet lens was used for visualization of the free supersonic airflow and of the discharges in it. An electric incandescent lamp with radiating body area about  $1 \text{ mm}^2$  was used as a light source for adjustment of the device. At registration of the airflow gas dynamical structure a pulsed ( $\tau=5 \text{ }\mu\text{s}$ ) xenon lamp was applied.

A spectrograph STE-1 and monochromator MDR-3 were used for registration of plasma radiation spectra. Either a highly sensitive photo film, or a CCD image sensor was fixed in the focal plane of the spectral devices. For an experimental investigation of a surface microwave discharge in supersonic flow it is necessary to use contactless methods and the optical diagnostics of plasma fully satisfy this requirement. The vibrational temperature  $T_v$  was measured by the relative intensity of the nitrogen and CN bands. The gas temperature  $T_g$  was determined by the distribution of the intensity of rotational lines of molecular bands of a second positive system of nitrogen.

Double ray pulsed oscilloscopes with pass band 10 MHz and sensitivity 1 mV/cm were used for registration of the discharge voltage characteristics and the electric photomultiplier tube signals.

For obtaining of the threshold characteristics of a surface microwave discharge the dependencies of the minimum input power, at which the discharge on an external surface of a dielectric body starts to be formed, on different values of air pressure in a vacuum chamber and on different durations of microwave pulses were measured. In experiments the moment of formation of the discharge was registered visually or on appearance of a signal on the screen of a double-beam oscilloscope from the collimated photoelectric multiplying tube, tuned on area of the antenna at an edge of a waveguide. Thus, on the second beam of an oscilloscope the signal from a microwave detector was applied. The amplitude of this signal was proportional to a pulsed microwave power.

The common view of a surface microwave discharge was registered on a film and a video camera in two projections (side view and top view). It has allowed to fix the longitudinal size of a surface discharge and to measure longitudinal velocity of its distribution at different air pressures, pulse durations and microwave powers.

For measurement of gas and vibration temperatures under condition of the surface microwave discharge in supersonic airflow, a diagnostic set up has been assembled. Radiation of the discharge that is formed in supersonic airflow, is projected on input slots of two spectral devices through the windows of chamber, the mirrors, and the focusing quartz lenses. The lens diameter and its focal length were chosen so that to provide projection of the discharge image

with reduction  $k=10$ , and use of all the light-gathering power of the devices. A spectrograph STE-1 and monochromator MDR-3 were used, their inverse linear dispersions being 0.35 and 1.3 nm/mm accordingly for the spectral region of 3000-6000 Å°. The measuring system (including the spectrograph STE-1, monochromator MDR-3 and the photo film) was calibrated by registration of standard iron arc spectrum (to get a wavelength scale) through a 9-step light reducer (to reveal the linear region of film darkening) on the same photo film together with the tested spectrum. The photo films were analysed with use of a microphotometer IFO-451.

The electronic analyzer of optical spectra on base of a personal computer registers plasma radiation in visible, ultraviolet and infrared spectral ranges. The system is designed on base of an IBM-compatible personal computer. The sensor of plasma radiation on base of a CCD image sensor forms a video signal directly proportional to the radiation intensity in the spectral band 3000-9000 Å°. The video signal is coded by an analog-to-digital converter situated on an Interface card and is sent to the PC memory as an array of data. The discharge spectra can be visualized on the monitor or printed out with use of program codes. The system can operate in two regimes: synchronous and asynchronous. At synchronous operation the pulses of discharge are synchronized with the CCD cycles of exposition and pickup. This regime makes it possible to research pulsed discharges or to integrate the information on pulsed-periodical discharges. The asynchronous operation yields spectra that are averaged during all the time of exposition.

The video signal formed by the CCD is passed to a broad-band differential amplifier for compensation of a constant component and amplification to the level sufficient for further coding by the analog-to-digital converter. Drivers of digital signals are necessary for formation of CCD controlling pulses.

The interface card contains a 12-bit analog-to-digital converter, a quartz generator and a scheme of generation of synchronizing pulses for controlling of CCD, a universal parallel interface of control of executive devices (valves, pumps etc.) and an interface logic for fitting the card with the ISA bus.

### **3.2. Set-up for creation of surface microwave discharge**

The system of creation of the surface microwave discharge in a boundary layer near to the bodies streamlined supersonic airflow was designed and manufactured. The modernization of the microwave generator used for creation of the surface microwave discharge inside a boundary layer, existing near bodies of different configuration streamlined supersonic airflow, is carried out. The experimental set-up is completed with the system of creation of supersonic airflow; the

special system of input of a microwave energy into discharge chamber and transformations of the microwave energy into the energy of a surface wave; the system of recording of the parameters of microwave radiation and supersonic airflow, the diagnostic instrumentation for measuring of plasma parameters of the discharge and for recording of the photo and video information about common view of the surface microwave discharge in supersonic airflow.

The pulsed magnetron generator of a centimetric wave frequency was used as a source of a microwave energy. The magnetron generator had the following characteristics: the wavelength  $\lambda=2,4$  cm; the pulsed microwave power  $W<600$  kW; the pulse duration  $\tau=1\div300$   $\mu$ s; the pulse period-to-pulse duration ratio  $Q=1000$ .

A pulsed modulator with the partial discharge of capacity, developed in our laboratory, was used for a feeding of magnetron. The work of the pulse modulator is based on a principle of rather long accumulation of energy during a pause between pulses and short-term its feedback to microwave generator during a pulse. The microwave energy introduced into the vacuum discharge chamber by the waveguide system of rectangular section  $9,5\times19$  mm through the directional coupler. All waveguide system was hermetic. It was filled by  $\text{SF}_6$  at pressures up to 5 atmospheres for avoidance of an electrical breakdown. The discharge was formed in a cylindrical chamber. The vacuum system allowed to investigate the surface microwave discharge at air pressures  $p=1,0\text{--}760$  torr. The waveguide entered into the discharge chamber ended the special antenna, on which the surface microwave discharge in supersonic airflow was created. The discharge was formed on an external surface of a dielectric body of rectangular section  $S=1\times2$  cm and length  $L=15$  cm. The direction of supersonic flow was opposite to the direction of the surface microwave discharge spreading.

The output signal from the microwave detector was registered on an oscillograph. The form of this signal was close to rectangular. The same signal acted on an input of the pulse digital voltmeter, under which indications the amplitude of a microwave pulse was determined. By meanings of this amplitude the microwave power supplied to the discharge chamber was measured. For it, the calibration of the voltmeter with the help of the power calorimeter was previously made. During calibration the power calorimeter was connected to an output of the basic shoulder of the directional branching-off.

The new set-up for realization of the investigations of the surface microwave discharge in large range of gas pressures  $p=10^{-3}\text{--}10^3$  torr is designed and assembled. The set-up consists of the vacuum booster pump permitting to execute the preliminary pumping-out of the discharge chamber up to pressures  $\sim 10^{-1}$  torr; the vacuum turbomolecular pump for pumping-out of the discharge chamber up to pressures  $\sim 10^{-5}$  torr; the glass discharge chamber with 35 cm in

diameter and 50 cm in length. The chamber has a metal flange for connection with the pumping and inlet gas system. The set-up has the system of measurement of gas pressure, the system of the supply of a microwave energy to dielectric bodies, the system of input into the discharge chamber of the dipole antenna and electrical probe permitting to measure of distributions of the electric field and electron concentration in zone of existence of plasma of the surface discharge.

### **3.3. Set-up for creation of surface transversal pulsed-periodical discharge**

The supply unit for obtaining the pulsed-periodic discharge on a surface of a plate placed at supersonic airflow is designed and created. The parameters of the supply unit allow to create the surface discharge in supersonic airflow at two modes:

1. A mode of single pulsed discharge at voltage  $U=3-25$  kV, current  $i=0,1-40$  A, pulse duration  $\tau=1\ \mu\text{s} - 1\ \text{ms}$ , maximal pulsed power  $W_p \leq 1\ \text{MW}$ .
2. A mode of pulsed-periodic discharge at voltage  $U=3-25$  kV, current  $i=0,1-10$  A, pulse duration  $\tau=1-300\ \mu\text{s}$ , pulse repetition frequency  $f=1-100\ \text{Hz}$ , mean power consumption about 1 kW.

The system of creation of a pulsed-periodic discharge on a surface of a dielectric plate streamlined supersonic airflow was designed and manufactured. The high-voltage pulses at  $U=1-25$  kV with the help of a high-voltage cable through the specially designed a vacuum cut-off point is lead to electrodes fixed into a dielectric plate. The special measures for avoidance of an electrical breakdown on the opposite surface of a dielectric plate outside of supersonic flow are undertaken. The plate can be installed under different angles to the direction of supersonic airflow.

### **3.4. Automated circuit of probe measuring**

The automated circuit of probe measuring with the optical isolator is designed and manufactured. The block-scheme of this circuit is submitted on Fig. 3.2.

The probe current signal from the resistor  $R$  feeds to an inlet of the agreeing amplifier for amplification up to value sufficient for effective coding by an analog-digital converter (ADC). In the experiment 12-bit 4096 levels the analog-digital converter are used. The time resolution of ADC is  $2\ \mu\text{s}$ . The signals from the analog-digital converter go to the optopair galvanic isolation scheme and further are transmitted in a computer memory. The transmission of the signals from

an analog-digital converter into the computer through the optical isolator takes place in parallel way. Accordingly, in the circuit 12 optopairs are utilized that allows to not reduce the operating speed of the scheme. The delay time in the optopair galvanic isolation scheme does not exceed  $9\text{ }\mu\text{s}$  and the permissible maximum voltage on its isolation is 7 kV. The potential difference between a probe and antiprobe (or between two probes) is generated by the computer. This potential difference is transmitted in a digital to analog converter (DAC) through the optopair galvanic isolation scheme and further through a compounding output equipment feeds to the probes. The time resolution of the DAC is  $0,5\text{ }\mu\text{s}$ , therefore the basic time is determined by the time resolution of the optopair galvanic isolation scheme. Thus, the cycle time, i.e. the time interval at which the circuit is ready to new measuring is  $20\text{ }\mu\text{s}$  at the intrinsic time of measuring of a signal of a current  $t=2\text{ }\mu\text{s}$ .

In the standard version the scan of voltages is linear with sampling of a step. The range of a voltage variation is situated in limits  $\pm 27\text{ V}$ , the minimum value of a step equals 15 mV. The scan of a voltage between probes in principle also can be set arbitrary, according to the program assigned to the computer.

The synchronizing circuit allows to synchronize the pulse of formation of the discharge with a cycle of measuring. It enables synchronously to store the information on a pulsed-periodical discharge.

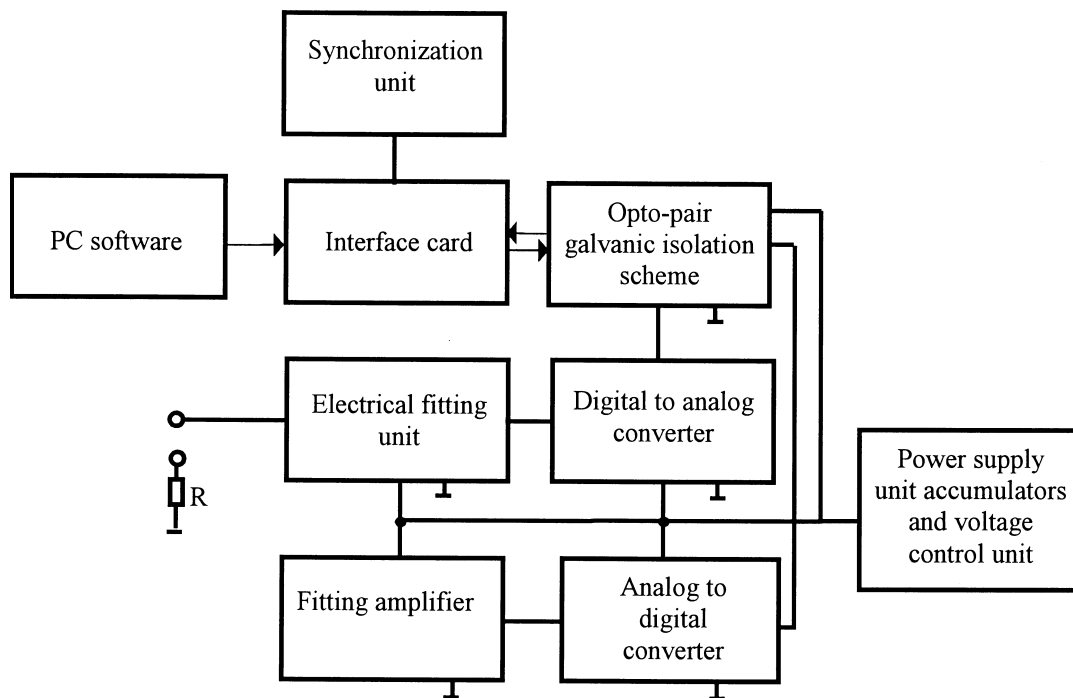


Fig. 3.2. Draft design of the set-up for measurement of voltage-current characteristic of the double probes.

## **CHAPTER IV**

### **DIAGNOSTICS METHODS**

#### **4.1. Probe application for diagnostics of the surface microwave discharge in supersonic flow**

The probe method permitting to conduct the measurements of local plasma parameters, is represented by the convenient tool of examination of the surface microwave discharges. It is concerned with the fact that the inhomogeneity of plasma parameters in a direction both perpendicular, and parallel surface of a dielectric surface is reference feature of such discharges.

However the probe method for diagnostics of such type of the discharge was not applied yet. Therefore for its correct application it is necessary to analyze problems not only interpretations of obtained results, but also technique of probe measurements, i.e. select of an electric scheme of a probe circuit, probe construction and sizes.

At measurements in a microwave plasma it is necessary to take into account that for a contact method, what is a probe method, the registration of action of a very high frequency field is principal moment. Especially it is important in a case of large pressure, as the very high frequency power which is necessary for creation of the surface microwave discharge grows with pressure.

Thus two major factors can be essential.

At first, it is the action of a very high frequency electric fields on a probe as a metal conductor. At application of probes, connected with recorded instrumentation by the radio-frequency cables, the difficulties arise. They are bound up with the fact that the conductors, placed at strong alternating fields, are the passive electrical vibrators.

Basically it can result in to occurrence around them the secondary discharges and essential change of the distribution of parameters of explored plasma. This influence is most essential in a high frequency region. However in conditions of a very high microwave powers, taking place in experiment, the elimination of this factor is advisable. Besides in conditions of very high microwave powers it is desirable to remove the recorded instrumentation on large enough distance.

The second factor is bound to action of a very high frequency electric field on a probe layer.



Due to effect of detection on a non-linearity of a probe layer of the variable electromotive force, existing between plasma and ground, a noticeable additional current, distorting a true current-voltage characteristic of a probe, appears in a probe circuit.

It is impossible to eliminate this effect completely. For its minimization a voltage divider on an alternating current on microwave frequency is organized. At this sequentially with a probe the filter, which impedance is much more than an impedance of a probe, is included. As a rule, the quarter wave short-circuited coaxial line, as such device in a microwave, is utilized [1]. However the probe should be prolongation of this line, otherwise the filter will be shunted. Therefore, the line should be placed in supersonic stream. However sizes of a line multiply exceed the size of a probe and on an order of magnitude are comparable with a dimensions of a plate. Apparently, it will lead in strongest deformation of stream, therefore it is impossible to use such approach.

Let's take into account, that the distorted influence of a microwave field of the discharge takes place only in the area of non-linearity of current-voltage characteristic of a probe. As a rule, the non-linearity is bound up with an electronic branch of current-voltage characteristic of probe. In plasma of low pressure this branch is most informative, allowing in a number of cases to measure not only temperature of electrons, but also electron energy distribution function. In a mode of a continuous medium the electronic branch of current-voltage characteristic of probe can give the information only about conductance of plasma, i.e. information, to within a portion of negative ions, does not distinguish from an ionic branch. The ionic part of current-voltage characteristic of a probe in supersonic flow at large pressures, as a rule, is close to linear [2]. Therefore the utilization of this part of the characteristic allows substantially to remove a problem of distortion of current-voltage characteristic.

It is known [2], that the diameter of a probe being flown about of supersonic stream should be selected minimum, if only the mode of a continuous medium was executed. However the high concentration of charged particles is feature of the surface microwave discharge. Therefore at a select of an ionic branch of current-voltage characteristic the value of a useful signal will be sufficient.

As the probe circuit should be closed one, in addition to probe the supporting probe should be placed into explored plasma. Arrangement of the supporting probe on a plate will give in deformation of the surface microwave discharge, therefore the supporting probe needs to be disposed in plasma. Taking into account, that we were restricted to an ionic branch, for minimization of gasdynamic perturbations it is more convenient to use a double probe. It is possible considerably to reduce the perturbations of investigated system and recording

instrumentation, about what was spoken above. For it an optical control by probe power supply and an optical transfer to the recording instrumentation the information about a probe current and voltage is used.

Then the scheme of the measurement of the plasma parameters under conditions of the surface microwave discharge practically will not differ from the scheme of a double probe with the optical isolator, designed within the framework of the ISTC projects #1867p [2].

The difference is bound up with the fact that the typical size of the surface microwave discharge in a direction, perpendicular surface of the antenna is equal some millimetres. If you want to use a spherical probe, its size should be the tenth of millimetre. However the size of a leg-holder then should be the 100-th shares of millimetre. The application of such construction under condition of supersonic flow practically is impossible. As a matter of fact, the unique solution in an explored situation is the application of a double cylindrical probe oriented along a surface of a plate, on which the surface microwave discharge is created. However in order to use the theory of an ionic current on a single probe under conditions a double probe, it is necessary, that the interference of probes was minimum. In practice it is reached by removal of probes on distance about  $10R$  (where  $R$  is probe radius), i.e. several millimetres. This value is not far from the size of the discharge in a transverse direction, therefore such construction of a probe is unacceptable. Therefore, it is possible the application only of double cylindrical symmetric probes oriented along supersonic stream. At this the plane of probes arrangement is parallel the plane of a discharge surface.

The conditions of operation of a probe outside of a boundary layer of a discharge surface being flown about are close to conditions, which were considered in the ISTC project #1867p [2]. However it is necessary to expect, that the properties of plasma will change noticeably inside a boundary layer at approaching to a surface. Apart from change of a degree of ionization of plasma and temperature its components, it is possible change of a composition of plasma because of an ablation of a surface. Besides arrangement of probes along a stream does not allow directly to utilize results, obtained in [2] for probes oriented across of a stream. The correct interpretation of obtained probe characteristics requires the special additional investigations.

## **4.2. Spectral methods of measurement of gas temperature**

Information about gas translation temperature  $T_g$  is important for study of plasma processes. The simplest possible case for molecular plasma corresponds to local thermodynamic equilibrium, then  $T_g = T_v = T_R$ , here  $T_v$  and  $T_R$  are vibration and rotation temperatures,

respectively.  $T_V$  and  $T_R$  are parameters of fitting of population of vibration and rotation energy states of molecules to the Boltzmann function, they characterise distribution function of molecules. Both  $T_V$  and  $T_R$  can be extracted from plasma radiation spectra.

In non-equilibrium plasmas  $T_g$  can be also determined on base of measurement of  $T_R$ . Spectra of plasma radiation provide information about rotation temperatures  $T_R^*$  of molecules in excited electron states. The dependence of  $T_R^*$  on intensity of a rotation structure spectral line  $I_{lk}$ , that corresponds to a transition between  $l$ -th and  $k$ -th states is given by a formula

$$\frac{k_B}{B^*} \ln \frac{I_{lk}}{i v_{lk}^4} = C - \frac{1}{T_R^*} j(j+1), \quad (4.1)$$

here  $k_B$  is the Boltzmann constant,  $j$  is a total molecular moment of momentum,  $i$  is a quantum mechanical coefficient of intensity,  $v_{lk}$  is the frequency of radiation quantum,  $C$  is a constant. One can extract  $T_R^*$  by plotting a function  $(k_B/B^*) \ln(I_{lk}/i v_{lk}^4)$  over  $j(j+1)$ , and measuring its slope  $\tan \alpha$ :

$$T_R^* = \frac{1}{\tan \alpha}. \quad (4.2)$$

For a stable molecule a possibility of change its rotation energy at excitation is negligible, and rotation distribution functions for excited and basic molecular states are identical,  $T_R = T_R^*$ . Effective exchange of translation and rotation energies at collisions results in equality of  $T_g$  and  $T_R$  of molecules in basic electron state. But at realistic conditions there are some peculiarities that must be paid account to. If molecules take part in plasma chemical reactions, a part of their activation energy can transfer to rotation energy, that results in distortion of initial rotation distribution function, and  $T_R \neq T_R^*$ . It is especially characteristic to chemically active radicals. Another source of errors is bound with the fact that spectra yield not  $T_R$  but  $B^*/T_R$ , here  $B^*$  is the rotation constant for upper state at radiation transition. At electron impact excitation of this state, rotation energy distribution can be conserved, but it corresponds to a temperature

$$T_R = T_g \frac{B^*}{B^0} \quad (4.3)$$

here  $B^0$  is the rotation constant for the basic state.

Thus, stable molecules with  $B^* \approx B^0$  should be chosen for measurement of  $T_g$ . The second positive band of nitrogen is widely used. Here one can take  $v_{lk}^4$  to be a constant (the corresponding error  $\approx 0.5\%$  is negligible),  $B^* = 1,826$ ; the formula for  $T_R$  looks like

$$0,89 \lg \frac{I_{ik}}{i} = C - \frac{1}{T_R} j(j+1). \quad (4.4)$$

In number of work it is suggested to determine the gas temperature of nitrogen at high pressure on base of unresolved cyan bands with threshold wavelengths  $3883\text{\AA}$  and  $3871\text{\AA}$ . At the present experiments cyan is generated at model erosion. Three ways of temperature measurement are available. These methods are based on: 1) – ratio of integrals of radiation of the two bands; 2) – ratio of threshold intensities of these bands; 3) – distribution of rotation transition intensities of (0;0) band with threshold wavelength  $3883\text{\AA}$ .

### 4.3. Spectral methods of measurement of vibration temperature

Vibration excitation in a molecular plasma as a rule affects ionization and gas heating. There is a method of determination of vibration levels population of nitrogen basic electron state  $X^1\Sigma_g^+$ . It is based on a measurement of radiation intensities in bands of the second positive nitrogen system. Conditions are pointed out, at which the electron state  $C^3\pi_u$  is populated due to electron impact excitation of the basic  $X^1\Sigma_g^+$  state. De-excitation of vibration levels of the state  $C^3\pi_u$  is bound with radiation, because its characteristic time ( $10^{-7}$  s) is much less than that of vibration and rotation relaxation and of diffusion.

Let the vibration levels  $v_X''$  of the basic nitrogen electron state are distributed according to a function  $f(v_X'')$ , i.e.

$$n(v_X'') = n_0 f(v_X''). \quad (4.5)$$

Then in case the conditions mentioned above are met, a stationary population of  $C^3\pi_u$  vibration levels  $v_C'$  is given by

$$n_{v_C'} = \frac{n_e n_0}{A_{v_C' v_B'}} \sum_{v_X''} \langle \sigma v_{v_C' v_X''} \rangle f(v_X''), \quad (4.6)$$

here  $n_0$  is a number of molecules in  $X^1\Sigma_g^+$  state with  $v_X'' = 0$ ;  $\langle \sigma v \rangle_{v_C' v_X''}$  is a mean cross section of excitation of  $v_C'$   $C^3\pi_u$  levels,  $n_e$  is electron concentration,  $A_{v_C' v_B'}$  is a probability of radiation of the second positive nitrogen system,  $v_X''$  are vibration quantum numbers of  $B^3\pi_g$  state.

As the process of excitation of the  $C^3\pi_u$  vibration levels due to electron impact of the basic  $X^1\Sigma_g^+$  state is fast in comparison with vibration period, these probabilities can be

considered to be in a direct proportion to the Franck-Condon coefficients for the Tanaka system  $C^3\pi_u \rightarrow X^1\Sigma_g^+$ . Then the previous equation takes form

$$n_{v_C'} = C \sum_{v_X''} q_{v_C'v_X''} f(v_X''), \quad (4.7)$$

here  $C$  is a constant independent on  $v_X''$ . At computation of the sum one can take only first 5 terms, because the population of the vibration levels is a steep falling function of  $v$ . Provided relative populations of the first 5 levels of the  $C^3\pi_u$  state are known, one can calculate relative populations  $v_X''$  of the basic electron states as a solution of a set of equations

$$n_{v_C'} = \alpha \sum_{v_X''=0}^4 q_{v_C'v_X''} n_{v_X''}, \quad (4.8)$$

here  $\alpha$  is a normalizing coefficient. The relative populations of the  $C^3\pi_u$  state levels can be determined experimentally with application of a usual method (on base of relative intensities of bands of the second positive nitrogen system  $C^3\pi_u \rightarrow B^3\pi_g$ ).

Molecular spectroscopy gives the following formula for a radiation intensity of a electron-vibration band:

$$I_{v_C'v_B''} = C' S_e n_{v_C'} v_{v_C'v_B''}^4 q_{v_C'v_B''}, \quad (4.9)$$

here  $S_e$  is a strength of electron transition,  $q_{v_C'v_B''}$  are the Franck-Condon factors,  $v_{v_C'v_B''}$  is a frequency of transition,  $C'$  is a constant independent on the quantum numbers  $v_C'$  and  $v_B''$ . After taking logarithm, one can get

$$\ln(n_{v_C'}) = \ln(C') + \ln \frac{I_{v_C'v_B''}}{v_{v_C'v_B''}^4 q_{v_C'v_B''}}. \quad (4.10)$$

Thus, one can get the relative populations  $v_X''$  and the vibration temperature of the nitrogen basic electron state on base of measurement of relative intensities of the electron-vibration bands  $v_C'$ .

direction of supersonic airflow at air pressure  $p=40$  torr, voltage on the discharge gap  $U=15$  kV, discharge current  $i=10$  A, and different values of gas velocity in supersonic airflow. The common view of the discharge in supersonic airflow on a surface of a dielectric body are given on Fig.5.22. It does not differ from the common view of the volumetric discharge in supersonic airflow. Without supersonic airflow the discharge represents the plasma channel existing on a surface of a dielectric body between two electrodes, fixed in a dielectric flush with a surface. The supersonic flow leads to blowing of plasma jets from each of electrodes which are overlapped among themselves downstream. The length of each jets depends on pulse duration, gas pressure, velocity of supersonic flow, and energy supplied into the discharge.

The electron density, measured by probe method under condition transversal pulsed-periodical surface discharge, changed from  $\sim 10^{11} \text{ cm}^{-3}$  at discharge current  $i=0.5$  A up to  $\sim 10^{13} \text{ cm}^{-3}$  at  $i=20$  A.

The time evolutions of the gas temperature of surface pulsed-periodic discharge on the surface of a flat plate at different values of discharge current is represented on Fig. 5.23. One can see, that at pulse duration  $\tau=100 \mu\text{s}$  the gas temperature increases from  $\sim 500$  K at discharge current  $i=0.7$  A up to  $\sim 3000$  K at  $i=18$  A.

The dependence of the gas heating rate on discharge current under condition of surface pulsed-periodic discharge on the flat plate is given on Fig.5.24. One can see, that under our conditions the gas heating rate grows with increasing of discharge current. This dependence very well coordinates with the gas heating rate dependence obtained from the non-stationary kinetical model worked out by us [9].

The vibrational temperature as a function of discharge current is represented on Fig.5.25. One can see that the vibrational temperature approximately equals 5000 K and almost does not dependent on discharge current under experimental conditions.

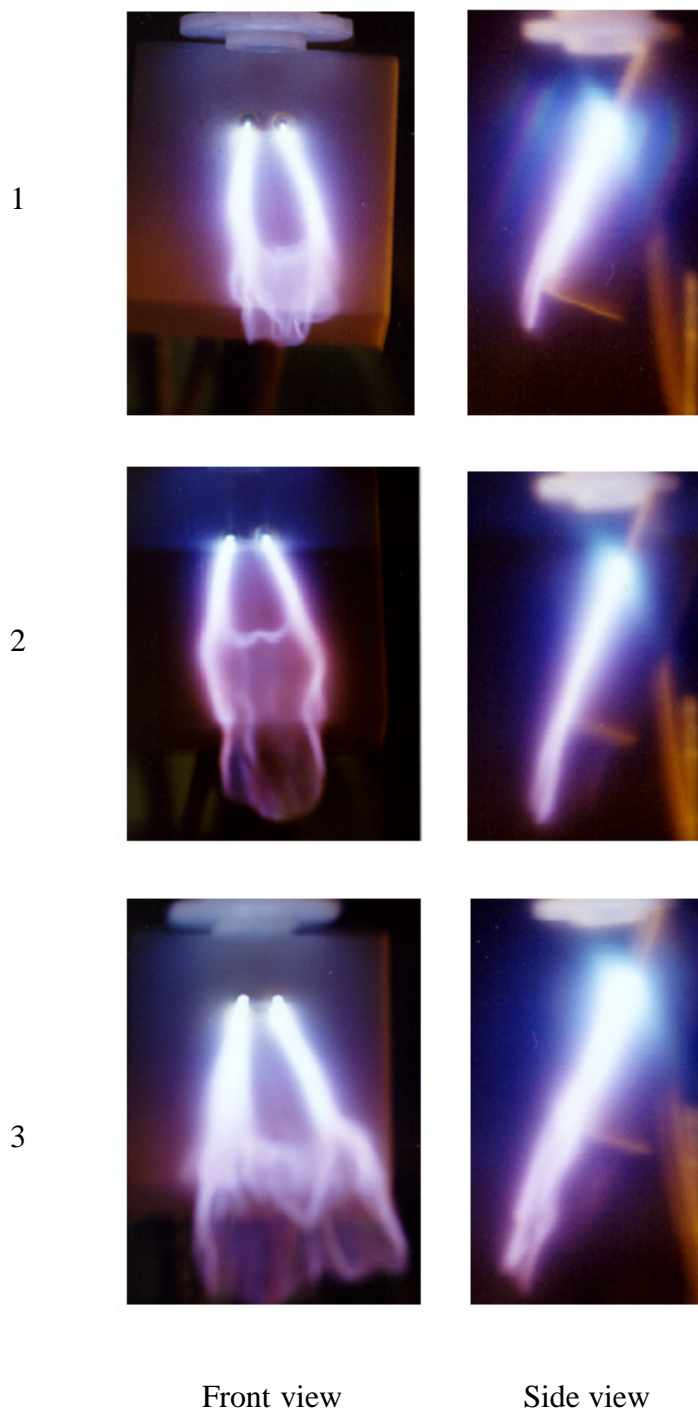


Fig.5.22. The common view of the pulsed-periodic discharge in supersonic airflow on a surface of flat plane at different values of air pressure in the high-pressure system  $p$ , atm: 1-1; 2-3; 3-6.

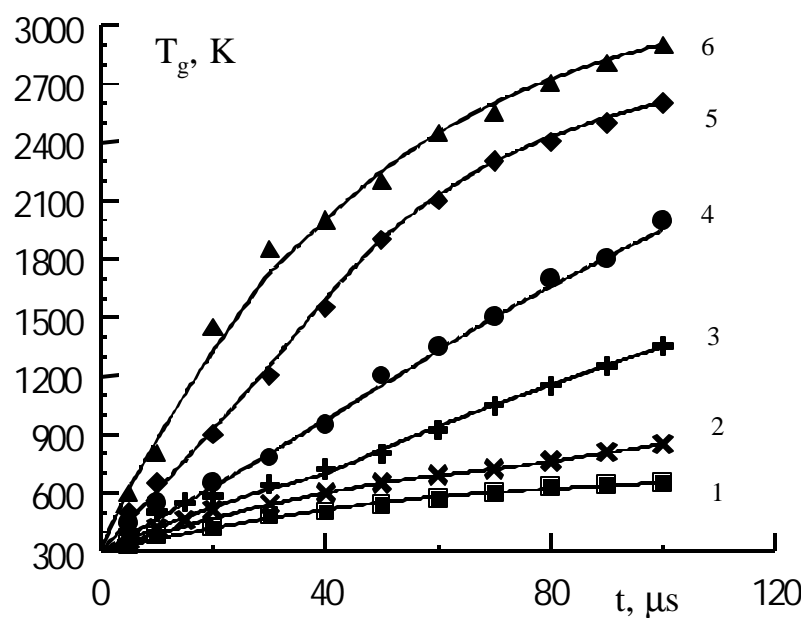


Fig.5.23. The gas temperature of surface pulsed-periodic discharge on the flat plate at different values of discharge current  $i$ , A: 1 – 0.7; 2 – 1.5; 3 – 3.0; 4 – 6.0; 5 – 9.0; 6 – 18.

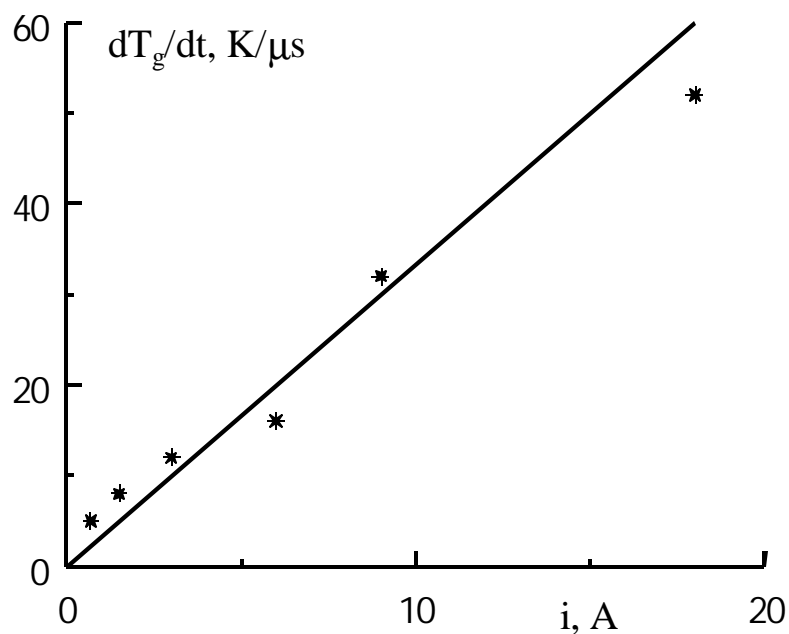


Fig.5.24. Dependence of the gas heating rate on discharge current under condition of surface pulsed-periodic discharge on the flat plate.



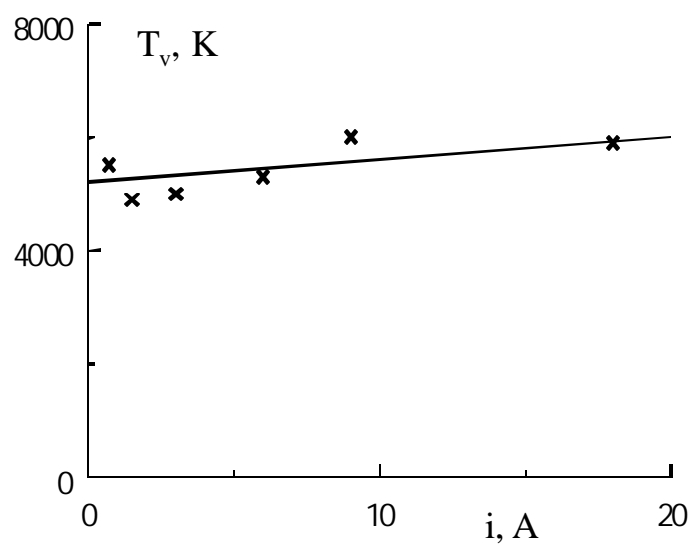


Fig.5.25. Dependence of the vibrational temperature on discharge current under condition of surface pulsed-periodic discharge on the flat plate.

## CONCLUSIONS

1. The literature review on the subject of the Project is carried out. The different regimes of action on laminar - turbulent transition and turbulent boundary layer resulting in to reduction of friction at subsonic and supersonic motion of flight vehicles in the Earth's atmosphere are analysed. The different ways of additional energy supply into a turbulent boundary layer are examined. The different modes of the gas discharges creation into a boundary layer are considered. The methods of plasma creation on the bodies surfaces with the help of the surface microwave discharges are examined.
2. The mathematical model of the discharge grounded on the joint solution of the balance equations of charged particles and Maxwell equations for an electromagnetic field are worked out. The theoretical analysis ensures following results: the calculation of the dispersion curves of a surface wave taking into account inhomogeneity of a plasma layer (self-consistent solution with the ionised non-linearity); the calculation of a field penetration depth in plasma and thickness of a plasma layer created by both direct and reflected surface waves, in dependence on wave amplitude and frequency, and also gas pressure and airflow velocity; the dependence of longitudinal length of the discharge supported by a surface wave from power, transferred by a microwave; the analysis of requirements of electromagnetic waves reflection from antenna butt-end at the different shape of the latter; the analysis of two dimensional field structure in a plane of the antenna.
3. The modernization of the discharge chamber available in laboratory is carried out with the purpose of creation of the surface microwave and pulsed-periodic discharges in supersonic airflow at gas pressure  $p=1-760$  torr. The system of formation of supersonic gas flow and the special system of input of a microwave energy into discharge chamber and transformations of the microwave energy into the energy of a surface wave is installed on the discharge chamber. The method of probe measurements of the charged particles concentration under conditions of surface microwave discharge plasma was worked out. It is shown that the perturbations of researched system and distortion of the probe characteristics can considerably be reduced by excluding the radio-frequency cables from constructions of devise and by supplied optical management of a probe feeding and transfer of the information about a probe current and voltage into the recording equipment. The automated circuit of probe measuring with the optical isolator is designed and manufactured. In the experiment 12-bit 4096 levels the analog-digital converter are used.

4. The surface microwave discharge on a dielectric antenna with length  $L=15$  cm of rectangular section  $S=1.2$  cm<sup>2</sup> is created at air pressure  $p=10^{-3}$ - $10^3$  torr. The magnetron generator had the following characteristics: the wavelength  $\lambda=2.4$  cm; the pulsed microwave power  $W=10$ - $300$  kW; the repetition frequency  $f=1$ - $100$  Hz; the pulse duration  $\tau=1$ - $300$   $\mu$ s; the pulse period-to-pulse duration ratio  $Q=1000$ . At air pressure  $p>1$  torr the discharge represents thin (thickness  $\Delta h=0.1$ - $1.0$  mm) plasma layer uniformly coating all antenna surface. The examination of dynamics of the discharge has shown that velocity of propagation of the discharge and its longitudinal length depend on microwave pulse duration and input power. Thus, on an initial stage of the discharge the velocity of its distribution reaches  $v\sim 10^7$  cm/s, that are much greater than the airflow velocity ( $v_f=5\cdot 10^4$  cm/s) under experimental conditions. The discharge propagation velocity decreases up to  $v\sim 10^4$  cm/s to the end of the microwave pulse with duration  $\tau=100$   $\mu$ s. The threshold characteristic of the surface microwave discharge appearance are determined. It is shown, that at air pressure  $p=0.1$ - $10$  torr the power necessary for creation of the surface microwave discharge is minimum and equals  $\sim 10$  kW.
5. In plasma of the surface microwave discharge the electron density, gas and vibrational temperature are measured at different values of gas pressure and microwave power. The electron density equals  $6\cdot 10^{12}$  cm<sup>-3</sup>. At growth of power the gas temperature is increased from  $\sim 500$  K at  $W=35$  kW up to  $\sim 1700$  K at  $W=175$  kW, whereas vibrational temperature remains practically constant under these conditions, insignificantly decreasing with increase of microwave power. At this the maximal gas heating is observed in a place of excitation of a surface microwave discharge and gas temperature decreases by the end of the discharge. On the initial stage of existence of the surface microwave discharge the fast gas heating with rate  $dT_g/dt=50$  K/ $\mu$ s is observed. It was shown, that the mechanism connected to effective excitation of electron-excited states of nitrogen molecules at large values of the reduced electrical field  $E/n\geq 100$  Td= $10^{-15}$  V·cm<sup>2</sup> and their subsequent quenching is responsible for the fast heating. At this the part of excitation energy of these states is transferred in the heat of air. As our estimations show, only the quenching of electron-excited long-living states of nitrogen molecules, which are effectively created in conditions of a surface microwave discharge in air, provides the gas heating rate.
6. The surface microwave discharges in supersonic airflow with Mach number of flow  $M=2$  are created. It was shown, that the supersonic flow of air at Mach number  $M=2$  does not influence on the common view of the surface discharge on the dielectric antenna of

rectangular section and on the microwave power which is necessary for creation of the surface microwave discharge. Thus the threshold of appearance of a surface microwave discharge does not depend on whether at first the discharge on a surface of a dielectric body is created and then the supersonic airflow is included or, on the contrary, at first the supersonic airflow is included, and only then the surface microwave discharge is created.

7. The system of creation of a pulsed-periodic discharge on a surface of a dielectric plate streamlined supersonic airflow was designed and manufactured. The high-voltage pulses at  $U=1-25$  kV with the help of a high-voltage cable through the specially designed a vacuum cut-off point is lead to electrodes fixed into a dielectric plate. The special measures for avoidance of an electrical breakdown on the opposite surface of a dielectric plate outside of supersonic flow are undertaken. The plate can be installed under different angles to the direction of supersonic airflow.
8. The surface pulsed-periodic discharge in supersonic airflow was created on a dielectric plate placed at the angle of approximately twenty degrees to the direction of supersonic airflow at air pressure  $p=40$  torr, voltage on the discharge gap  $U=15$  kV, and discharge current  $i=10$  A. The common view of the discharge in supersonic airflow on a surface of a dielectric body does not differ from the common view of the volumetric discharge in supersonic airflow. Without supersonic airflow the discharge represents the plasma channel existing on a surface of a dielectric body between two electrodes, fixed in a dielectric flush with a surface. The supersonic flow leads to blowing of plasma jets from each of electrodes which are overlapped among themselves downstream. The length of each jets depends on pulse duration, gas pressure, velocity of supersonic flow, and energy deposition in the discharge. The electron density, measured by probe method under condition transversal pulsed-periodical surface discharge, changed from  $\sim 10^{11} \text{ cm}^{-3}$  at discharge current  $i=0.5$  A up to  $\sim 10^{13} \text{ cm}^{-3}$  at  $i=20$  A. The time evolutions of the gas temperature of surface pulsed-periodic discharge on the surface of a flat plate at different values of discharge current is obtained. It is shown, that under experimental conditions the gas heating rate grows with increasing of discharge current. The vibrational temperature approximately equals 5000 K.

## REFERENCES

### References to chapter I

1. International Space Planes and Hypersonic System and Technologies Conference. Workshop on Weakly Ionized Gases. Proceedings: Colorado, USA, AIAA-1997; Norfolk, USA, AIAA-1998; Norfolk, USA, AIAA-99.
2. The First and Second Workshops on Magneto- and Plasma Aerodynamics for Aerospace Applications. Proceedings: Mocsow, Russia, IVTAN-1999; Mocsow, Russia, IVTAN-2000.
3. A.Yu.Gridin, B.G.Efimov, A.V.Zabrodin, et.al. Preprint Keldish Institut Prikladnoi Mekhaniki RAN, No 19, 1995 (In Rus).
4. A.F.Alexandrov, I.B.Timofeev, S.N.Chuvashev. Bezudarnoe sverkhzvukovoe dvizhenie v atmosfere: printsipialnaya vozmozhnost i prakticheskaya realizatsiya. -Prikladnaya Fizika. 1996, No 3, p.112-117 (In Rus).
5. S.N.Chuvashev, A.P.Ershov, A.I.Klimov, S.B.Leonov, V.M.Shibkov, I.B.Timofeev. Flow around body and characteristics of AD/CD discharges in plasma aerodynamic experiment. Proceedings Norfolk, VA, 1998.
6. Lowry, J.Blanks, C.Stepanek, M.Smith, L.Crosswy, P.Sherrouse, J.Felderman. Characterization of the shock structure of a spherical projectile in weakly ionized air through ballistic range test technique. Proceedings Norfolk, VA, 1998.
7. L.M.Biberman, V.S.Vorob'ev, I.T.Yakubov. Kinetika neravnovesnoi nizkoterperaturnoi plasmi. Moscow: Nauka, 1982 (In Rus).
8. A.S.Zarin, A.A.Kuzovnikov, V.M.Shibkov. Freely localized MW discharge in air. Moscow: Oil & Gas. 1996, 204 p (In Rus).
9. V.M.Batenin, I.I.Klimovskii, P.V.Lisov, V.N.Troitskii. Sverkhvisokochastotnie generatori plasmi. Moscow: Energoatomizdat. 1988 (In Rus).
10. P.L.Kapitsa. Svobodnii plasmennii shnur v visokochastotnom pole pri visokom davlenii. – Zhurnal eksperimentalnoi i teoreticheskoi fiziki, 1969, vol.57, No 6(12), p.1801-1866 (In Rus).
11. J.Allison, A.L.Cullen, A.A.Zavody. A microwave plasma discharge. -Nature, 1962, vol.193, No 4811, p.72.
12. W.E.Scharfman, W.C.Taylor, T.Morita. Breakdown limitations on the transmission of microwave power through the atmosphere. -IEEE Trans. on Antennas and Propagation. 1964, vol.AP-12, No 6, p.709.

13. A.M.Devyatov, A.A.Kuzovnikov, V.V.Lodinev, V.M.Shibkov. The mechanism of molecular gas heating in a pulsed free-localizing RF discharge. -Moscow University Physics Bulletin. Fizika, 1991, vol.46, No 2, p.28-31.
14. A.A.Kuzovnikov, V.M.Shibkov, L.V.Shibkova. Free-localized pulse-periodic MW discharge in air. Kinetics of gas heating. -High Temperature, 1996, vol.34, No 3, p.343-348.
15. V.M.Shibkov. Free-localized pulse-periodic MW discharge in air. Electric field strength in plasma. -High Temperature, 1996, vol.34, No 4, p.519-524.
16. A.A.Kuzovnikov, V.M.Shibkov, L.V.Shibkova. Kinetics of charged particles in a free-localized pulse-periodic MW discharge in air. -High Temperature, 1996, vol.34, No 5, p.651-655.
17. A.V.Kalinin, V.M.Shibkov, L.V.Shibkova. Vliyanie kisloroda na kinetiku nagreva molekulyarnogo gasa v azotno-kislorodnoi smesi. –Vestnik Moskovskogo Universiteta. Seriya 3, Fizika, astronomiya, 1996, No 1, p.38-42 (In Rus).
18. V.V.Zlobin, A.A.Kuzovnikov, V.M.Shibkov. Concentration of electrons in a stimulated MW discharge channel in nitrogen. -Moscow University Physics Bulletin. Fizika, 1988, vol.43, No 1, p.98-100.
19. V.V.Lodinev, V.M.Shibkov, L.V.Shibkova. Gas heating kinetics in pulse-periodic air discharge. -Moscow University Physics Bulletin. Fizika, 1996, vol.51, No 2, , p.26-31.
20. A.A.Kuzovnikov, V.M.Shibkov, L.V.Shibkova. Kinetics of electrons in plasma of discharge, created in free space by focused microwave beam. -Zhurnal Tekhnicheskoi Fiziki, 1997, vol.67, No 6, p.10-14 (In Rus).
21. A.F.Alexandrov, A.S.Zarin., A.A.Kuzovnikov, V.M.Shibkov, L.V.Shibkova. Plasma parameters of non-consistent microwave discharge, created in programmable pulse. - Zhurnal Tekhnicheskoi Fiziki, 1997, vol.67, No 7, p.19-23 (In Rus).
22. V.M.Shibkov. Heating of gas under conditions of free-localized microwave discharge in air. Mathematical simulation. -High Temperature, 1997, vol.35, No 5, p.681-689.
23. V.M.Shibkov. Heating of gas under conditions of free-localized microwave discharge in air: Experiment. -High Temperature, 1997, vol.35, No 6, p.858-862.
24. Yu.V.Zlobina, V.M.Shibkov, L.V.Shibkova. Kinetics of heating and dissociation of molecules in pulsed discharge in hydrogen. –Fizika plasmi, 1998, vol.24, No 7, p.667-671 (In Rus).
25. A.V.Kazakov, M.N.Kogan, V.A.Kuparev. Delay of laminar-turbulent transition by means of intensive localized heating of the surface in the vicinity of the leading edge of the plate. - High Temperature, 1996, vol.34, No 1, p.42-47.

26. A.A.Pilipenko, G.K.Shapovalov. Upravlenie sostoyaniem pograničnogo sloya putem vvedeniya iskusstvennikh vozmushenii. –Uchenie zapiski TsAGI, 1986, vol.17, No 4, p.73-78 (In Rus).
27. Yu.S.Kachanov, V.V.Kozlov, V.Ya.Levchenko. Vozniknovenie turbulentnosti v pograničnom sloe. -Novosibirsk, Nauka, 1982, 151p (In Rus).
28. A.V.Kazakov, M.N.Kogan, V.A.Kuparev. Laminirizatsiya pograničnogo sloya pri otritsatel'nom gradiente davleniya i nagreve poverkhnosti. –Teplofizika visokikh temperatur, 1996, v.34, No 2, p.244-249 (In Rus).
29. V.V.Kozlov. Physics of flow structures. Flow separation. –Soros Education Journal, 1998, No 4, p.86-94.
30. V.V.Kozlov. Otriv potoka ot perednej kromki i vliyanie na nego akusticheskikh vozmushenii. –Prikladnaya mekhanika i tekhnicheskaya fizika. 1985, No 2, p.112-115 (In Rus).
31. A.A.Maslov, N.A.Semenov. Vozbuzhdenie sobstvennikh kolebaniy pograničnogo sloya vneshnim akusticheskim putem. –Mekhanika zhidkosti i gasa. 1986, No 3, p. (In Rus).
32. A.V.Kazakov, M.N.Kogan, V.A.Kuparev. Ob ustojchivosti dozvukovogo pograničnogo sloya pri nagreve poverkhnosti ploskoi plastini vblizi perednei kromki. –Izvestiya AN SSSR. Mekhanika zhidkosti i gasa, 1985, No 3, p.68 (In Rus).
33. A.V.Kazakov, M.N.Kogan, A.P.Kuryachii. O vliyaniy lokal'nogo nagreva poverkhnosti na trenie v turbulentnom pograničnom sloe na plastine. -Teplofizika visokikh temperatur, 1995, v.33, No 6, p.888-894 (In Rus).
34. A.V.Kazakov, A.P.Kuryachii. The effect of viscous-nonviscous interaction on turbulent flow past a plate under conditions of local heating of its surface. -High Temperature, 1998, vol.36, No 3, p.395-400.
35. Yu.V.Lapin. Turbulentnii pograničnii sloi v sverkhzvukovikh potokakh gasa. -Moscow: Nauka, 1982. 312 p (In Rus).
36. C.Carvin, J.F.Debieve, A.J.Smits. The Near-Wall Temperature Profile of Turbulent Boundary Layer. -AIAA Paper. 1988, No 136, 8 p.
37. A.V.Kazakov, M.N.Kogan, A.P.Kuryachii. Vliyanie na trenie lokal'nogo podvoda tepla v turbulentnii pograničnii sloi. –Izvestiya RAN. Mekhanika zhidkosti i gasa, 1997, No 1, p.48 (In Rus).
38. A.V.Kazakov, M.N.Kogan, A.P.Kuryachii. The effect of the thermal properties of a body being flown about on friction and heat transfer under conditions of local heat input to a turbulent boundary layer. -High Temperature, 1997, v.35. No 1, p.61-66.

39. Chien K.Y. Prediction of Channel and Boundary-Layer Flows with a Low-Reynolds-Number Turbulence Model. -AIAA Journal, 1982, vol. 20, No 1, p.33.
40. M.Moisan, C.M.Ferreira, Y.Hajlaoui, D.Henry, J.Hubert, R.Pantel, A.Ricard, Z.Zakrzewski. Properties and applications of surface wave produced plasmas. -Revue Phys. Appl., 1982, vol.17, p.707-727.
41. M.Moisan, Z.Zakrzewski. -J. Phys. D: Appl. Phys., 1991, vol. 24, p.1025.
42. S.Daviaud, C.Boisse-Laporte, P.Leprince, J.Marec. Description of surface-wave-produced microwave discharge in helium at low pressure in the presence of a gas flow. -J.Phys.D: Phys. Appl., 1989, vol.22, p.770-779.
43. A.Granier, C.Boisse-Laporte, P.Leprince, J.Marec, P.Nghiem. Wave propagation and diagnostics in argon surface-wave discharges up to 100 Torr. -Phys. Appl., 1989, vol.20, p.204-209.
44. A.Granier, C.Boisse-Laporte, P.Leprince, J.Marec, E.Dervisevic. Microwave discharges produced by surface waves in argon gas. -Phys. Appl., 1987, vol.20, p.197-203.
45. C.Boisse-Laporte, P.Leprince, J.Marec, R.Darchicourt, S.Pasquiers. Influence of the radial electron density profile on the determination of the characteristics of surface-wave-produced discharges. -Phys. Appl., 1988, vol.21, p.293-300.
46. M.Moisan, C.M.Ferreira The similarity laws for the maintenance field per electron in low-pressure surface wave produced plasmas and their extension to HF plasmas in general. - Physica Scripta, 1998, vol.38, p.382-399.
47. J.Marec, P.Leprince. Recent trends and developments of microwave discharges. -Journal de Physique IV. France, 1998, vol.8, Pr7-21-32.
48. M.Moisan, C.Beaudry, P.Leprince. -IEEE Trans.Plasma Sci., 1975, PS-3, p.55.
49. M.Moisan, Z.Zakrzewski, R.Pantel. -J.Phys.D, 1979, vol.12, p.219.
50. M.Moisan, Z.Zakrzewski. -Microwave excited plasmas (Amsterdam Elsevier 1992), p.92.
51. J.Marec, P.Leprince. -Microwave discharges: Fundamentals and applications, C.M.Ferreira and M.Moisan Eds. (New York and London Plenum, 1993), p.45.
52. C.Boisse-Laporte. -Microwave discharges: Fundamentals and applications, C.M.Ferreira and M.Moisan Eds. (New York and London Plenum, 1993), p.25.
53. Z.Rakern, P.Leprince, J.Marec. -Rev. Phys. Appl., 1990, vol.25, p.125.
54. Z.Rakern, P.Leprince, J.Marec. -J. Phys. D: Appl. Phys., 1992, vol.25, p.953.
55. C.M.Ferreira. -J. Phys. D: Appl. Phys., 1989, vol.22, p.705.
56. U.Kortshagen, H.Schluter, A.Shivarova. -J. Phys. D: Appl. Phys., 1991, vol.24, p.1571.
57. U.Kortshagen, H.Schluter, A.Shivarova. -J. Phys. D: Appl. Phys., vol.24, p.1585.



58. C.Boisse-Laporte, P.Leprince, J.Marec. -CIP 95, Xth. Int. Coil., Antibes, 1995.
59. S.Bechu, C.Boisse-Laporte, P.Leprince, J.Marec. -AVS 43rd Symp., Philadelphia, 1996.
60. S.Bechu, C.Boisse-Laporte, J.Marec. -J. Vac. Sci. Technol., 1997, vol. A15.
61. Ohl A. Fundamentals and limitations of large area planar microwave discharges using slotted waveguides. -Journal de Physique IV. France, 1998, vol.8, Pr7-83-98.
62. M.Moisan, C.Barbeau, R.Claude, C.M.Ferreira, J.Margot, J.Paraszczak. A.B.Sa, G.Sauve, M.R.Wertheuner. -J. Vac. Sci. Technol., 1991, vol. B9, p.8-25.
63. M.Kummer. -Mikrowellentechnik (Verlag Technik, Berlin, 1986), p. 40-41.
64. D.Korzec, F.Werner, R.Winter, J.Engemann. -Plasma Sources Sci. Technol., 1996, vol.5, p.216-234.
65. T.Yasui, J.Kitayama, H.Tahara, T.Yoshikawa. Production of wide plasmas using microwave slot antennas on a rectangular waveguide. -Proceedings ICRP-2/SPP-11, Yokohama 19-21 January 1994, T. Goto Ed. (Organizing Committee of ICRP-2/SPP-11, Yokohma, 1994), p.367-370.
66. A.Ohl. Large area planar microwave discharges. -Microwave Discharges: Fundamentals and Applications, C.M. Ferreira and M. Moisan Eds. (Plenum Press, New York and London, 1993), p.205-214.
67. Z.Zakrzewski, M.Moisan. -Plasma Sources Sci. Technol., 1995, vol.4, p.379-397.
68. W.H.Watson. The physical principles of wave guide transmission and antenna systems (University Press, Oxford, 1949), p. 80-154.
69. G.Sauve, M.Moisan, Z.Zakrzewski. -J. Microwave Power Electromagn. Energy, 1993, vol.28, p.123-131.
70. M.Wakatsuchi, S.Ishii, Y.Kato, F.Tani, M.Sunagawa. -Plasma Sources Sci. Technol., 1996, vol.5, p.327-332.
71. M.Nagatsu, G.Xu, M.Yamaga, M.Kanoh, H.Sugai. -Jpn. J. Appl. Phys., 1996, vol.35, L341.
72. P.Werner, D.Korzec, J.Engemann. -Plasma Sources Sci. Technol., 1994, vol.3, p.473.
73. Z.Zakrzewski, M.Moisan. -Plasma Sources Sci. Technol., 1995, vol.4, p.379.
74. Z.Zakrzewski, M.Moisan. Linear field applicators. -Journal de Physique IV. France, 1998, vol.8, Pr7-109-118.
75. E.Rauchle. Duo-plasmaline, a surface wave sustained linearly extended discharge. -Journal de Physique IV. France, 1998, vol.8, Pr7-99-108.
76. K.Komachi. -J. Vac. Sci. Technol., 1994, vol.A12, p.769.
77. T.Kiimura, Y.Yoshida, S.Mizuguchi. -Jpn. J. Appl. Phys., 1995, vol.34, L1076.
78. Y.Yoshida, Y.Miyazawa, A.Kazama. -Rev. Sci. Instrum., 1997, vol.68, p.1.

79. Y.Yoshida. -Journal de Physique IV. France, 1998, vol.8, Pr7-195-203.

## References to chapter II

1. H.Schluter. Self-consistent modeling of surface wave sustained discharges. -Journal de Physique IV. France, 1998, vol.8, Pr7-43-60.
2. Z.Zakrzewski, M.Moisan. Linear field applicators. -Journal de Physique IV. France, 1998, vol.8, Pr7-109-120.
3. S.A.Dvinin, V.A.Dovzhenko, G.S.Solntsev. Ob izmerenii energeticheskikh kharakteristik SVCH razryada pri razvitii ionizatsionnoi neustoichivosti na poverkhnostnoi volne. -Fizika plasmi, 1983, vol.9, No 5, p.1058-1067 (In Rus).
4. S.A.Dvinin, V.A.Dovzhenko. Diffusive propagation of ionization front in UHF wave field. Fizika plasmi, 1988, vol.14, No 1, p. 66–76 (In Rus).
5. T.A.Grotjohn. Modeling electromagnetic fields for the excitation of microwave discharges used for material processing. -Journal de Physique IV. France, 1998, vol.8, Pr7-61-82.
6. E.Rauchle. Duo-plasmaline, a surface wave sustained linearly extended discharges. -Journal de Physique IV. France, 1998, vol.8, Pr7-83-99.
7. A.Kh.Mnatsakanyan, G.V.Naidis. Processes of formation and loss of charged particles in nitrogen-oxygen plasma. In book: Khimiya plasmi. Vipusk 14. Pod redaktsiei B.M.Smirnov. Moscow. Energoizdat, 1987 (In Rus).
8. O.E.Krivososova, S.A.Losev, V.P.Nalivayko et al. -In book: Khimiya plasmi. Vipusk 14. Pod redaktsiei B.M.Smirnov. Moscow. Energoizdat, 1987 (In Rus).
9. C.Park. -AIAA Rep. 89-1740, 1989.
10. I.A.Kossyi, A.Yu.Kostinsky, A.A.Matveyev et al. -Plasma Sources Sci. Technol., 1992, vol.1, p.207.
11. N.L.Aleksndrov, E.M.Bazelyan. -J. Phys. D: Appl. Phys., 1996, vol.29, p.2873.
12. N.L.Aleksndrov, E.M.Bazelyan, N.A.Dyatko, I.V.Kochetov. -J. Phys. D: Appl. Phys., 1997, vol.30, p.1616.
13. E.M.Bazelyan, Yu.P.Raizer. Intergrowth of the streamer channel: a field and density of plasma behind a wave of ionization, initial electrons before it. -High temperature, 1997, vol.35, p.181–186.
14. N.L.Aleksndrov, E.M.Bazelyan, N.A.Dyatko, I.V.Kochetov. Streamer break-down of lengthy air gaps. -Plasma phys. report, 1998, vol. 24, No7, p.587–602.
15. K.U.Riemann. -J. Phys D: Appl. Phys. 1991, vol. 24, p.1991.

16. K.B.Riemann. -Physics of plasmas, 1997, vol.4, p.4158.
17. Alexandrov A.F., Rukhadze A.A. "Lectures on Electrodynamics of Plasma-like Media", Moscow, Pub. House Moscow University, 1999 (In Rus).
18. Alexandrov A.F., Bogdankevich L.S., Rukhadze A.A. "Waves and Oscillations in Plasma-like Media", Moscow, Pub. House Moscow University, 1990 (In Rus).
19. Alexandrov A.F., Bogdankevich L.S., Rukhadze A.A. "Principles of Plasma Electrodynamics", Moscow, Pub. House "Visshay Skola" (1978, 1988), English Trans. "Springer Verlag", Heidelberg (1984).
20. Ginzburg V.L., Rukhadze A.A. "Waves in Magnetoactive Plasma", Moscow, Pub. House "Nauka" (1970, 1975); English trans. Hand Physics v.49, "Springer Verlag", (1972).
21. Kondratenko A.N. Surface and Volume waves in restricted plasma. Energoatomizdat, 1985 (In Rus).
22. Kondratenko A.N. Electromagnetic field penetration into plasma. Energoatomizdat, 1979 (In Rus).
23. Kondratenko A.N. Surface waves in plasma. Atomizdat, 1976 (In Rus).
24. Zhelyazkov I., Atanassov V. Axial structure of low pressure high frequency discharges, sustained by travelling electromagnetic surface wave. Physics reports, 255, 1995, p.79-201.
25. Microwave plasma and its application. Ed. Yuri Lebedev. Moscow, Moscow Physical society, 1995.
26. Microwave discharge and its applications. III International workshop. Ed. C. Bousse-Laport, J. Marec. J de physique IV, v.8, pr7, Oct 1998.
27. Felsen L., Marcuvitz N. Radiation and Scattering of waves. Prentice-Hall, Inc., Englewood Cliffs, New Jersey, 1973.
28. Zeldovich Ya.B., Rayzer Yu.P. Fizika udarnihk voln i vysokotemperaturnihk gazodinamicheskikh yavleniy. Moscow: Nauka, 1966 (In Rus).
29. Alexandrov A.F., Rukhadze A.A. Fizika silnotochnihk elektrorazryadnihk istochnikov sveta. Moscow: Nauka, 1966 (In Rus).
30. Granovskiy V.L. Elektricheskiy tok v gaze. Ustanovivshiysya tok. Moscow: Nauka, 1971. p.253.
31. Ginzburg V.L. Propagation of electromagnetic waves in plasma Moscow: Nauka, 1965 (In Rus).
32. Denisov N.G. About one feature of an electromagnetic wave field propagating in inhomogeneous plasma. Sov. Phys: ZhETP, 1956, p.1931 (In Rus).

33. V.N.Ponomarev, G.S.Solntsev. -Jurnal Tekhnicheskoi Fiziki. 1966, vol.36, (Sov. Phys., JTP, 1966, v.36).
34. A.G.Boev. To the theory of nonlinear surface waves in plasma. -Sov. Phys. JETP, 1979, v.77, No 1, p.92-100.
35. A.G.Boev. To the nonlinear theory of penetration of p-polarized electromagnetic waves in plasma. -Sov. Phys. JETP, 1980, v.79, No 1(7), p.134-142.
36. A.G.Boev. Threshold values of plasma electronic density created by an electromagnetic field. -Dokladi AN USSR, Seriya ?, 1981, No 2, p.65-67 (In Rus).
37. A.G.Boev. Plasma column formed by a running ionizing electromagnetic wave. -Fizika plazmi, 1982, v.8, No 4, p.729-735 (In Rus).
38. V.B.Gildenburg, A.V.Kochetov, A.G.Litvak, A.M.Feigin. Self-sustaining waveguide channels in plasma. -Sov. Phys. JETP, 1983, v.84, No 1 (In Rus)
39. Braginskiy S.I. Yavleniya perenosa v plasme. Voprosi teorii plazmi. 1964, v.1, p.183–272 (In Rus).
40. Gurevich A.V., Shvartsburg A.B. Nelineynaya teoriya rasprostraneniya radiovoln v ionosfere. Moscow: Nauka, 1973, p.221 (In Rus).
41. Kim A.V., Frayman A.G. Fizika plazmi, 1983, v.9, No.3, p.619 (In Rus).
42. Kostinsky A.Y., Matveev A.A., Silakov V.P. Kinetical processes in the non-equilibrium nitrogen-oxygen plasma. Moscow.: Academy of sciences of the USSR. General physics institute. Plasma physics division. Preprint ? 87. 29. p. 1990.

#### **References to chapter IV**

1. Ivanov Yu.A., Lebedev Yu.A., Polak L.S. Methods of contact diagnostics in non-equilibrium plasmachemistry. Moscow, Nauka, 1981 (In Rus).
2. Ershov A.P. Final scientific report on ISTC project #1867p between International Science and Technology Center, Department of Physics of Moscow State University and the European Office of Aerospace Research and Development (EOARD), 2001.

#### **References to chapter V**

1. Zarin A.S., Kuzovnikov A.A., Shibkov V.M.. Freely localized microwave discharge in air. - Moscow: Oil and gas, 1996, 204p (In Rus).
2. Shibkov V.M. -High Temperature. 1997, 35, No.5, p.681.

3. Shibkov V.M. -High Temperature. 1997, 35, No.6, p.858.
4. Shibkov V.M. Kinetics of gas heating in plasma created in supersonic airflow. -9<sup>th</sup> Intern. Space Planes and Hypersonic Systems and Technologies Conf. Norfolk, Virginia, USA, 1999, AIAA-99-4965.

direction of supersonic airflow at air pressure  $p=40$  torr, voltage on the discharge gap  $U=15$  kV, discharge current  $i=10$  A, and different values of gas velocity in supersonic airflow. The common view of the discharge in supersonic airflow on a surface of a dielectric body are given on Fig.5.22. It does not differ from the common view of the volumetric discharge in supersonic airflow. Without supersonic airflow the discharge represents the plasma channel existing on a surface of a dielectric body between two electrodes, fixed in a dielectric flush with a surface. The supersonic flow leads to blowing of plasma jets from each of electrodes which are overlapped among themselves downstream. The length of each jets depends on pulse duration, gas pressure, velocity of supersonic flow, and energy supplied into the discharge.

The electron density, measured by probe method under condition transversal pulsed-periodical surface discharge, changed from  $\sim 10^{11} \text{ cm}^{-3}$  at discharge current  $i=0.5$  A up to  $\sim 10^{13} \text{ cm}^{-3}$  at  $i=20$  A.

The time evolutions of the gas temperature of surface pulsed-periodic discharge on the surface of a flat plate at different values of discharge current is represented on Fig. 5.23. One can see, that at pulse duration  $\tau=100 \mu\text{s}$  the gas temperature increases from  $\sim 500$  K at discharge current  $i=0.7$  A up to  $\sim 3000$  K at  $i=18$  A.

The dependence of the gas heating rate on discharge current under condition of surface pulsed-periodic discharge on the flat plate is given on Fig.5.24. One can see, that under our conditions the gas heating rate grows with increasing of discharge current. This dependence very well coordinates with the gas heating rate dependence obtained from the non-stationary kinetical model worked out by us [9].

The vibrational temperature as a function of discharge current is represented on Fig.5.25. One can see that the vibrational temperature approximately equals 5000 K and almost does not dependent on discharge current under experimental conditions.

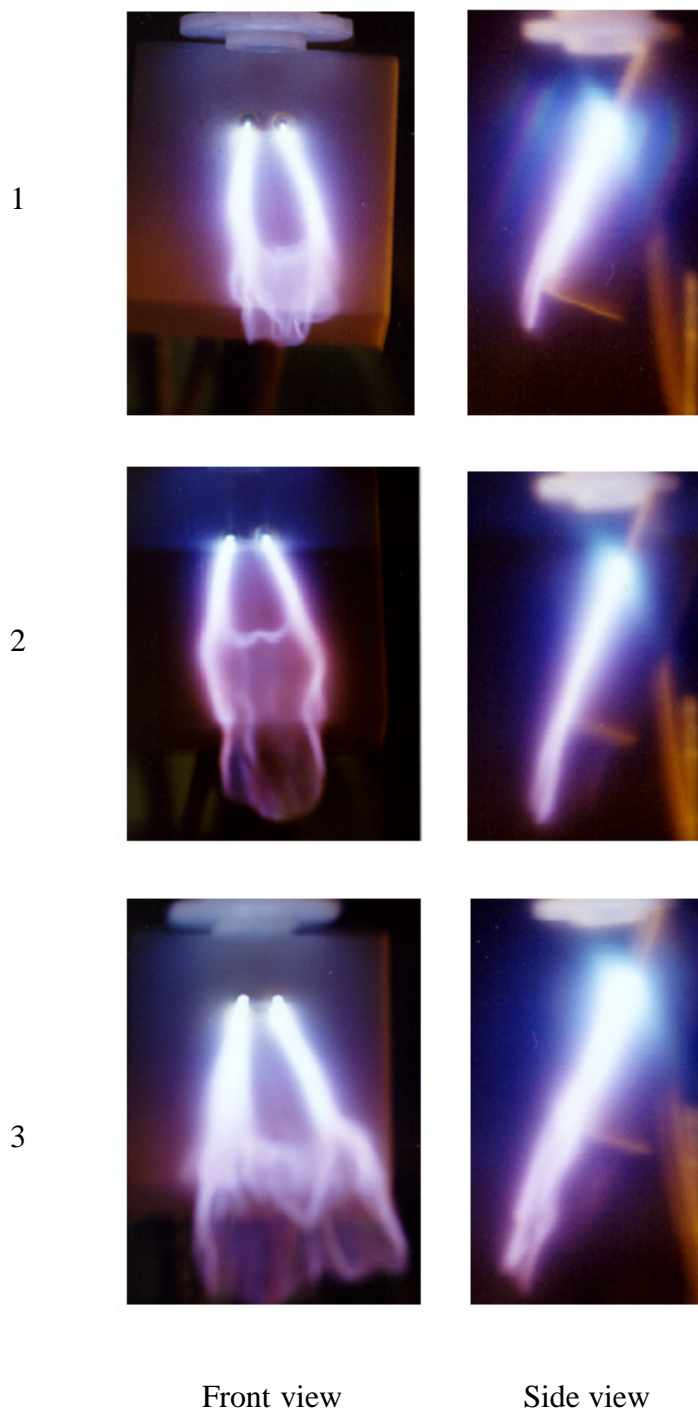


Fig.5.22. The common view of the pulsed-periodic discharge in supersonic airflow on a surface of flat plane at different values of air pressure in the high-pressure system  $p$ , atm: 1-1; 2-3; 3-6.

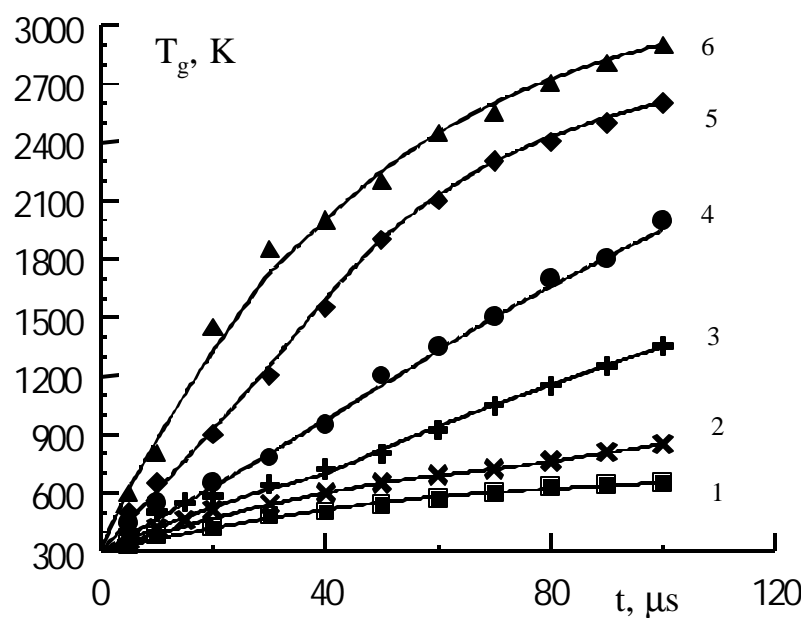


Fig.5.23. The gas temperature of surface pulsed-periodic discharge on the flat plate at different values of discharge current  $i$ , A: 1 – 0.7; 2 – 1.5; 3 – 3.0; 4 – 6.0; 5 – 9.0; 6 – 18.

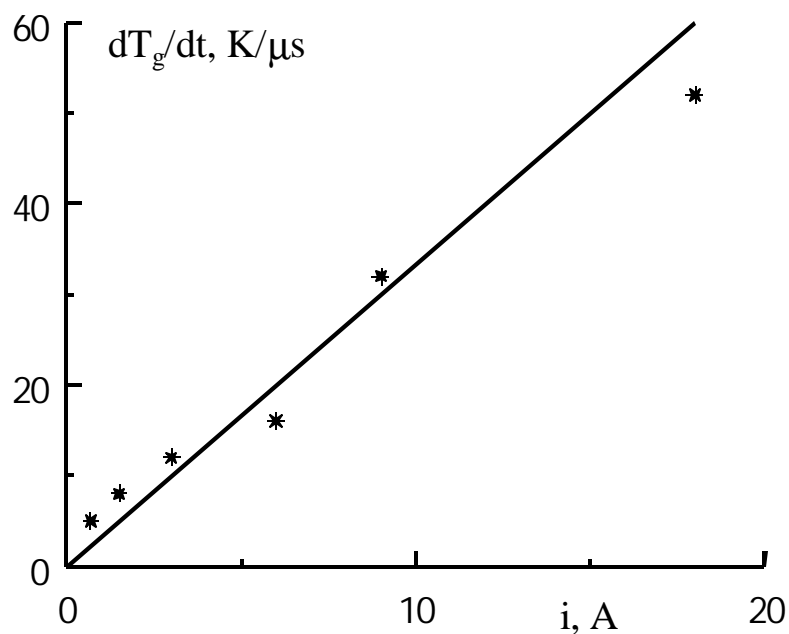


Fig.5.24. Dependence of the gas heating rate on discharge current under condition of surface pulsed-periodic discharge on the flat plate.



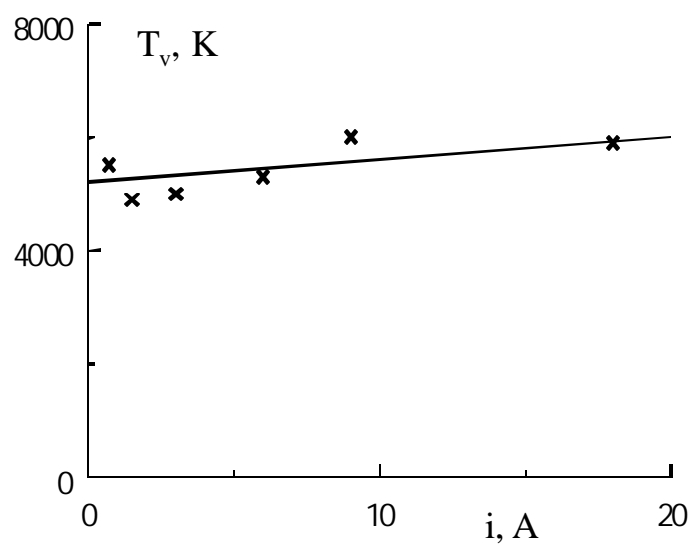


Fig.5.25. Dependence of the vibrational temperature on discharge current under condition of surface pulsed-periodic discharge on the flat plate.

## CONCLUSIONS

1. The literature review on the subject of the Project is carried out. The different regimes of action on laminar - turbulent transition and turbulent boundary layer resulting in to reduction of friction at subsonic and supersonic motion of flight vehicles in the Earth's atmosphere are analysed. The different ways of additional energy supply into a turbulent boundary layer are examined. The different modes of the gas discharges creation into a boundary layer are considered. The methods of plasma creation on the bodies surfaces with the help of the surface microwave discharges are examined.
2. The mathematical model of the discharge grounded on the joint solution of the balance equations of charged particles and Maxwell equations for an electromagnetic field are worked out. The theoretical analysis ensures following results: the calculation of the dispersion curves of a surface wave taking into account inhomogeneity of a plasma layer (self-consistent solution with the ionised non-linearity); the calculation of a field penetration depth in plasma and thickness of a plasma layer created by both direct and reflected surface waves, in dependence on wave amplitude and frequency, and also gas pressure and airflow velocity; the dependence of longitudinal length of the discharge supported by a surface wave from power, transferred by a microwave; the analysis of requirements of electromagnetic waves reflection from antenna butt-end at the different shape of the latter; the analysis of two dimensional field structure in a plane of the antenna.
3. The modernization of the discharge chamber available in laboratory is carried out with the purpose of creation of the surface microwave and pulsed-periodic discharges in supersonic airflow at gas pressure  $p=1-760$  torr. The system of formation of supersonic gas flow and the special system of input of a microwave energy into discharge chamber and transformations of the microwave energy into the energy of a surface wave is installed on the discharge chamber. The method of probe measurements of the charged particles concentration under conditions of surface microwave discharge plasma was worked out. It is shown that the perturbations of researched system and distortion of the probe characteristics can considerably be reduced by excluding the radio-frequency cables from constructions of devise and by supplied optical management of a probe feeding and transfer of the information about a probe current and voltage into the recording equipment. The automated circuit of probe measuring with the optical isolator is designed and manufactured. In the experiment 12-bit 4096 levels the analog-digital converter are used.

4. The surface microwave discharge on a dielectric antenna with length  $L=15$  cm of rectangular section  $S=1.2$  cm<sup>2</sup> is created at air pressure  $p=10^{-3}$ - $10^3$  torr. The magnetron generator had the following characteristics: the wavelength  $\lambda=2.4$  cm; the pulsed microwave power  $W=10$ - $300$  kW; the repetition frequency  $f=1$ - $100$  Hz; the pulse duration  $\tau=1$ - $300$   $\mu$ s; the pulse period-to-pulse duration ratio  $Q=1000$ . At air pressure  $p>1$  torr the discharge represents thin (thickness  $\Delta h=0.1$ - $1.0$  mm) plasma layer uniformly coating all antenna surface. The examination of dynamics of the discharge has shown that velocity of propagation of the discharge and its longitudinal length depend on microwave pulse duration and input power. Thus, on an initial stage of the discharge the velocity of its distribution reaches  $v\sim 10^7$  cm/s, that are much greater than the airflow velocity ( $v_f=5\cdot 10^4$  cm/s) under experimental conditions. The discharge propagation velocity decreases up to  $v\sim 10^4$  cm/s to the end of the microwave pulse with duration  $\tau=100$   $\mu$ s. The threshold characteristic of the surface microwave discharge appearance are determined. It is shown, that at air pressure  $p=0.1$ - $10$  torr the power necessary for creation of the surface microwave discharge is minimum and equals  $\sim 10$  kW.
5. In plasma of the surface microwave discharge the electron density, gas and vibrational temperature are measured at different values of gas pressure and microwave power. The electron density equals  $6\cdot 10^{12}$  cm<sup>-3</sup>. At growth of power the gas temperature is increased from  $\sim 500$  K at  $W=35$  kW up to  $\sim 1700$  K at  $W=175$  kW, whereas vibrational temperature remains practically constant under these conditions, insignificantly decreasing with increase of microwave power. At this the maximal gas heating is observed in a place of excitation of a surface microwave discharge and gas temperature decreases by the end of the discharge. On the initial stage of existence of the surface microwave discharge the fast gas heating with rate  $dT_g/dt=50$  K/ $\mu$ s is observed. It was shown, that the mechanism connected to effective excitation of electron-excited states of nitrogen molecules at large values of the reduced electrical field  $E/n\geq 100$  Td= $10^{-15}$  V·cm<sup>2</sup> and their subsequent quenching is responsible for the fast heating. At this the part of excitation energy of these states is transferred in the heat of air. As our estimations show, only the quenching of electron-excited long-living states of nitrogen molecules, which are effectively created in conditions of a surface microwave discharge in air, provides the gas heating rate.
6. The surface microwave discharges in supersonic airflow with Mach number of flow  $M=2$  are created. It was shown, that the supersonic flow of air at Mach number  $M=2$  does not influence on the common view of the surface discharge on the dielectric antenna of

rectangular section and on the microwave power which is necessary for creation of the surface microwave discharge. Thus the threshold of appearance of a surface microwave discharge does not depend on whether at first the discharge on a surface of a dielectric body is created and then the supersonic airflow is included or, on the contrary, at first the supersonic airflow is included, and only then the surface microwave discharge is created.

7. The system of creation of a pulsed-periodic discharge on a surface of a dielectric plate streamlined supersonic airflow was designed and manufactured. The high-voltage pulses at  $U=1-25$  kV with the help of a high-voltage cable through the specially designed a vacuum cut-off point is lead to electrodes fixed into a dielectric plate. The special measures for avoidance of an electrical breakdown on the opposite surface of a dielectric plate outside of supersonic flow are undertaken. The plate can be installed under different angles to the direction of supersonic airflow.
8. The surface pulsed-periodic discharge in supersonic airflow was created on a dielectric plate placed at the angle of approximately twenty degrees to the direction of supersonic airflow at air pressure  $p=40$  torr, voltage on the discharge gap  $U=15$  kV, and discharge current  $i=10$  A. The common view of the discharge in supersonic airflow on a surface of a dielectric body does not differ from the common view of the volumetric discharge in supersonic airflow. Without supersonic airflow the discharge represents the plasma channel existing on a surface of a dielectric body between two electrodes, fixed in a dielectric flush with a surface. The supersonic flow leads to blowing of plasma jets from each of electrodes which are overlapped among themselves downstream. The length of each jets depends on pulse duration, gas pressure, velocity of supersonic flow, and energy deposition in the discharge. The electron density, measured by probe method under condition transversal pulsed-periodical surface discharge, changed from  $\sim 10^{11} \text{ cm}^{-3}$  at discharge current  $i=0.5$  A up to  $\sim 10^{13} \text{ cm}^{-3}$  at  $i=20$  A. The time evolutions of the gas temperature of surface pulsed-periodic discharge on the surface of a flat plate at different values of discharge current is obtained. It is shown, that under experimental conditions the gas heating rate grows with increasing of discharge current. The vibrational temperature approximately equals 5000 K.

## REFERENCES

### References to chapter I

1. International Space Planes and Hypersonic System and Technologies Conference. Workshop on Weakly Ionized Gases. Proceedings: Colorado, USA, AIAA-1997; Norfolk, USA, AIAA-1998; Norfolk, USA, AIAA-99.
2. The First and Second Workshops on Magneto- and Plasma Aerodynamics for Aerospace Applications. Proceedings: Mocsow, Russia, IVTAN-1999; Mocsow, Russia, IVTAN-2000.
3. A.Yu.Gridin, B.G.Efimov, A.V.Zabrodin, et.al. Preprint Keldish Institut Prikladnoi Mekhaniki RAN, No 19, 1995 (In Rus).
4. A.F.Alexandrov, I.B.Timofeev, S.N.Chuvashev. Bezudarnoe sverkhzvukovoe dvizhenie v atmosfere: printsipialnaya vozmozhnost i prakticheskaya realizatsiya. -Prikladnaya Fizika. 1996, No 3, p.112-117 (In Rus).
5. S.N.Chuvashev, A.P.Ershov, A.I.Klimov, S.B.Leonov, V.M.Shibkov, I.B.Timofeev. Flow around body and characteristics of AD/CD discharges in plasma aerodynamic experiment. Proceedings Norfolk, VA, 1998.
6. Lowry, J.Blanks, C.Stepanek, M.Smith, L.Crosswy, P.Sherrouse, J.Felderman. Characterization of the shock structure of a spherical projectile in weakly ionized air through ballistic range test technique. Proceedings Norfolk, VA, 1998.
7. L.M.Biberman, V.S.Vorob'ev, I.T.Yakubov. Kinetika neravnovesnoi nizkotemperaturnoi plazmi. Moscow: Nauka, 1982 (In Rus).
8. A.S.Zarin, A.A.Kuzovnikov, V.M.Shibkov. Freely localized MW discharge in air. Moscow: Oil & Gas. 1996, 204 p (In Rus).
9. V.M.Batenin, I.I.Klimovskii, P.V.Lisov, V.N.Troitskii. Sverkhvisokochastotnie generatori plazmi. Moscow: Energoatomizdat. 1988 (In Rus).
10. P.L.Kapitsa. Svobodnii plasmennii shnur v visokochastotnom pole pri visokom davlenii. – Zhurnal eksperimentalnoi i teoreticheskoi fiziki, 1969, vol.57, No 6(12), p.1801-1866 (In Rus).
11. J.Allison, A.L.Cullen, A.A.Zavody. A microwave plasma discharge. -Nature, 1962, vol.193, No 4811, p.72.
12. W.E.Scharfman, W.C.Taylor, T.Morita. Breakdown limitations on the transmission of microwave power through the atmosphere. -IEEE Trans. on Antennas and Propagation. 1964, vol.AP-12, No 6, p.709.

13. A.M.Devyatov, A.A.Kuzovnikov, V.V.Lodinev, V.M.Shibkov. The mechanism of molecular gas heating in a pulsed free-localizing RF discharge. -Moscow University Physics Bulletin. Fizika, 1991, vol.46, No 2, p.28-31.
14. A.A.Kuzovnikov, V.M.Shibkov, L.V.Shibkova. Free-localized pulse-periodic MW discharge in air. Kinetics of gas heating. -High Temperature, 1996, vol.34, No 3, p.343-348.
15. V.M.Shibkov. Free-localized pulse-periodic MW discharge in air. Electric field strength in plasma. -High Temperature, 1996, vol.34, No 4, p.519-524.
16. A.A.Kuzovnikov, V.M.Shibkov, L.V.Shibkova. Kinetics of charged particles in a free-localized pulse-periodic MW discharge in air. -High Temperature, 1996, vol.34, No 5, p.651-655.
17. A.V.Kalinin, V.M.Shibkov, L.V.Shibkova. Vliyanie kisloroda na kinetiku nagreva molekulyarnogo gasa v azotno-kislorodnoi smesi. -Vestnik Moskovskogo Universiteta. Seriya 3, Fizika, astronomiya, 1996, No 1, p.38-42 (In Rus).
18. V.V.Zlobin, A.A.Kuzovnikov, V.M.Shibkov. Concentration of electrons in a stimulated MW discharge channel in nitrogen. -Moscow University Physics Bulletin. Fizika, 1988, vol.43, No 1, p.98-100.
19. V.V.Lodinev, V.M.Shibkov, L.V.Shibkova. Gas heating kinetics in pulse-periodic air discharge. -Moscow University Physics Bulletin. Fizika, 1996, vol.51, No 2, , p.26-31.
20. A.A.Kuzovnikov, V.M.Shibkov, L.V.Shibkova. Kinetics of electrons in plasma of discharge, created in free space by focused microwave beam. -Zhurnal Tekhnicheskoi Fiziki, 1997, vol.67, No 6, p.10-14 (In Rus).
21. A.F.Alexandrov, A.S.Zarin., A.A.Kuzovnikov, V.M.Shibkov, L.V.Shibkova. Plasma parameters of non-consistent microwave discharge, created in programmable pulse. - Zhurnal Tekhnicheskoi Fiziki, 1997, vol.67, No 7, p.19-23 (In Rus).
22. V.M.Shibkov. Heating of gas under conditions of free-localized microwave discharge in air. Mathematical simulation. -High Temperature, 1997, vol.35, No 5, p.681-689.
23. V.M.Shibkov. Heating of gas under conditions of free-localized microwave discharge in air: Experiment. -High Temperature, 1997, vol.35, No 6, p.858-862.
24. Yu.V.Zlobina, V.M.Shibkov, L.V.Shibkova. Kinetics of heating and dissociation of molecules in pulsed discharge in hydrogen. -Fizika plasmi, 1998, vol.24, No 7, p.667-671 (In Rus).
25. A.V.Kazakov, M.N.Kogan, V.A.Kuparev. Delay of laminar-turbulent transition by means of intensive localized heating of the surface in the vicinity of the leading edge of the plate. - High Temperature, 1996, vol.34, No 1, p.42-47.

26. A.A.Pilipenko, G.K.Shapovalov. Upravlenie sostoyaniem pograničnogo sloya putem vvedeniya iskusstvennikh vozmushenii. –Uchenie zapiski TsAGI, 1986, vol.17, No 4, p.73-78 (In Rus).
27. Yu.S.Kachanov, V.V.Kozlov, V.Ya.Levchenko. Vozniknovenie turbulentnosti v pograničnom sloe. -Novosibirsk, Nauka, 1982, 151p (In Rus).
28. A.V.Kazakov, M.N.Kogan, V.A.Kuparev. Laminirizatsiya pograničnogo sloya pri otritsatel'nom gradiente davleniya i nagreve poverkhnosti. –Teplofizika visokikh temperatur, 1996, v.34, No 2, p.244-249 (In Rus).
29. V.V.Kozlov. Physics of flow structures. Flow separation. –Soros Education Journal, 1998, No 4, p.86-94.
30. V.V.Kozlov. Otriv potoka ot perednej kromki i vliyanie na nego akusticheskikh vozmushenii. –Prikladnaya mekhanika i tekhnicheskaya fizika. 1985, No 2, p.112-115 (In Rus).
31. A.A.Maslov, N.A.Semenov. Vozbuzhdenie sobstvennikh kolebaniy pograničnogo sloya vneshnim akusticheskim putem. –Mekhanika zhidkosti i gasa. 1986, No 3, p. (In Rus).
32. A.V.Kazakov, M.N.Kogan, V.A.Kuparev. Ob ustojchivosti dozvukovogo pograničnogo sloya pri nagreve poverkhnosti ploskoi plastini vblizi perednei kromki. –Izvestiya AN SSSR. Mekhanika zhidkosti i gasa, 1985, No 3, p.68 (In Rus).
33. A.V.Kazakov, M.N.Kogan, A.P.Kuryachii. O vliyaniy lokalnogo nagreva poverkhnosti na trenie v turbulentnom pograničnom sloe na plastine. -Teplofizika visokikh temperatur, 1995, v.33, No 6, p.888-894 (In Rus).
34. A.V.Kazakov, A.P.Kuryachii. The effect of viscous-nonviscous interaction on turbulent flow past a plate under conditions of local heating of its surface. -High Temperature,1998, vol.36, No 3, p.395-400.
35. Yu.V.Lapin. Turbulentnii pograničnii sloi v sverkhzvukovikh potokakh gasa. -Moscow: Nauka, 1982. 312 p (In Rus).
36. C.Carvin, J.F.Debieve, A.J.Smits. The Near-Wall Temperature Profile of Turbulent Boundary Layer. -AIAA Paper. 1988, No 136, 8 p.
37. A.V.Kazakov, M.N.Kogan, A.P.Kuryachii. Vliyanie na trenie lokalnogo podvoda tepla v turbulentnii pograničnii sloi. –Izvestiya RAN. Mekhanika zhidkosti i gasa, 1997, No 1, p.48 (In Rus).
38. A.V.Kazakov, M.N.Kogan, A.P.Kuryachii. The effect of the thermal properties of a body being flown about on friction and heat transfer under conditions of local heat input to a turbulent boundary layer. -High Temperature, 1997, v.35. No 1, p.61-66.

39. Chien K.Y. Prediction of Channel and Boundary-Layer Flows with a Low-Reynolds-Number Turbulence Model. -AIAA Journal, 1982, vol. 20, No 1, p.33.
40. M.Moisan, C.M.Ferreira, Y.Hajlaoui, D.Henry, J.Hubert, R.Pantel, A.Ricard, Z.Zakrzewski. Properties and applications of surface wave produced plasmas. -Revue Phys. Appl., 1982, vol.17, p.707-727.
41. M.Moisan, Z.Zakrzewski. -J. Phys. D: Appl. Phys., 1991, vol. 24, p.1025.
42. S.Daviaud, C.Boisse-Laporte, P.Leprince, J.Marec. Description of surface-wave-produced microwave discharge in helium at low pressure in the presence of a gas flow. -J.Phys.D: Phys. Appl., 1989, vol.22, p.770-779.
43. A.Granier, C.Boisse-Laporte, P.Leprince, J.Marec, P.Nghiem. Wave propagation and diagnostics in argon surface-wave discharges up to 100 Torr. -Phys. Appl., 1989, vol.20, p.204-209.
44. A.Granier, C.Boisse-Laporte, P.Leprince, J.Marec, E.Dervisevic. Microwave discharges produced by surface waves in argon gas. -Phys. Appl., 1987, vol.20, p.197-203.
45. C.Boisse-Laporte, P.Leprince, J.Marec, R.Darchicourt, S.Pasquiers. Influence of the radial electron density profile on the determination of the characteristics of surface-wave-produced discharges. -Phys. Appl., 1988, vol.21, p.293-300.
46. M.Moisan, C.M.Ferreira The similarity laws for the maintenance field per electron in low-pressure surface wave produced plasmas and their extension to HF plasmas in general. - Physica Scripta, 1998, vol.38, p.382-399.
47. J.Marec, P.Leprince. Recent trends and developments of microwave discharges. -Journal de Physique IV. France, 1998, vol.8, Pr7-21-32.
48. M.Moisan, C.Beaudry, P.Leprince. -IEEE Trans.Plasma Sci., 1975, PS-3, p.55.
49. M.Moisan, Z.Zakrzewski, R.Pantel. -J.Phys.D, 1979, vol.12, p.219.
50. M.Moisan, Z.Zakrzewski. -Microwave excited plasmas (Amsterdam Elsevier 1992), p.92.
51. J.Marec, P.Leprince. -Microwave discharges: Fundamentals and applications, C.M.Ferreira and M.Moisan Eds. (New York and London Plenum, 1993), p.45.
52. C.Boisse-Laporte. -Microwave discharges: Fundamentals and applications, C.M.Ferreira and M.Moisan Eds. (New York and London Plenum, 1993), p.25.
53. Z.Rakern, P.Leprince, J.Marec. -Rev. Phys. Appl., 1990, vol.25, p.125.
54. Z.Rakern, P.Leprince, J.Marec. -J. Phys. D: Appl. Phys., 1992, vol.25, p.953.
55. C.M.Ferreira. -J. Phys. D: Appl. Phys., 1989, vol.22, p.705.
56. U.Kortshagen, H.Schluter, A.Shivarova. -J. Phys. D: Appl. Phys., 1991, vol.24, p.1571.
57. U.Kortshagen, H.Schluter, A.Shivarova. -J. Phys. D: Appl. Phys., vol.24, p.1585.



58. C.Boisse-Laporte, P.Leprince, J.Marec. -CIP 95, Xth. Int. Coil., Antibes, 1995.
59. S.Bechu, C.Boisse-Laporte, P.Leprince, J.Marec. -AVS 43rd Symp., Philadelphia, 1996.
60. S.Bechu, C.Boisse-Laporte, J.Marec. -J. Vac. Sci. Technol., 1997, vol. A15.
61. Ohl A. Fundamentals and limitations of large area planar microwave discharges using slotted waveguides. -Journal de Physique IV. France, 1998, vol.8, Pr7-83-98.
62. M.Moisan, C.Barbeau, R.Claude, C.M.Ferreira, J.Margot, J.Paraszczak. A.B.Sa, G.Sauve, M.R.Wertheuner. -J. Vac. Sci. Technol., 1991, vol. B9, p.8-25.
63. M.Kummer. -Mikrowellentechnik (Verlag Technik, Berlin, 1986), p. 40-41.
64. D.Korzec, F.Werner, R.Winter, J.Engemann. -Plasma Sources Sci. Technol., 1996, vol.5, p.216-234.
65. T.Yasui, J.Kitayama, H.Tahara, T.Yoshikawa. Production of wide plasmas using microwave slot antennas on a rectangular waveguide. -Proceedings ICRP-2/SPP-11, Yokohama 19-21 January 1994, T. Goto Ed. (Organizing Committee of ICRP-2/SPP-11, Yokohma, 1994), p.367-370.
66. A.Ohl. Large area planar microwave discharges. -Microwave Discharges: Fundamentals and Applications, C.M. Ferreira and M. Moisan Eds. (Plenum Press, New York and London, 1993), p.205-214.
67. Z.Zakrzewski, M.Moisan. -Plasma Sources Sci. Technol., 1995, vol.4, p.379-397.
68. W.H.Watson. The physical principles of wave guide transmission and antenna systems (University Press, Oxford, 1949), p. 80-154.
69. G.Sauve, M.Moisan, Z.Zakrzewski. -J. Microwave Power Electromagn. Energy, 1993, vol.28, p.123-131.
70. M.Wakatsuchi, S.Ishii, Y.Kato, F.Tani, M.Sunagawa. -Plasma Sources Sci. Technol., 1996, vol.5, p.327-332.
71. M.Nagatsu, G.Xu, M.Yamaga, M.Kanoh, H.Sugai. -Jpn. J. Appl. Phys., 1996, vol.35, L341.
72. P.Werner, D.Korzec, J.Engemann. -Plasma Sources Sci. Technol., 1994, vol.3, p.473.
73. Z.Zakrzewski, M.Moisan. -Plasma Sources Sci. Technol., 1995, vol.4, p.379.
74. Z.Zakrzewski, M.Moisan. Linear field applicators. -Journal de Physique IV. France, 1998, vol.8, Pr7-109-118.
75. E.Rauchle. Duo-plasmaline, a surface wave sustained linearly extended discharge. -Journal de Physique IV. France, 1998, vol.8, Pr7-99-108.
76. K.Komachi. -J. Vac. Sci. Technol., 1994, vol.A12, p.769.
77. T.Kiimura, Y.Yoshida, S.Mizuguchi. -Jpn. J. Appl. Phys., 1995, vol.34, L1076.
78. Y.Yoshida, Y.Miyazawa, A.Kazama. -Rev. Sci. Instrum., 1997, vol.68, p.1.

79. Y.Yoshida. -Journal de Physique IV. France, 1998, vol.8, Pr7-195-203.

## References to chapter II

1. H.Schluter. Self-consistent modeling of surface wave sustained discharges. -Journal de Physique IV. France, 1998, vol.8, Pr7-43-60.
2. Z.Zakrzewski, M.Moisan. Linear field applicators. -Journal de Physique IV. France, 1998, vol.8, Pr7-109-120.
3. S.A.Dvinin, V.A.Dovzhenko, G.S.Solntsev. Ob izmerenii energeticheskikh kharakteristik SVCH razryada pri razvitii ionizatsionnoi neustoichivosti na poverkhnostnoi volne. -Fizika plasmi, 1983, vol.9, No 5, p.1058-1067 (In Rus).
4. S.A.Dvinin, V.A.Dovzhenko. Diffusive propagation of ionization front in UHF wave field. Fizika plasmi, 1988, vol.14, No 1, p. 66–76 (In Rus).
5. T.A.Grotjohn. Modeling electromagnetic fields for the excitation of microwave discharges used for material processing. -Journal de Physique IV. France, 1998, vol.8, Pr7-61-82.
6. E.Rauchle. Duo-plasmaline, a surface wave sustained linearly extended discharges. -Journal de Physique IV. France, 1998, vol.8, Pr7-83-99.
7. A.Kh.Mnatsakanyan, G.V.Naidis. Processes of formation and loss of charged particles in nitrogen-oxygen plasma. In book: Khimiya plasmi. Vipusk 14. Pod redaktsiei B.M.Smirnov. Moscow. Energoizdat, 1987 (In Rus).
8. O.E.Krivososova, S.A.Losev, V.P.Nalivayko et al. -In book: Khimiya plasmi. Vipusk 14. Pod redaktsiei B.M.Smirnov. Moscow. Energoizdat, 1987 (In Rus).
9. C.Park. -AIAA Rep. 89-1740, 1989.
10. I.A.Kossyi, A.Yu.Kostinsky, A.A.Matveyev et al. -Plasma Sources Sci. Technol., 1992, vol.1, p.207.
11. N.L.Aleksndrov, E.M.Bazelyan. -J. Phys. D: Appl. Phys., 1996, vol.29, p.2873.
12. N.L.Aleksndrov, E.M.Bazelyan, N.A.Dyatko, I.V.Kochetov. -J. Phys. D: Appl. Phys., 1997, vol.30, p.1616.
13. E.M.Bazelyan, Yu.P.Raizer. Intergrowth of the streamer channel: a field and density of plasma behind a wave of ionization, initial electrons before it. -High temperature, 1997, vol.35, p.181–186.
14. N.L.Aleksndrov, E.M.Bazelyan, N.A.Dyatko, I.V.Kochetov. Streamer break-down of lengthy air gaps. -Plasma phys. report, 1998, vol. 24, No7, p.587–602.
15. K.U.Riemann. -J. Phys D: Appl. Phys. 1991, vol. 24, p.1991.

16. K.B.Riemann. -Physics of plasmas, 1997, vol.4, p.4158.
17. Alexandrov A.F., Rukhadze A.A. "Lectures on Electrodynamics of Plasma-like Media", Moscow, Pub. House Moscow University, 1999 (In Rus).
18. Alexandrov A.F., Bogdankevich L.S., Rukhadze A.A. "Waves and Oscillations in Plasma-like Media", Moscow, Pub. House Moscow University, 1990 (In Rus).
19. Alexandrov A.F., Bogdankevich L.S., Rukhadze A.A. "Principles of Plasma Electrodynamics", Moscow, Pub. House "Visshay Skola" (1978, 1988), English Trans. "Springer Verlag", Heidelberg (1984).
20. Ginzburg V.L., Rukhadze A.A. "Waves in Magnetoactive Plasma", Moscow, Pub. House "Nauka" (1970, 1975); English trans. Hand Physics v.49, "Springer Verlag", (1972).
21. Kondratenko A.N. Surface and Volume waves in restricted plasma. Energoatomizdat, 1985 (In Rus).
22. Kondratenko A.N. Electromagnetic field penetration into plasma. Energoatomizdat, 1979 (In Rus).
23. Kondratenko A.N. Surface waves in plasma. Atomizdat, 1976 (In Rus).
24. Zhelyazkov I., Atanassov V. Axial structure of low pressure high frequency discharges, sustained by travelling electromagnetic surface wave. Physics reports, 255, 1995, p.79-201.
25. Microwave plasma and its application. Ed. Yuri Lebedev. Moscow, Moscow Physical society, 1995.
26. Microwave discharge and its applications. III International workshop. Ed. C. Bousse-Laport, J. Marec. J de physique IV, v.8, pr7, Oct 1998.
27. Felsen L., Marcuvitz N. Radiation and Scattering of waves. Prentice-Hall, Inc., Englewood Cliffs, New Jersey, 1973.
28. Zeldovich Ya.B., Rayzer Yu.P. Fizika udarnihk voln i vysokotemperaturnihk gazodinamicheskikh yavleniy. Moscow: Nauka, 1966 (In Rus).
29. Alexandrov A.F., Rukhadze A.A. Fizika silnotochnihk elektrorazryadnihk istochnikov sveta. Moscow: Nauka, 1966 (In Rus).
30. Granovskiy V.L. Elektricheskiy tok v gaze. Ustanovivshiysya tok. Moscow: Nauka, 1971. p.253.
31. Ginzburg V.L. Propagation of electromagnetic waves in plasma Moscow: Nauka, 1965 (In Rus).
32. Denisov N.G. About one feature of an electromagnetic wave field propagating in inhomogeneous plasma. Sov. Phys: ZhETP, 1956, p.1931 (In Rus).

33. V.N.Ponomarev, G.S.Solntsev. -Jurnal Tekhnicheskoi Fiziki. 1966, vol.36, (Sov. Phys., JTP, 1966, v.36).
34. A.G.Boev. To the theory of nonlinear surface waves in plasma. -Sov. Phys. JETP, 1979, v.77, No 1, p.92-100.
35. A.G.Boev. To the nonlinear theory of penetration of p-polarized electromagnetic waves in plasma. -Sov. Phys. JETP, 1980, v.79, No 1(7), p.134-142.
36. A.G.Boev. Threshold values of plasma electronic density created by an electromagnetic field. -Dokladi AN USSR, Seriya ?, 1981, No 2, p.65-67 (In Rus).
37. A.G.Boev. Plasma column formed by a running ionizing electromagnetic wave. -Fizika plazmi, 1982, v.8, No 4, p.729-735 (In Rus).
38. V.B.Gildenburg, A.V.Kochetov, A.G.Litvak, A.M.Feigin. Self-sustaining waveguide channels in plasma. -Sov. Phys. JETP, 1983, v.84, No 1 (In Rus)
39. Braginskiy S.I. Yavleniya perenosa v plasme. Voprosi teorii plazmi. 1964, v.1, p.183–272 (In Rus).
40. Gurevich A.V., Shvartsburg A.B. Nelineynaya teoriya rasprostraneniya radiovoln v ionosfere. Moscow: Nauka, 1973, p.221 (In Rus).
41. Kim A.V., Frayman A.G. Fizika plazmi, 1983, v.9, No.3, p.619 (In Rus).
42. Kostinsky A.Y., Matveev A.A., Silakov V.P. Kinetical processes in the non-equilibrium nitrogen-oxygen plasma. Moscow.: Academy of sciences of the USSR. General physics institute. Plasma physics division. Preprint ? 87. 29. p. 1990.

#### **References to chapter IV**

1. Ivanov Yu.A., Lebedev Yu.A., Polak L.S. Methods of contact diagnostics in non-equilibrium plasmachemistry. Moscow, Nauka, 1981 (In Rus).
2. Ershov A.P. Final scientific report on ISTC project #1867p between International Science and Technology Center, Department of Physics of Moscow State University and the European Office of Aerospace Research and Development (EOARD), 2001.

#### **References to chapter V**

1. Zarin A.S., Kuzovnikov A.A., Shibkov V.M.. Freely localized microwave discharge in air. - Moscow: Oil and gas, 1996, 204p (In Rus).
2. Shibkov V.M. -High Temperature. 1997, 35, No.5, p.681.

3. Shibkov V.M. -High Temperature. 1997, 35, No.6, p.858.
4. Shibkov V.M. Kinetics of gas heating in plasma created in supersonic airflow. -9<sup>th</sup> Intern. Space Planes and Hypersonic Systems and Technologies Conf. Norfolk, Virginia, USA, 1999, AIAA-99-4965.